

Biogeomorphic modelling of tropical sheltered bays

Assessment of the role of seagrass ecosystems in
tropical sheltered bays in the Caribbean

C. Taaban

Biogeomorphic modelling of tropical sheltered bays

Assessment of the role of seagrass ecosystems in
tropical sheltered bays in the Caribbean

by

C. Taaban

in partial fulfillment of the requirements for the degree of

Master of Science
in Hydraulic Engineering

at the Delft University of Technology,
to be defended publicly on 21 November 2019, at 10:00 AM.

Thesis committee

| | |
|----------------------------------|---------------------|
| Prof. dr. J. D. Pietrzak (Chair) | TU Delft |
| Prof. dr. P. M. J. Herman | TU Delft & Deltares |
| Dr. R. E. M. Riva | TU Delft |
| Ir. B. P. Smits | Deltares |
| Ir. L. M. Keyzer | TU Delft |

An electronic version of this thesis is available at <http://repository.tudelft.nl/>.



Cover image adapted from Martin (2019).

Acknowledgments

This thesis results from my research on the biogeomorphic role of seagrass ecosystems in tropical, sheltered bays. This research was part of the NWO Caribbean Research Program (SCENES project) and was carried out at Deltares, under the department of Ecosystems & Sediment Dynamics, which provided financial and academic support. After a long period of hard work and dedication, I am proud to show the results of my thesis research. But first, I would like to highlight a few important people that helped me along my journey and made this possible. I most definitely have forgotten many names, therefore please forgive me and know that I am very appreciative of your help.

All the courses during my study program at TU Delft provided me with the necessary knowledge and tools to successfully complete my research. I would like to thank all my teachers and professors for their contribution to inspiring new generations of students who choose to embark on this same journey.

I want to show my immense appreciation to my committee members. Thank you all for your contribution. You helped me find (and often re-find) my way to my objective. Thank you, Julie, for sharing your passion for your expertise, continued encouragement and inspiration throughout my graduation. Thank you, Peter. I enjoyed the technical conversations with you and loved your constructive feedback. You formulated this in such an efficient manner (you often needed a few words to convey the message) which allowed me to understand immediately and kept me critical. Thank you, Bob, for your daily supervision at Deltares that especially in the beginning stage of my research was very needed. I learned a lot about your professionalism and how you tackle challenges. Your problem analysis and subsequent decomposition of the issues helped me often to solve my overwhelming model issues. Thank you, Lennart, for sharing your recent graduation experiences and knowledge of your model to continue this fascinating research topic. Thank you, Riccardo, for being part of my committee and your input during the meetings is also greatly appreciated.

I also want to thank Rebecca James. You provided me with important knowledge and measurements of the coastal bays of St. Martin and this data was crucial during my model setup.

To my fellow students and friends, thank you all for sharing this journey with me. Many talks, joyful moments, and futsal matches made this period much less lonely. I would like to highlight the help of Said, Tolga, and Khaled for reading my report and for being available to answer one of my questions (again), thank you.

I would like to thank my family, in particular, my mum and dad. Thank you for your unconditional love and support. Thank you, grandma. You are not with us anymore, but you meant a lot to me and you were are a great inspiration. I dedicate this thesis to you for your endless love and believing in me (even though I was a little kid).

Above all, I want to thank Allah, the Almighty, for blessing me with great people who support me in my personal and professional life and for granting me the opportunity, dedication, and strength to complete my thesis satisfactorily.

Enjoy reading my thesis!

Chahid Taaban
Delft, November 2019

الحمد لله

“Alhamdulillah”

Quran: Al-Fatihah [I;2]

Abstract

Coastal bays in the Caribbean accommodate different marine ecosystems, including seagrass meadows and coral reefs, which provide important ecosystem services. However, these marine ecosystems are endangered. Seagrass ecosystems have a key role in coastal bays, but despite their alarming rates of loss, they receive little attention compared to other marine ecosystems. This study aims to provide a better understanding of the role of seagrass ecosystems in coastal bays by assessing their impact on the morphodynamic behavior. In order to achieve this, an existing hydrodynamic model has been extended to include morphodynamics. Two different bays have been investigated: Baie Orientale and Baie de l'Embouchure (St. Martin). These bays represent a partially exposed and fully sheltered bay, respectively. Both regular wave conditions, as well as extreme storm conditions, have been investigated to understand the consequences of seagrass loss on coastal erosion for different environmental climates.

The coastal erosion has been found to be more prominent in the exposed region, whereas the more sheltered areas are more resilient. The erosion takes place in shallow waters but remains limited under regular swell conditions. The increased wave energy, during the extreme storm event, increases the erosion rates considerably. However, the regular swell conditions are normative in shaping the morphological development of these coastal bays when longer timescales are considered.

The seagrass counters erosion most effectively in the foreshore and much less in deeper regions. Removal of seagrass in the foreshore (between 1-3m) halves the sediment stabilization. In contrast, the sediment stabilization increases if the meadows are able to spread especially towards the shore. In addition, the wave energy and waveform have a significant impact on the sediment stabilization. The stabilization typically decreases for higher and shorter (storm) waves, whereas it increases for smaller and longer (swell) waves.

The long-distance interactions between seagrass meadows and coral reefs have led to their mutual coexistence, which is also found to be beneficial for the erosion control of the coastal bays. The dissipation of wave energy on top of the reefs fosters the sediment stabilization by seagrass. Moreover, the impact of the reefs on sediment stabilization also increases in the presence of seagrass meadows due to the additional drag exerted by the seagrass. The seagrass meadows are typically more effective under swell waves, whereas the reefs are more dominant in the dissipation of storm waves. Seagrass meadows and coral reefs form thus a synergy, in which the stabilization of sediments provided by the individual ecosystems is facilitated, reinforced, and complemented by the proximate presence of the other ecosystem.

Finally, the role of seagrass on sediment stabilization has been explored under climate change. The coastal erosion increases for the considered sea-level rise scenarios. The impact of the seagrass on sediment stabilization decreases when the bays, seagrass and reef ecosystems are not able to keep up with sea-level rise. The synergy between seagrass and reefs emphasizes that the responses of both ecosystems are of importance for the future of tropical sheltered bays and should therefore not be managed in isolation.

Table of Contents

| | |
|--|-------------|
| Acknowledgments | i |
| Abstract | iii |
| List of Figures | ix |
| List of Tables | xiii |
| 1 Introduction | 1 |
| 1.1 Tropical sheltered bays | 1 |
| 1.2 Conceptual research design | 2 |
| 1.2.1 Problem description | 2 |
| 1.2.2 Research objective and questions | 3 |
| 1.2.3 Research scope. | 4 |
| 1.2.4 Research hypothesis | 4 |
| 1.3 Thesis outline | 5 |
| 2 Background information | 7 |
| 2.1 Coastal behavior | 7 |
| 2.1.1 Hydrodynamic behavior of coastal bays | 8 |
| 2.1.2 Shear resistance by vegetation | 9 |
| 2.1.3 Wave dissipation by vegetation | 10 |
| 2.1.4 Morphological behavior of coastal bays | 11 |
| 2.2 Ecosystems | 11 |
| 2.2.1 Seagrass meadows | 11 |
| 2.2.2 Coral reefs | 13 |
| 2.3 Climate change | 14 |
| 2.3.1 Extreme storm events | 15 |
| 2.3.2 Sea-level rise | 15 |
| 2.3.3 Vulnerability reefs | 16 |
| 3 Case study area | 17 |
| 3.1 Introduction St. Martin | 17 |
| 3.2 Environmental climate | 18 |
| 3.3 Hydrodynamic conditions | 19 |
| 3.4 Geomorphological conditions | 19 |
| 3.5 Presence of ecosystems | 21 |
| 4 Methodology | 23 |
| 4.1 Research strategy | 23 |
| 4.2 Model description | 23 |
| 4.3 Adaptations of hydrodynamic model | 24 |
| 4.3.1 Bed shear stress | 24 |
| 4.3.2 Ecosystems | 24 |

| | | |
|----------|--|-----------|
| 4.4 | Morphological model setup | 25 |
| 4.4.1 | Morphological settings | 25 |
| 4.4.2 | Sediment transport formulation | 26 |
| 4.5 | Sensitivity analysis | 27 |
| 4.6 | Model validation | 28 |
| 4.6.1 | Validation of hydrodynamics | 28 |
| 4.6.2 | Validation of morphology | 29 |
| 4.7 | Simulations and scenarios | 32 |
| 4.7.1 | Simulations base cases | 32 |
| 4.7.2 | Simulations seagrass effectiveness | 33 |
| 4.7.3 | Simulations seagrass-reef interaction | 34 |
| 4.7.4 | Future scenarios | 35 |
| 5 | Morphodynamic behavior of coastal bays | 37 |
| 5.1 | Hydrodynamic behavior of bays | 37 |
| 5.1.1 | Hydrodynamics under regular wave climate | 37 |
| 5.1.2 | Hydrodynamics under extreme storm event | 38 |
| 5.2 | Morphological behavior of bays | 40 |
| 5.2.1 | Morphology under regular wave climate | 40 |
| 5.2.2 | Morphology under extreme storm event | 42 |
| 6 | Role of seagrass | 45 |
| 6.1 | Hydrodynamic attenuation by seagrass | 45 |
| 6.2 | Sediment stabilization by seagrass | 46 |
| 6.3 | Effectiveness seagrass | 47 |
| 6.3.1 | Impact of seagrass for various wave conditions | 47 |
| 6.3.2 | Impact of seagrass for different vegetation heights | 49 |
| 6.3.3 | Impact of seagrass for different spatial distributions | 51 |
| 6.4 | Seagrass and reef interaction | 51 |
| 6.5 | Future role of seagrass | 52 |
| 7 | Discussion | 55 |
| 7.1 | Model setup | 55 |
| 7.1.1 | Morphodynamic development | 55 |
| 7.1.2 | Vegetation formulation | 56 |
| 7.2 | Effectiveness seagrass | 57 |
| 7.3 | Seagrass and reef interaction | 57 |
| 7.4 | Future role of seagrass | 57 |
| 8 | Conclusion and recommendations | 59 |
| 8.1 | Conclusion | 59 |
| 8.2 | Recommendations | 60 |
| 8.2.1 | Model extensions | 60 |
| 8.2.2 | Innovative research applications | 60 |
| 8.2.3 | Managing coastal bays | 61 |
| | Bibliography | 63 |
| A | Additional literature | 71 |
| A.1 | Hydrodynamic behavior of coastal bays | 71 |
| A.2 | Morphological behavior of coastal bays | 73 |

| | | |
|----------|--|-----------|
| B | Delft3D-FM model description | 77 |
| B.1 | D-Flow | 77 |
| B.2 | D-Waves | 78 |
| B.3 | D-Morphology | 78 |
| B.4 | Vegetation formulation | 79 |
| C | Hydrodynamic model setup by Keyzer | 81 |
| C.1 | Computational domain | 81 |
| C.2 | Flow module setup | 82 |
| C.3 | Wave module setup | 83 |
| D | Bed shear stress analysis | 85 |
| D.1 | Total bed shear stress | 85 |
| D.2 | Individual components | 87 |
| E | Morphological sensitivity analysis | 91 |
| E.1 | Wave height | 91 |
| E.2 | Wave period. | 92 |
| E.3 | Wave direction | 94 |
| E.4 | Sediment grain size | 95 |
| F | Hydrodynamic attenuation by seagrass | 97 |
| F.1 | Attenuation under regular wave climate | 97 |
| F.2 | Attenuation under extreme storm event | 99 |
| F.3 | Hydrodynamic sensitivity to vegetation characteristics | 100 |

List of Figures

| | | |
|------|--|----|
| 1.1 | Schematic representation of a tropical coastal beach | 1 |
| 1.2 | Critical transitions in disturbance driven vegetation ecosystems | 3 |
| 2.1 | Schematization of a coastal profile | 7 |
| 2.2 | Schematization of wave-driven circulation in reef environments | 8 |
| 2.3 | Non-linear interaction between the wave-induced and flow-induced bed shear stress | 9 |
| 2.4 | Velocity profile in presence of vegetation | 9 |
| 2.5 | Global seagrass distribution | 12 |
| 2.6 | Schematization of anatomy of seagrass meadows | 12 |
| 2.7 | Schematization of coral reef types | 13 |
| 2.8 | Different zones of a barrier reef | 14 |
| 2.9 | Overview of potential impacts of climate change in coastal bays | 14 |
| 2.10 | Projections of globally averaged sea-level rise | 15 |
| 2.11 | Regional sea level rise | 16 |
| 3.1 | Topographic map of Saint Martin | 17 |
| 3.2 | Baie Orientale and Baie de l'Embouchure | 18 |
| 3.3 | Wind rose of annually-averaged recorded winds in Gustavia | 18 |
| 3.4 | Bed substrates and marine ecosystems in Saint Martin bays | 20 |
| 3.5 | Mean sediment grain size measurements | 20 |
| 3.6 | Seagrass species in Baie de l'Embouchure | 21 |
| 4.1 | Seagrass and reef cover | 24 |
| 4.2 | Initial spatial sediment cover | 25 |
| 4.3 | Analysis of sediment transport formulations | 26 |
| 4.4 | Morphological sensitivity to the wave conditions | 27 |
| 4.5 | Locations of measurements | 28 |
| 4.6 | Morphological development for base cases | 30 |
| 4.7 | Observed development of Saint Martin coastal bays | 30 |
| 4.8 | Sediment transport and shear velocities | 31 |
| 4.9 | Verification of morphological up-scaling factor | 32 |
| 4.10 | Different spatial seagrass covers | 33 |
| 4.11 | Bathymetry with and without reef structures | 34 |
| 4.12 | Adapted bathymetry (keep up) and seagrass cover (catch up) for future scenarios | 35 |
| 5.1 | Hydrodynamic behavior of coastal bays | 38 |
| 5.2 | Increase of hydrodynamic forces during the extreme storm event | 39 |
| 5.3 | Water depth increase during the extreme storm event | 39 |
| 5.4 | Morphological changes in the coastal domain under regular wave climate | 40 |
| 5.5 | Morphological changes in coastal bays under regular wave climate | 41 |
| 5.6 | Development of coastal profile A-A' under regular swell wave climate | 41 |
| 5.7 | Morphological changes in coastal bays under regular wave climate & extreme storm event event | 42 |

| | | |
|------|---|----|
| 5.8 | Development of coastal profile A-A' under extreme storm and regular wave conditions | 43 |
| 6.1 | Spatially-averaged seagrass attenuation | 45 |
| 6.2 | Relative impact of seagrass on sediment stabilization under regular swell conditions | 46 |
| 6.3 | Relative impact of seagrass on sediment stabilization under extreme storm conditions | 47 |
| 6.4 | Impact of seagrass on total sediment stabilization under varying wave conditions | 48 |
| 6.5 | Wave-induced set-up | 48 |
| 6.6 | Effect of wave period on bed shear stress | 49 |
| 6.7 | Impact of vegetation height on total sediment stabilization | 50 |
| 6.8 | Relative sediment stabilization and vegetation height | 50 |
| 6.9 | Impact of different spatial distributions of seagrass meadows on sediment stabilization | 51 |
| 6.10 | Impact ecosystems and inter-ecosystem interactions on sediment stabilization | 52 |
| 6.11 | Morphological development for the climate change scenarios | 53 |
| 6.12 | Stabilization role of seagrass under climate change | 54 |
| 7.1 | Morphological development of observation points (O1-O4) | 56 |
| A.1 | Wave-induced orbital motion of fluid particles in intermediate to shallow water | 71 |
| A.2 | Wave-induced velocity profile close to the boundary layer | 72 |
| A.3 | Velocity profile of a confined flow by a solid and free surface | 73 |
| A.4 | Schematization of fores acting on an individual sediment particle | 73 |
| A.5 | Schematization turbulent suspension of an individual sediment particle | 74 |
| A.6 | Dimensionless plot of the Rouse profile | 75 |
| B.1 | Schematic representation of sediment transfer between the bed and suspension layer | 79 |
| C.1 | Computational grids and bathymetry | 81 |
| C.2 | Constructed tidal signal for one solar month. | 82 |
| C.3 | Chèzy smoothness of the bed | 82 |
| D.1 | Bed shear stress components for Flow-Wave & vegetation case | 86 |
| D.2 | Total bed shear stress for Flow-Wave & No vegetation case | 87 |
| D.3 | Bed shear stress components for a simulation without distinct reef friction field | 88 |
| D.4 | Impact of wave set-up activation on hydrodynamics | 89 |
| D.5 | Bed shear stress components with wave set-up activated in D-Waves | 90 |
| E.1 | Morphological changes in coastal bays for regular wave climate ($H_s = 0.5\text{m}$) | 91 |
| E.2 | Morphological changes in coastal bays for regular wave climate ($H_s = 1\text{m}$) | 92 |
| E.3 | Difference of wave height and bed shear stresses between normal & small wave conditions | 92 |
| E.4 | Wave height difference between long and short waves | 93 |
| E.5 | Simulated diffraction around Île Tintamarre | 93 |
| E.6 | Observed diffraction around Île Tintamarre | 94 |
| E.7 | Sensitivity of morphological changes for different wave periods | 94 |
| E.8 | Sensitivity of morphological changes for different wave directions | 95 |
| E.9 | Sensitivity of morphological changes for different sediment properties | 95 |
| F.1 | Impact of seagrass on flow and water level | 97 |
| F.2 | Impact of seagrass on wave forces | 98 |
| F.3 | Wave propagation and transformation | 98 |
| F.4 | Impact of seagrass on bed shear stresses | 99 |

| | | |
|----|--|-----|
| F5 | Hydrodynamic attenuation during the extreme storm event | 99 |
| F6 | Hydrodynamic sensitivity for the vegetation characteristics (+/-50%) | 100 |

List of Tables

| | | |
|-----|--|----|
| 3.1 | Seasonal variation of the wave height in the eastern part of the Caribbean Sea | 19 |
| 4.1 | Vegetation characteristics of singular seagrass class | 24 |
| 4.2 | Sediment characteristics of the average sediment class | 25 |
| 4.3 | Validation water depth | 28 |
| 4.4 | Validation of wave height | 29 |
| 4.5 | Measurements of critical shear velocities | 31 |
| 4.6 | Environmental conditions of the two base cases | 33 |
| C.1 | Components of constructed astronomic tidal signal | 82 |
| D.1 | Bed shear stress issues | 85 |

1

Introduction

Section 1.1 introduces the broader context of tropical sheltered bays and marine ecosystems. The conceptual design of the research is given in Section 1.2 in which the problem description, research objective, questions, scope, and hypothesis are defined. Lastly, the outline for this thesis is given in Section 1.3.

1.1. Tropical sheltered bays

Coastal bays in the Caribbean accommodate different marine ecosystems, forming an intricate network. These ecosystems affect the hydrodynamic and morphological behavior of coastal bays and hold many interdependencies (Gillis et al., 2014). The tropical marine ecosystems consist of, amongst others, coral reefs and seagrass meadows (Figure 1.1). Reefs provide a sheltering function and the magnitude of the wave dissipation depends on the section of the reef where waves break. Interactions between seagrass and wave action are important in shaping the spatial distribution of seagrass meadows (Van Der Heide et al., 2010). The sheltered conditions behind the reefs form, therefore, suitable habitat for seagrass meadows. (Saunders et al., 2014). Seagrass further attenuates the hydrodynamic energy via the leaf structure and stem density (Gillis et al., 2014). Moreover, seagrass stabilizes sediments and provides a filter mechanism to dissolved nutrients, which are beneficial factors for the reefs to thrive, and the seagrass itself (F. T. Short & Short, 1984).

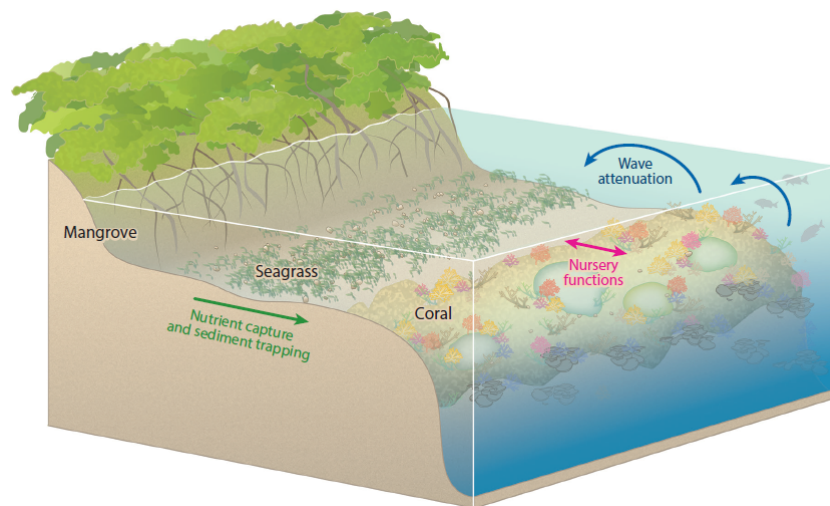


Figure 1.1: Schematic representation of a tropical coastal beach including seagrass meadows and coral reefs including their interdependencies (van de Koppel et al., 2015). Reefs provide a sheltering function for the region behind. Seagrass further attenuates the hydrodynamic energy via the leaf structure and stem density, stabilizes sediments and filters dissolved nutrients.

Marine ecosystems are endangered and belong to the most threatened natural systems around the world (Lotze et al., 2006; Worm et al., 2006). Although the status of seagrass in 2025 may somewhat improve in developed countries due to active protection, the majority of seagrass meadows are found in developing, tropical countries that suffer the most of environmental degradation (Duarte, 2002). Waycott et al. (2009) showed that seagrass across the globe has been disappearing at a rate of $110 \text{ km}^2\text{yr}^{-1}$ since 1980 and the rates of decline accelerated over time. Seagrass could be classified among the most threatened ecosystems on earth and the rates of loss are expected to accelerate in the Caribbean (Waycott et al., 2009; Duarte, 2002). The widespread loss of seagrass results, amongst other causes, from direct human impacts (e.g. coastal development, dredging, overfishing, pollution, and anchoring) and the corresponding lack of awareness and attention on the value of the seagrass ecosystem services (Duarte, 2002; Talbot & Wilkinson, 2001; Unsworth et al., 2019; Dewsbury et al., 2016). Moreover, indirect human impacts through the effects of anthropogenic climate change (e.g. increased coastal erosion, turbidity, storminess, and ultraviolet irradiance) also pose a threat to seagrass (Duarte, 2002). Seagrass meadows have a key role in coastal ecosystems, but despite their alarming rates of loss, they receive little attention compared to other coastal ecosystems (Duarte et al., 2008).

Reefs also suffer from climate change. Global warming and ocean acidification will lead to structural deterioration of the corals (i.e. coral bleaching) and a decline of the coral reef growth rates (Hoegh-Guldberg et al., 2007). Hence, drowning of the reefs under sea-level rise might be a serious danger and might also impact the neighboring seagrass meadows.

Seagrass and reef ecosystems are a valuable part of coastal bays and contribute to human and ecological well-being. These ecosystems provide coastal protection against floods, erosion control, recreational territory, water purification, natural habitat for multiple tropical species and foster the biological productivity and diversity (Barbier et al., 2011). Any threat to these coastal ecosystems should, therefore, be taken seriously otherwise, it could have profound consequences on these marine ecosystems, coastal bays, and coastal communities.

1.2. Conceptual research design

1.2.1. Problem description

Coastal bays could be considered as complex networks formed by many different interdependent (eco)systems. Seagrass meadows provide beneficial ecosystem services but are endangered from extinction. A disturbance or loss of seagrass due to altered conditions could, therefore, have profound effects on neighboring (eco)systems and might even have severe consequences on the entire coastal bay. This could lead to a loss of resilience and a shift to an alternative state of the coastal bay. For instance, seagrass meadows might not keep pace with sea-level rise, leading to a violation of the vertical tolerance limits of the seagrass. Ultimately, this will cause a shift of the seagrass to another state, for instance, a state in which the seagrass dies off (Figure 1.2). Therefore, increased coastal erosion might be expected and could even trigger a positive feedback system. This shift could be reversed if the forcing conditions have been lowered sufficiently, but reversing to the original state might be less straightforward.

The rate at which seagrass meadows are disappearing is reason enough to make the assessment of seagrass ecosystem services in coastal bays an important necessity. In order to obtain a better understanding of the role that seagrass ecosystems provide in coastal bays, the impact of seagrass on the hydrodynamic and morphological behavior could be investigated. In this way, predictions of the development of coastal bays can be provided due to the consequences of future seagrass losses. From a practical point of view, the knowledge of seagrass ecosystem services and of the conditions for which these seagrass impacts are expected to be dominant could be incorporated to enhance the development of appropriate management plans of regional coastal bays.

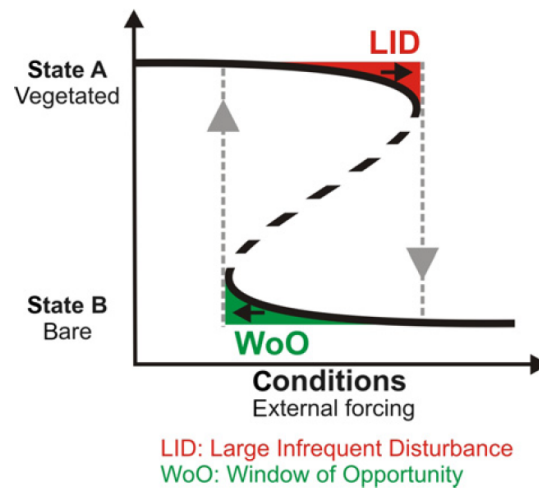


Figure 1.2: Critical transitions in disturbance driven vegetation ecosystems (Balke et al., 2014). For example, a threat to seagrass meadows might be caused by increasing sea levels. Potential acclimation and adaptation to new conditions might be a counterpart to such threats.

1.2.2. Research objective and questions

The main investigation in this thesis is the assessment of the role of seagrass ecosystems on the morphodynamic behavior of tropical, sheltered bays. The research objective has been defined as follows:

To provide a better understanding of seagrass ecosystem services by assessing the impact of seagrass meadows on the morphodynamic behavior of tropical, sheltered bays.

A biogeomorphic model is utilized to perform numerical analysis on the sediment stabilization by seagrass. The considered coastal bays, which are classified as tropical, sheltered bays, are characterized by the presence of barrier reefs and seagrass meadows in the sheltered bays. Two different bays have been investigated, Baie Orientale and Baie de l'Embouchure (St. Martin), which represent a partially exposed and fully sheltered bay, respectively. Both regular wave conditions, as well as extreme storm conditions, have been investigated to understand the consequences of seagrass loss on coastal erosion under different environmental climates.

Tropical, sheltered bays are mainly protected by reefs against the incoming wave energy and coastal erosion. Therefore, the following paradoxical research question has been defined:

Are seagrass meadows in tropical, sheltered bays only functional and effective against coastal erosion where it is not needed?

To answer the main question, the following sub-questions have been defined:

1. Do seagrass ecosystems provide substantial hydrodynamic attenuation?
2. Which vegetation characteristics mainly contribute to the stabilization of sediments?
3. Is sediment stabilization a considerable seagrass ecosystem service under regular wave conditions?
4. Do seagrass meadows significantly increase coastal resilience under extreme storm events?
5. How is the future role of seagrass going to develop under climate change?

1.2.3. Research scope

This research is part of a major project of NIOZ, TUDelft and Utrecht University called SCENES: Stability of Caribbean Ecosystems uNder future Extreme Sea level changes. In order to fulfill the main objective: “to determine the effects of global change on the coastal ecosystems in the Caribbean, a comprehensive multi-disciplinary project is formulated involving analysis of regional ocean observations and global high-resolution ocean modelling (sub-project A), high-resolution biogeomorphological modelling (subproject B) and field work on sediment dynamics, wave climate, temperature and pH dynamics (subproject C)” (NIOZ, 2014). This thesis pays attention to the biogeomorphological modelling of Caribbean coastal bays.

To make the research feasible and the results interpretable, the complexity of the investigation has been reduced in the following way:

- **The ecosystem services** have been simplified to incorporate the core essence of the hydrodynamic attenuation. The seagrass meadows have been included by taking a vegetation roughness into account which affects the hydrodynamic behavior and hence the morphology by stabilizing sediments. The coral reefs have been incorporated as bathymetric structures that dissipate the wave energy by the exerted drag and wave breaking.
- **Existing vegetation formulations** for the roughness and wave energy dissipation have been adopted. This research study does not encompass the derivation of new formulations.
- **The development of the ecosystems** has not been simulated but incorporated by taking different scenarios of the ecosystem presence and coexistence into account.
- **Sea-level rise** has been investigated with scenarios in which an increased water level has been imposed. The continuous adaption of the coastal bays to the rising sea levels could, therefore, not be studied. Other environmental conditions that might vary due to climate change are not adapted. Possible degradation of the seagrass meadows as a consequence of the new environmental conditions has been considered, whilst new opportunities for habitat extension have not been considered.

1.2.4. Research hypothesis

The vegetation roughness and dissipation of wave energy are found to be highly influenced by the ratio between the vegetation height and water depth (M. S. Fonseca & Fisher, 1986; M. S. Fonseca & Cahalan, 1992). Therefore, the seagrass meadows are expected to be effective in providing hydrodynamic attenuation and sediment stabilization in shallow regions in the foreshore. Whereas, the impact of the seagrass is expected to be less significant in deeper regions of the bays.

Reefs are able to dissipate the wave energy to a large extent (Ferrario et al., 2014). The morphological activity is, therefore, not expected to be enormous in the sheltered regions of both bays under moderate wave conditions. The seagrass impact on sediment stabilization might not be noticeable under these smaller wave conditions and might be more prominent under higher and extreme wave conditions.

The climate is a complex system with many variables and interdependencies. These complexities increase the uncertainty to predict outcomes of sea-level rise rates (IPCC, 2014) and the corresponding responses of coastal bays. It can be expected that the increased water levels and potential drowning of coral reefs (Hoegh-Guldberg et al., 2007) will lead to more wave energy that will propagate inside the sheltered bays which increases the coastal erosion. At the same time, the sediment stabilization by seagrass is expected to decrease due to the increased water levels. Dependent on the significance of the sediment stabilization by seagrass, the coast will either conduct resiliently or will be directed towards a new equilibrium state. If the seagrass does not function effectively or if the coastal erosion is too large, a shift of the coastal state is likely to be triggered in which it is expected that the shores will regress.

1.3. Thesis outline

Chapter 1 provides an introduction of tropical, sheltered bays and the accommodated marine ecosystems. Furthermore, the social and scientific relevance for developing a better understanding of the role of seagrass ecosystems in coastal bays is indicated. Besides, the conceptual research design is given in which the problem description and research objective, questions, scope, and hypothesis are stated. Background information of this research, based on the performed literature research, is given Chapter 2. This includes the description of the coastal behavior, marine ecosystems, and the impact of climate change on tropical coastal bays. Chapter 3 provides background information about Saint Martin and the investigated coastal bays: Baie Orientale and Baie de l'Embouchure. The technical design of the research is given in Chapter 4. It gives a description of the research approach and model setup to obtain answers to the posed research questions. Thereafter, the simulated morphodynamic behavior of the coastal bays, in the presence of seagrass, is described in Chapter 5. The results of the impact of seagrass on the morphodynamic behavior are presented in Chapter 6. The discussion about the results and performed research can be subsequently found in Chapter 7. Finally, the conclusions and recommendations are stated in Chapter 8.

2

Background information

This chapter provides background information on tropical sheltered bays. In section 2.1 the hydrodynamic and morphological behavior of coastal bays is treated. The seagrass and reef ecosystems are described in section 2.2. Finally, the impacts of climate change on tropical coastal bays are highlighted in section 2.3.

2.1. Coastal behavior

Coastal areas are transition zones between ocean and land. The coastal profile can be separated into an offshore zone and the shoreface (Figure 2.1). The shoreface zone starts with the shoaling zone where the waves are influenced by the bottom. Ultimately, in the surf/littoral zone, the waves start to break and their energy is dissipated. The shoreface zone is very dynamic on various spatial and temporal scales. The morphological and hydrodynamic behavior continuously and mutually adapt to each other to reach a morphodynamic equilibrium (Bosboom & Stive, 2015, P.16-22). Morphological changes occur if sediment transport gradients exist. As long as there are no gradients there will be no net changes, even though the transport is non-zero (Bosboom & Stive, 2015, P.9).

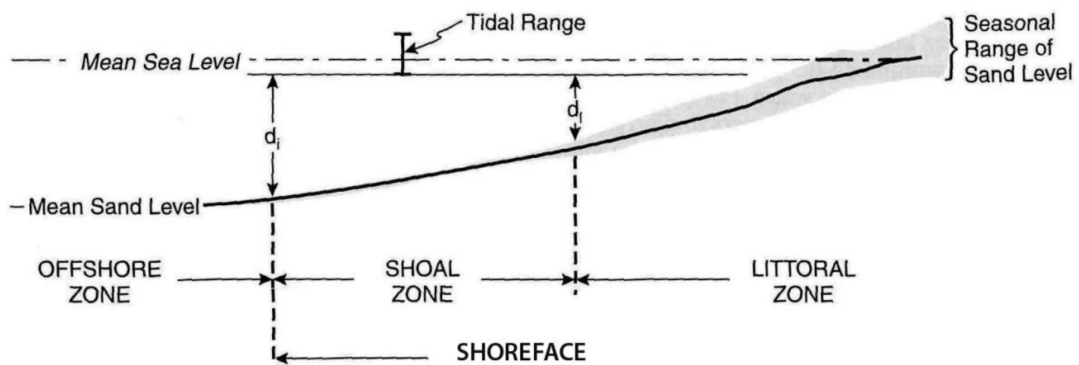


Figure 2.1: Schematization of a coastal profile. Different zone can be distinguished: an offshore zone, shoaling zone and surf/littoral zone (Bosboom & Stive, 2015, P.17). In the shoaling zone, the waves start to be influenced by the bottom. Initially, the wave height slightly decreases and thereafter the depth-induced energy bunching of the waves starts. The wave increases until the waves start to break in the surf/littoral zone.

2.1.1. Hydrodynamic behavior of coastal bays

Coral reefs substantially influence the hydrodynamic behavior by the altered bathymetry and rugosity. Wave breaking is dominant on top of the reefs and initiates a circulation flow beyond the reefs (Lowe et al., 2009). The reef structures can be seen as natural, submerged breakwaters in which depth-induced wave breaking increases from the forereef towards the reef flat. This results in an increase in the water level due to the wave-induced setup (Figure 2.2). The spatial differences in water level result in a pressure gradient which initiates a flow across the reef towards the shore. Ultimately, the water can not pile up at the shore and hence continuity requires a return flow towards the ocean. This return flow is concentrated in one or multiple channels.

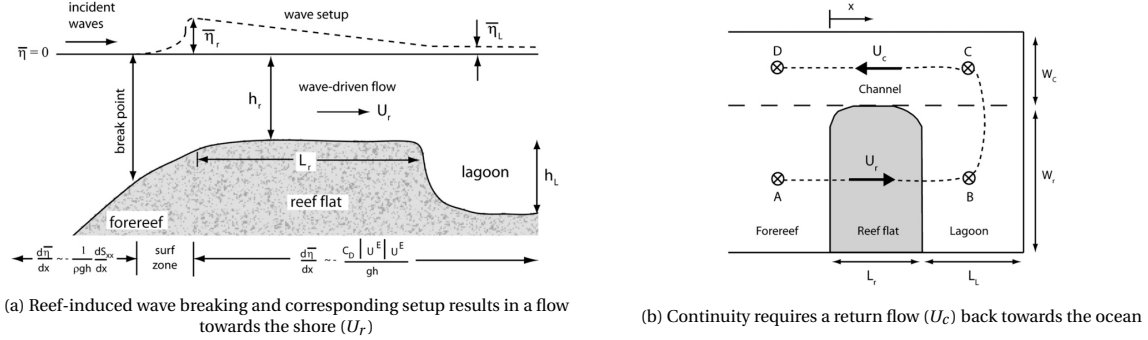


Figure 2.2: Schematization of wave-driven circulation in reef environments characterized by a sloping forereef, shallow reef flat, relatively deep lagoon and a channel (Lowe et al., 2009).

The flow-induced and wave-induced currents cause shear stresses that act on the bed. For a more detailed description of the wave-induced and flow-induced bed shear stresses, one is referred to Appendix A.1. The bed shear stress caused by flow-induced currents can be characterized by a quadratic friction law:

$$\tau_b = \rho_w c_f |U|U \quad (2.1)$$

where ρ_w is the density of water, c_f represents a dimensionless friction factor, and U is the depth-averaged flow velocity (Bosboom & Stive, 2015, P.184).

In analogy with the formulation of flow-induced bed shear stress and the friction factor, a similar formulation for wave-induced bed shear stress has been derived:

$$\hat{\tau}_w = 0.5 \rho_w f_w |\hat{u}_0| \hat{u}_0 \quad (2.2)$$

in which f_w represents a dimensionless friction factor and u_0 is the amplitude of the wave-induced, oscillatory currents (Bosboom & Stive, 2015, P.183).

The combined total bed shear stress has a non-linear character and is generally larger than the linear superposition of the wave-induced and flow-induced bed shear stress components (Figure 2.3). Furthermore, the waves and currents generally have different directions. Therefore, both the magnitude and direction of the bed shear stress vary continuously during a wave cycle (Bosboom & Stive, 2015, P.209-210). The non-linear enhancement decreases when the relative wave-flow angle increases from 0° (parallel) to 90° (perpendicular). It is important to distinguish between the wave-averaged bed shear stress and the maximum bed shear stress regarding sediment transport. The maximum bed shear stress during a wave cycle determines the threshold of the initiation of motion and entrainment of sediment particles. And the transport of sediment particles is determined by the wave-averaged bed shear stress (Soulsby et al., 1993).

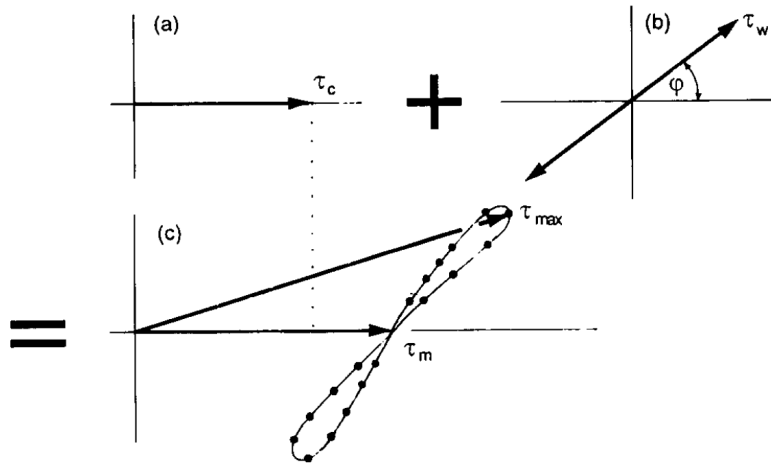


Figure 2.3: Non-linear interaction between the wave-induced (τ_w) and flow-induced (τ_c) bed shear stress (Soulsby et al., 1993). The wave-period averaged mean (τ_m) and maximum bed shear stress (τ_{max}) are generally larger than the individual components. The angle between the wave- and flow-induced bed shear stresses is indicated by ϕ .

2.1.2. Shear resistance by vegetation

Vegetation exerts a certain shear on the flow and reduces the flow velocity. Moreover, vegetation alters the velocity profile (Figure 2.4). Four distinct zones can be distinguished. The first zone is located close to the bed in which the velocity is highly influenced by the bed. The distribution of the velocity in this zone is described by a logarithmic boundary layer profile. The second zone is located inside the vegetation, in which the velocity can be considered uniform. The third zone is a transitional zone from the uniform flow to the logarithmic profile, which can be found in the fourth zone above the vegetation (Baptist et al., 2007).

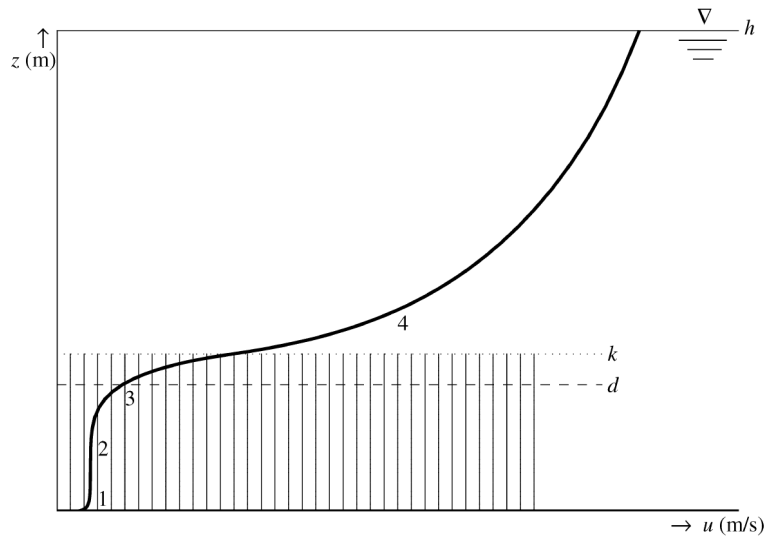


Figure 2.4: Velocity profile $u(z)$ in presence of vegetation (Baptist et al., 2007). The flow velocity inside the vegetation height (k) can be considered uniform, except for the boundary layers. Above the vegetation a logarithmic profile can be observed, which has a zero-place displacement boundary condition just inside the vegetation at level d .

The uniform flow velocity inside the vegetation layer has been derived by Baptist et al. (2007) and follows from the momentum balance for flow through vegetation:

$$u_c = \sqrt{\frac{hi}{\frac{1}{C_b^2} + \frac{C_d m D h_v}{2g}}} \quad (2.3)$$

where C_b represents the alluvial bed roughness, i is the hydraulic gradient, n m is the number of stems per square meter, D is the stem diameter, h_v the vegetation height, and C_D the vegetation drag coefficient..

The logarithmic velocity profile above the vegetation is given as (Baptist et al., 2007):

$$u_u(z) = \frac{u_*}{\kappa} \ln\left(\frac{z - h_v}{z_0}\right) + u_c \quad (2.4)$$

Baptist et al. (2007) developed a formulation for the (Chézy) roughness which includes the resistance exerted by the vegetation and is based on a dimensionally aware approach:

$$C = \sqrt{\frac{1}{\frac{1}{C_b^2} + \frac{C_d m D h_v}{2g}} + \frac{\sqrt{g}}{\kappa} \ln\left(\frac{h}{h_v}\right)} \quad (2.5)$$

where κ is the Von Kármán constant. This vegetation resistance formulation takes the combined contributions of both flows in the vegetation layer and in the free layer above the vegetation into account. The formulation has been developed with the use of results of a 1DV numerical model and is validated with various cases with different vegetation characteristics, types and water depths. This formulation yields the best fit with data from laboratory flume experiments in comparison to two alternative analytical expressions.

2.1.3. Wave dissipation by vegetation

Vegetation also attenuate wave energy and is most effective for relatively shallow waters (Koch et al., 2006). The vegetation can be characterized as rigid cylinders that exert a certain drag force on the waves as derived by Dalrymple et al. (1984). The wave attenuation depends on the geometric and physical characteristics of the vegetation field (Mendez & Losada, 2004). Assuming that the linear wave theory does hold and considering a constant depth with normal incident, regular waves, the conservation of wave energy is given as:

$$\frac{\partial E c_g}{\partial x} = -\epsilon_D \quad (2.6)$$

in which $E = \frac{1}{8} \rho g H^2$ is the wave energy per unit area and H the wave height. The wave group celerity $c_g = n c$, with $n = \frac{1}{2} \left(1 + \frac{2kh}{\sinh(2kh)}\right)$ and the individual wave celerity $c = \frac{gT}{2\pi} \tanh\left(\frac{2\pi h}{L}\right)$. $k = \frac{2\pi}{L}$ represents the wave number, L the wave length and h the water depth. The depth-averaged energy dissipation ϵ_D caused by the vegetation drag force (F_D) over the vegetation height is expressed as:

$$\epsilon_D = \int_h^{h+h_v} F_D u dz \quad (2.7)$$

$$F_D = \frac{1}{2} \rho C_D A u |u| \quad (2.8)$$

where $A = b_v N$ the projected vegetation area per volume, b_v represents the plant area per unit height, and N the number of shoots per unit bottom area. The average bulk drag coefficient C_D serves as a calibration parameter to represent the total drag force of a vegetation field.

2.1.4. Morphological behavior of coastal bays

Reciprocal interactions lead to a coastal bay that continuously is directing towards a morphodynamic equilibrium. Coastal protection is an important service provided by the shore. As waves propagate towards the shore, the beach slope induces breaking of the waves and dissipates wave energy (Holthuijsen, 2010, P.242-243). The shore is also affected by the hydrodynamic forces and shows natural variety.

The sediment morphology in a coastal bay is of dynamic nature with spatial and temporal variations. The sediment budget in a coastal system depends on the supply and demand of sediment and determines whether the coastal system will erode or accrete. Wright and Short (1984) classified beaches into a spectrum of six different states. The highest state is the dissipative beach and the lowest state is the reflective beach. Dissipative beaches are characterized by a wide and flat sandy shoreface with possible bars and dunes. The flat beach slope results from high wave energy which dissipates gradually towards the shoreline. The dissipative beach states are linked to storm wave climates and are highly variable. Reflective beaches have a relatively steep and narrow shoreface with a berm at the shore. Often the steep beach slopes consist of relatively coarse sand particles. Reflective beaches result from mild wave conditions and are therefore often found in swell wave climates. Due to the low variability of these wave climates, the morphodynamic behavior is also less dynamic compared to dissipative beaches (Bosboom & Stive, 2015, 316-320).

The morphology of coastal systems is directly influenced by the hydrodynamic forces and vice versa. Therefore, disturbances in the hydrodynamic or morphological conditions will force a disequilibrium. This will lead to an adaptation of the morphodynamics such that a new equilibrium state is reached. However, when the changes in environmental conditions happen at a rapid rate and the sediment budget of a coastal system is distorted, the coastal protection offered by sand shores might be compromised (Ruggiero et al., 2010).

The transport of sediment can be separated into bed-load and suspended-load transport. Bed-load transport is located in a thin layer close to the bed and takes place under low shear stresses. When shear stresses increase, the likelihood of a turbulent flow character and suspension of sediment is larger and suspended-load transport takes place. The mechanisms that cause the transport modes are quite different and therefore separate transport formulations are used to describe the sediment transport modes (Bosboom & Stive, 2015, P.267-272). A more detailed description of the transport mechanisms is given in Appendix A.2.

2.2. Ecosystems

2.2.1. Seagrass meadows

Seagrass meadows are flowering plants (*angiosperms*) found in marine areas. A schematization of the anatomy of seagrass is shown in Figure 2.6. Seagrass settle in shallow, marine habitats on soft substrates and are encountered across the world (Figure 2.5). In tropical regions, seagrass meadows generally show minor variability throughout the seasons and develop highly productive ecosystems (Duarte, 2002; Barbier et al., 2011).

All seagrass species are rhizomatous, clonal plants in which the reiteration of the shoots results in habitat extension. The elongation of the leaves and rhizomes leads to the vertical growth (M. A. Hemminga & Duarte, 2000, P.27 & 52). The seagrass meadows are generally located between water depth of 0 and up to 30m (Duarte, 2002). According to Koch et al. (2007) as cited in Barbier et al. (2011) seagrass meadows favor sheltered conditions and often are located alongside coral reefs (Dutch Caribbean Nature Alliance, n.d.-b).

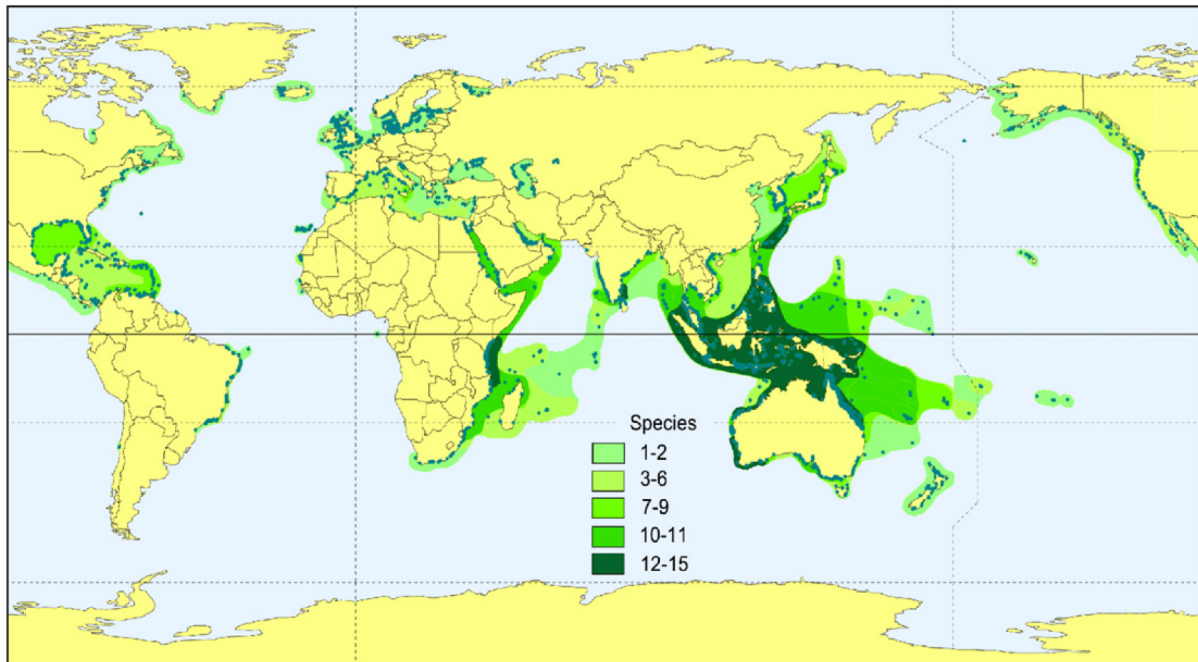


Figure 2.5: Global seagrass distribution (F. Short et al., 2007).

Seagrass meadows require light for their photosynthetic activity and are, therefore, affected by disturbances in water quality and light conditions. Seagrass species grow less efficiently under decreased light conditions and reduced productivity has been observed for *T. testudinum* (Tomasko & Dawes, 1990) and *H. wrightii* (Dunton, 1994). The downslope depth limit is determined by the light intensity requirement of $\sim 11\%$ of the surface light (Duarte, 1991). The upslope depth limit is determined by the requirement for sufficient immersion and tolerable hydrodynamic conditions (M. A. Hemminga & Duarte, 2000, P.16). The dynamic character of morphological changes also influences the habitat of seagrass meadows. The sporadic character of these disturbances are reflected on the meadows and also have dynamic behavior (Fourqurean & Robblee, 1999; Duarte, 2002).

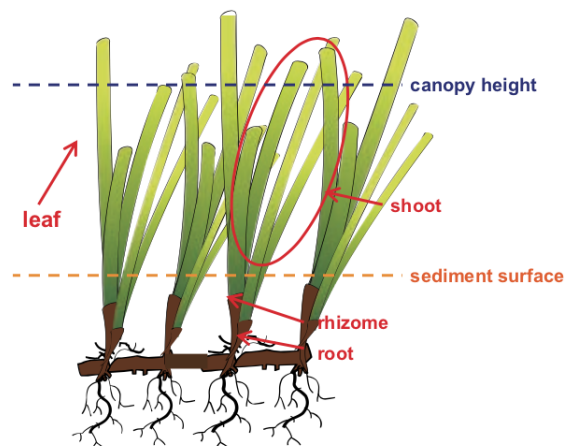


Figure 2.6: Schematization of anatomy of seagrass meadows and nomenclature to describe different parts of seagrass. Note that the canopy height is usually obtained by averaging the tallest two-thirds of the leaves (Koch et al., 2006).

Seagrass meadows are considered to belong to the most valuable ecosystems of the biosphere (Costanza et al., 1997; Barbier et al., 2011). Seagrass meadows are able to attenuate flows and wave energy. The attenuation is highest in shallow waters or for plants with large vegetation heights. Seagrass also stabilize sediments and stimulate soil retention in the vegetation roots. Therefore, seagrass ecosystems contribute to erosion control and coastal protection (M. Hemminga & Nieuwenhuize, 1990; Barbier et al., 2011).

Besides the coastal protection, seagrass provide several ecological ecosystem services. For instance, seagrass purifies the water by filtering dissolved nutrients and stabilizing sediments (F. T. Short & Short, 1984; Gacia et al., 1999). Moreover, seagrass ecosystems provide oxygenation of seawater by their photosynthetic activity, a buffer of carbon dioxide (15% of the oceanic carbon storage) by means of carbon sequestration, and accommodation for benthic life (Barbier et al., 2011; Duarte & Chiscano, 1999; F. T. Short & Neckles, 1999). Seagrass also conserve the pH level which might enhance the coral reef resilience to future ocean acidification (Unsworth et al., 2012).

2.2.2. Coral reefs

Coral reefs are complex structural habitats formed by limestone and can be found in tropical coastal waters. Reefs are made out of individual corals (*sedentary cnidarians*) and accrete calcium carbonate. Corals feed on zooplankton and maintain a mutualistic symbiosis with algae (photosynthetic dinoflagellates). Furthermore, coralline algae stabilize and cement coral reef structures (Barbier et al., 2011). Coral reefs require a hard substrate as a base in contrast to seagrass meadows. Moreover, corals require warm and clear water with sufficient sunlight irradiance. The corals are negatively affected by excessive sediment concentrations. The fastest growth rate of branching corals is 10 cm per year, where other corals grow at much slower paces (order of few millimeters for several years) (Dutch Caribbean Nature Alliance, n.d.-a).

Several types of reefs can be distinguished (Figure 2.7). Reefs that are closely attached to the coastline, are called fringing reefs. When the reef is separated from the coastline by a lagoon or open water it is called a barrier reef. Lastly, coral reef atolls are reefs that are shaped in a ring surrounding open water or land (Elliff & Silva, 2017; Dutch Caribbean Nature Alliance, n.d.-a).

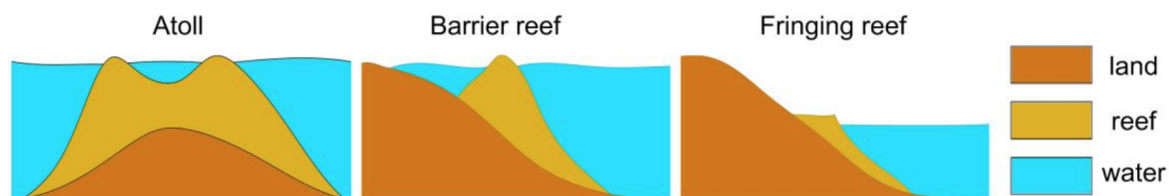


Figure 2.7: Schematization of coral reef types (Bosboom & Stive, 2015, P66). Atolls are shaped in a ring and surround open water or land. Barrier reefs are separated from the coastline by a lagoon or open water. Fringing reef are closely attached to the coastline.

Coral reefs provide coastal protection from (extreme) wave conditions (Figure 2.8). This allows other coastal ecosystems (e.g. seagrass meadows) to develop under desired, milder conditions. (Barbier et al., 2011). The hydrodynamic environment is altered by means of wave attenuation and reducing the currents. The wave energy is dissipated by means of depth-induced breaking on the forereef and reef crests and by bottom friction on the reef flat due to the rugosity of the reef. According to Ferrario et al. (2014) coral reefs are able to attenuate 97% of the wave energy (globally averaged). However, it has been shown that coral mortality and deterioration reduces the sheltering function provided by reefs (Sheppard et al., 2005).

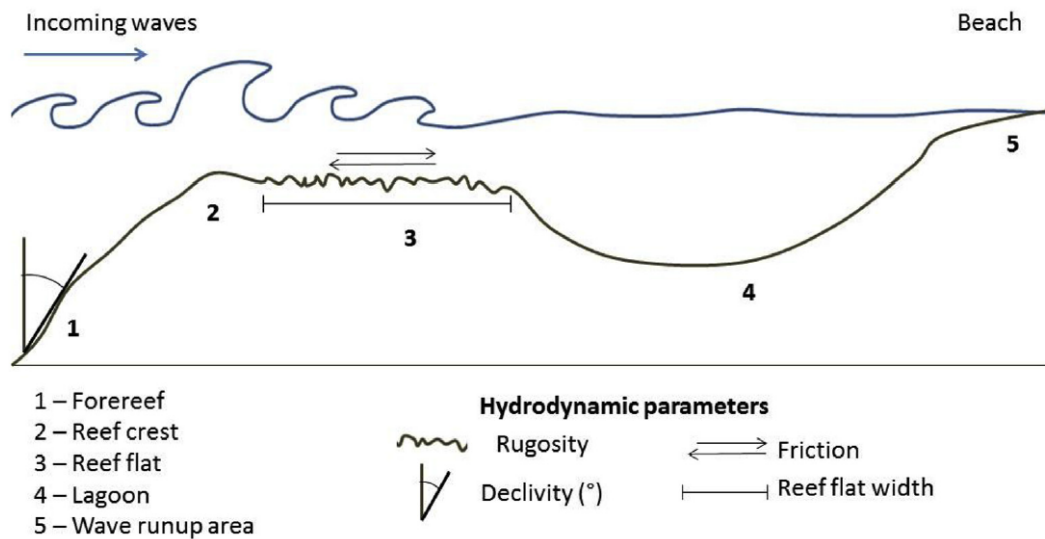


Figure 2.8: Different zones of a barrier reef and the parameters that influence the wave attenuation (Elliff & Silva, 2017). One of the important ecosystem services coral reefs provide is coastal protection from (extreme) wave conditions and therefore could be seen as natural variants of submerged breakwaters.

2.3. Climate change

The atmospheric concentration of carbon dioxide is increasing and predictions indicate significant changes in climate behavior (Cox et al., 2000). The consequences of climate change are considered to become unacceptably dangerous when global warming surpasses the 2°C threshold (above the preindustrial temperature). The climate is a complex system with many variables and, therefore, it remains difficult to predict precise outcomes of climate change on the environmental conditions. Climate change causes coastal bays and marine ecosystems to be under pressure and it is uncertain how the coastal bays will be affected. A schematic overview of climate change effects that might impact coastal bays and marine ecosystems are shown in Figure 2.9.

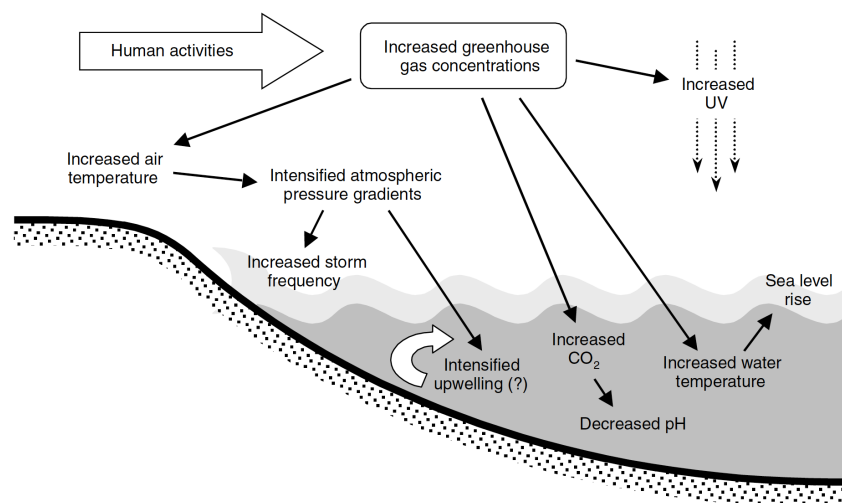


Figure 2.9: Overview of potential impacts of climate change in coastal bays (Harley et al., 2006).

2.3.1. Extreme storm events

In September 2017, Hurricane Irma (Category 5) destroyed 95% of the buildings on the French side of Saint Martin, impacting more than 36,000 inhabitants and left a devastating impact on the economy of Saint Martin (damage estimated at 3 billion euros) (Central Intelligence Agency [US], 2018; Rosaz & Azzar, 2018). Such extreme disturbances might have severe impacts on coastal bays and the marine ecosystems (Preen et al., 1995).

The Nature Foundation St. Maarten (NFSXM) found that seagrass meadows and coral reefs around St. Martin have been damaged during Irma (Dutch Caribbean Nature Alliance, 2017). Although, minor to no long-term permanent effects of hurricanes on well-developed Caribbean seagrass communities have been recorded Van Tussenbroek et al. (2014). These ecosystems can recover themselves if the frequency of these episodic events is small enough and sufficient time is provided. However, climate change might reinforce hurricanes and increase the frequency of these rare events.

2.3.2. Sea-level rise

Sea-level rise forms a threat to low-lying coastal areas (Nurse et al., 2014; IPCC, 2014) and also to seagrass ecosystems (Orth et al., 2006). The sea level rises as a consequence of the thermal expansion of the oceanic waters and the direct and indirect effects of melting ice caps (i.e. extra fluid water volume & Glacial Isostatic Adjustment: the elastic response of the Earth's mantle to redistribution of mass and gravitational effects).

Global sea levels have increased throughout the 20th century and are expected to accelerate through the 21st century (Nicholls & Cazenave, 2010). However, the pace remains uncertain. Important contributors to this uncertainty are prospective roles of the Greenland and West Antarctic ice sheets and the sea-level changes on a regional scale (Nicholls & Cazenave, 2010). Different scenarios of the emission of greenhouse gasses (GHG) are taken into account in predictions of sea-level rise (Figure 2.10).

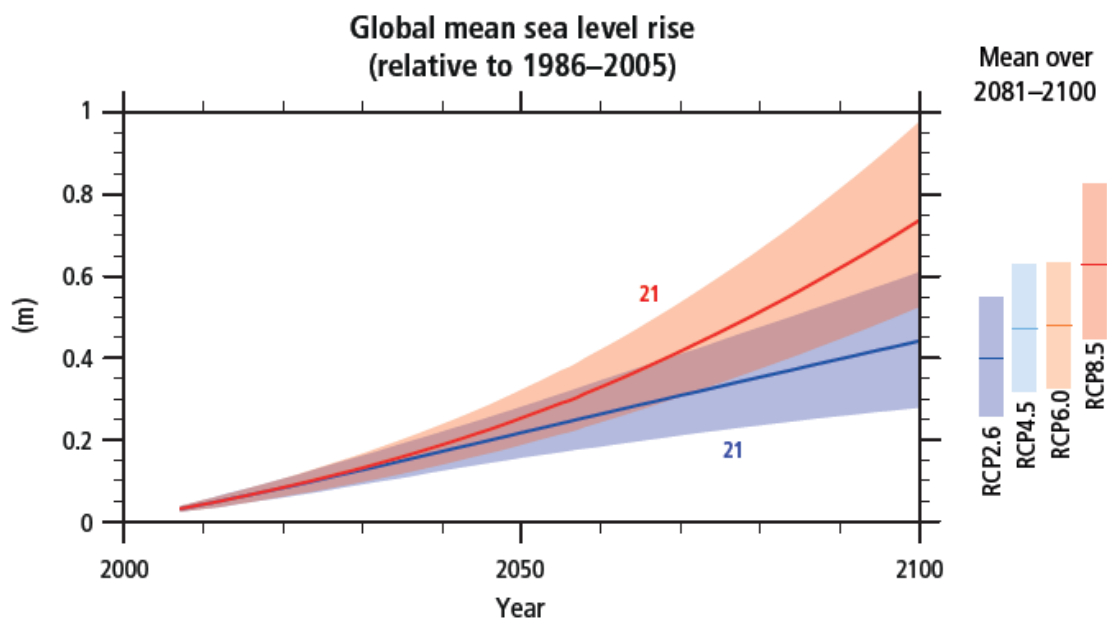


Figure 2.10: Projections of globally averaged sea-level rise. The mean sea-level projections (solid lines) and uncertainties (shaded area) are shown for RCP2.6 and RCP8.5. Furthermore, the mean sea-level rise and associated uncertainties averaged over 2081–2100 for all four GHG emission scenarios are indicated by the different colored bars (IPCC, 2014).

The rate of the sea-level rise by the year 2100 will be larger than any time during human civilization (Jevrejeva et al., 2016). This will lead to a very limited transition time for vulnerable tropical coastal ecosystems to adapt to the increased sea levels. The global sea-level rise for 2081-2100, will likely be in the ranges of 0.26-0.55m under RCP2.6 and 0.45-0.82m under RCP8.5 (IPCC, 2014). The sea levels do not rise uniformly, but rather vary across the globe as shown in Figure 2.11 (IPCC, 2014). Estimates for global sea-level rise do not provide sufficient detail since coastal areas are also affected by regional and local influences. The local sea level trends are, therefore, of importance for coastal areas (NIOZ, 2014).

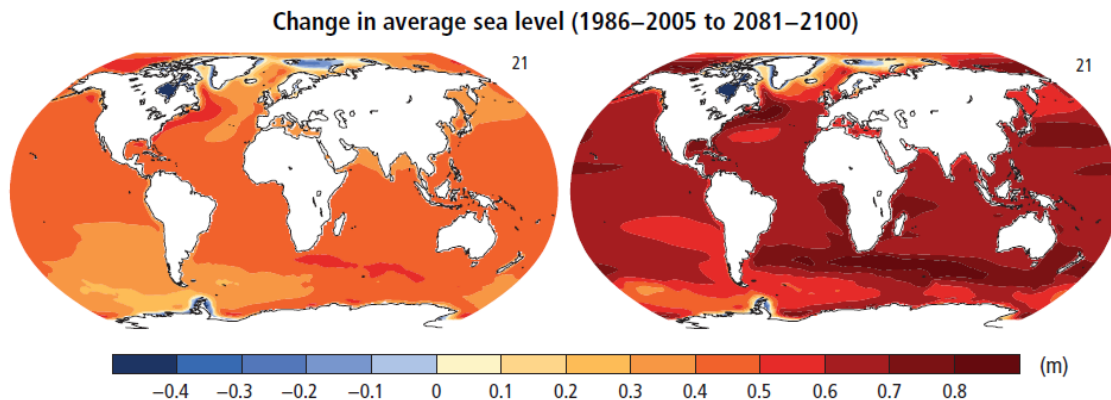


Figure 2.11: Regional sea level rise for RCP2.6 (left) and RCP8.5 (right) for the period 2081-2100 relative to the period 1986-2005 (IPCC, 2014).

2.3.3. Vulnerability reefs

According to Hoegh-Guldberg (1999), the temperature of oceanic waters is increasing at a rate of $\sim 1 - 2^{\circ}\text{C}$ per century. Whilst, corals and their photosynthetic symbionts (zooxanthellae) already live close to the upper thermal tolerance condition (Hoegh-Guldberg, 1999). The increase of oceanic temperatures and ocean acidification are considered to be among the most relevant effects of climate change that will impact coral reefs (Ateweberhan et al., 2013).

Thermal-induced coral bleaching occurs when the symbiotic algae abandon the corals due to the increased temperatures. Although bleaching events are reversible, the corals are left physiologically compromised (Wild et al., 2011). Ocean acidification reduces the coral calcification capacity and hence the formation of coral skeleton (Pandolfi et al., 2011).

Higher frequency of coral bleaching events is expected and the adaptation time might be limited for the reefs to overcome these events (Hoegh-Guldberg, 1999). Global warming and ocean acidification will compromise the reproduction of coral reef and will lead to smoother reef flats (Quataert et al., 2015). Eventually, this will increase the mortality of coral reefs and the former coral space can be inhabited with non-reef-building organisms (Hoegh-Guldberg et al., 2007; Elliff & Silva, 2017).

Sea-level rise and its pace are also important effects that impact the development of coral reefs (Saunders et al., 2016). Numerical simulations for coral reef development Graus and Macintyre (1998) demonstrated that Caribbean coral reefs will most likely not be able to keep up with future sea-level rise for the scenario defined by Hoffman et al. (1983). The drowning of the coral reefs might, therefore, be a serious danger and is enhanced due to structural deterioration of coral reefs.

3

Case study area

In this chapter, the Caribbean island of St. Martin and coastal bays of interest have been mapped out based on the work of the Association de Gestion de la réserve Naturelle Nationale de SAINT MARTIN (AGRNSM, 2009b).

3.1. Introduction St. Martin

Saint Martin is a tropical island in the Caribbean and is part of the Leeward Islands (northern) subgroup of the Lesser Antilles Island group (Figure 3.1). The economy of Saint Martin predominantly depends on the tourism industry, where 85% of the labor force is directly or indirectly involved in this sector (Central Intelligence Agency [US], 2018). Saint Martin has many bays and two examples of adjacent bays are Baie Orientale and Baie de l’Embouchure (Figure 3.1 & 3.2), located at the east coast of the French part of Saint Martin. Coral reefs and seagrass meadows are present in these coastal bays and are part of a protected nature reserve.

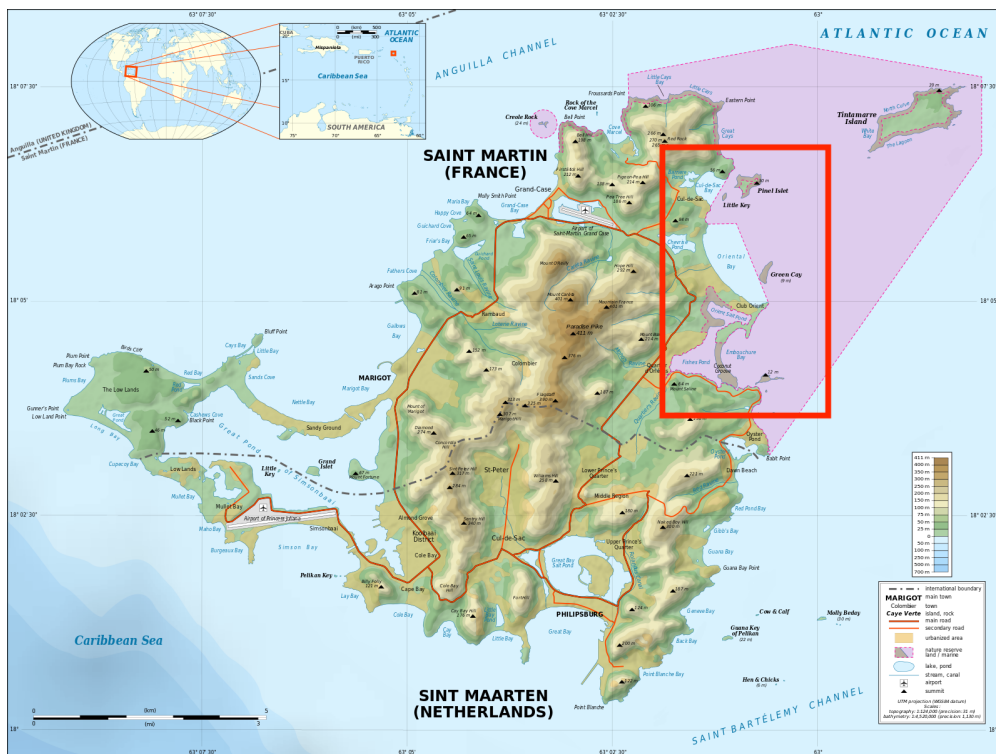


Figure 3.1: Topographic map of Saint Martin adapted from Gaba (2015). Baie Orientale and Baie de l’Embouchure are indicated in red rectangle. The purple area indicates the protected nature reserve.

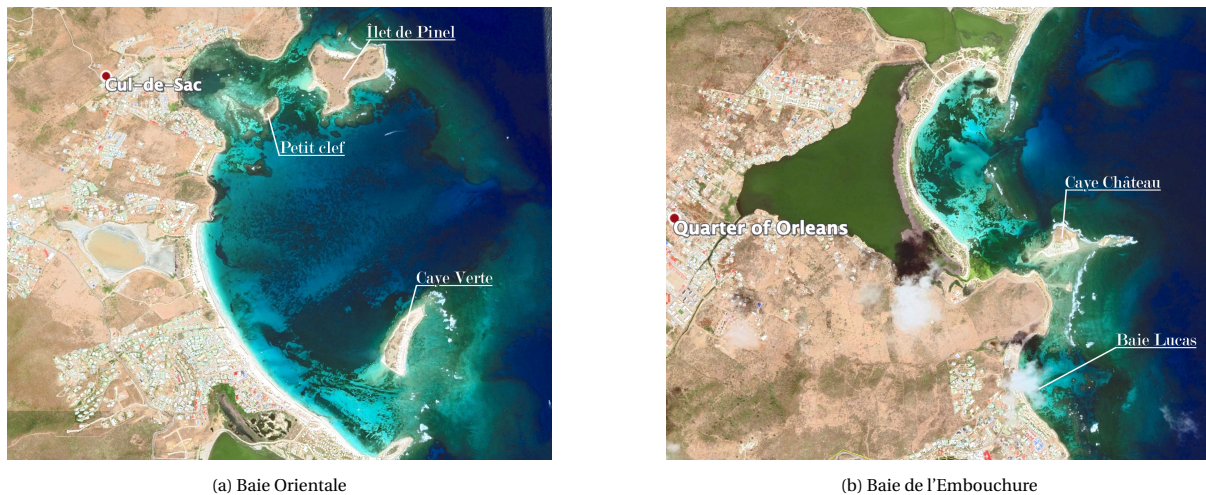


Figure 3.2: Baie Orientale and Baie de l'Embouchure with indicated characteristic spots. Adapted from (Google Maps, 2019).

3.2. Environmental climate

The climate of Saint Martin is driven by the atmospheric circulation of high pressure (Hadley) cells of the North Atlantic (Pietrzak, 2017). This results in a year-round hot and humid climate with variable (trade) winds (Figure 3.3). Strong trade winds are recorded in the northern Caribbean islands from December to March, weakened in April and May, and reinforce again in June and July.

Saint Martin is also subjected to tropical hurricanes. Hurricanes are extreme storm events that are characterized by strong winds, waves, and heavy rainfall. A fundamental condition for hurricanes to form is a sufficient ocean temperature (minimum 26° Celsius at 60 m water depth). In the North Atlantic Ocean, these conditions are met from August to November which could initiate or intensify a hurricane.

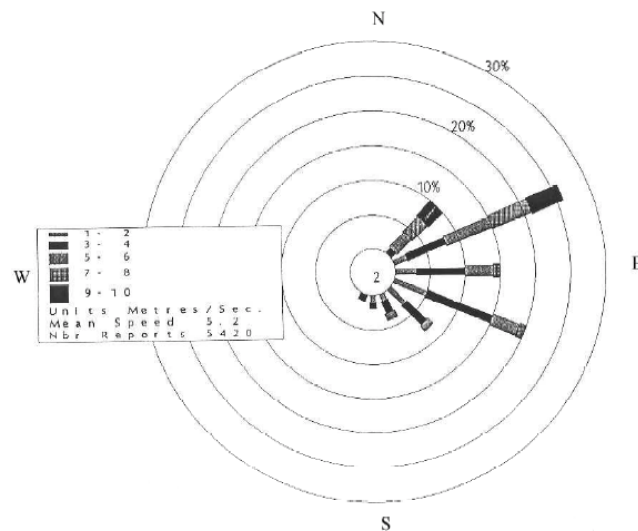


Figure 3.3: Wind rose of annually-averaged recorded winds in Gustavia, Saint Barthelemy (nearby Saint Martin). The mean wind speed is 5.2 m/s. From (Meteo France, 1977-1999) as cited in AGRNSM (2009b).

3.3. Hydrodynamic conditions

The tidal environment can be classified by the tidal range and the tidal character. The tides are generally low in the northern Caribbean islands with a tidal range of approximately 0.2 m for an average spring tide. The tidal character can be characterized as a mainly diurnal mixed tide. The generated tidal currents are generally weak and most of the time the wave-induced currents are more dominant.

The waves in Saint Martin can be characterized as swell waves that are generated from the trade winds in the Atlantic Ocean. The wave directions are similar to the wind directions and range from the northeast to the southeast sectors. The wave height typically ranges between 1 and 2.5 m.

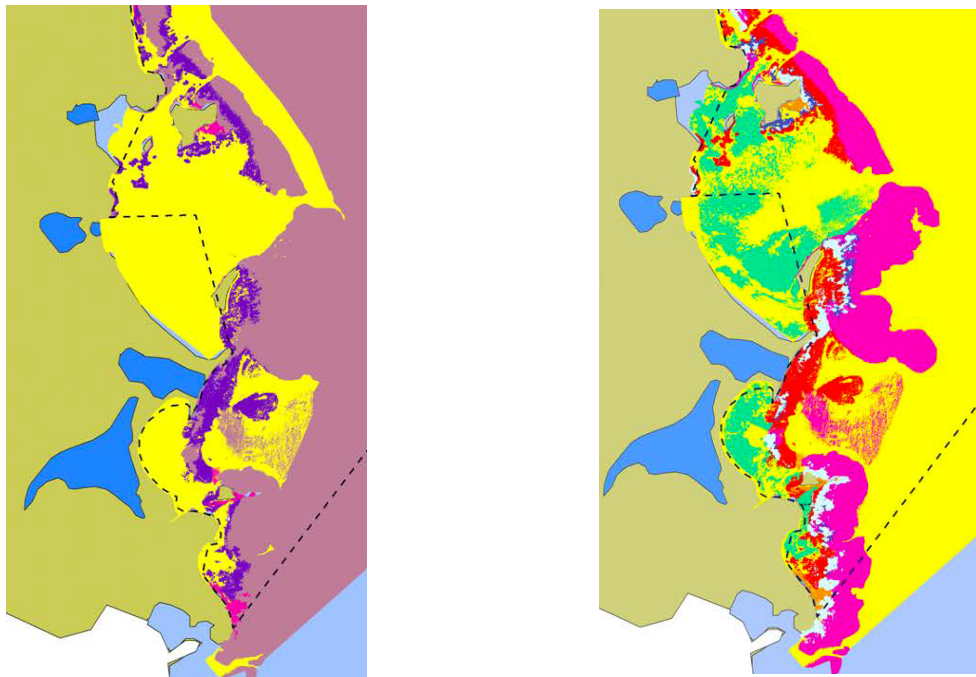
| Wave height [m] | January | April | July | October |
|-----------------|---------|-------|------|---------|
| < 1.5 | 68% | 78% | 66% | 88% |
| 1.5 - 3.0 | 26% | 19% | 29% | 11% |
| 3.0 - 4.0 | 5% | 2% | 4% | 1% |
| > 4.0 | 1% | 1% | 1% | 0% |

Table 3.1: Seasonal variation of the wave height in the eastern part of the Caribbean Sea. From (SAFEGE Guadeloupe, 2005) as cited in AGRNSM (2009b).

The sea surface temperature ranges between 25° and 29° Celsius and results generally in a homogeneous distribution without significant stratification patterns between the surface and bottom. The (surface) salinity is also homogeneously distributed and equals approximately 35‰.

3.4. Geomorphological conditions

Saint Martin emerges from the central part of a submarine shelf forming an archipelago. The bed near the coast consists of a rocky platform covered with a thick layer of sand (Figure 3.4a). The sand is predominately calcareous and organic sediment. This sediment either originates from physical erosion of coral reefs or is produced by calcifying macro-algae e.g. *Halimeda Opuntia* (AGRNSM, 2009b). The sediment is typically less dense compared to regular Quartz sand (P. M. J. Herman, personal communication, July 5, 2019). The grain sizes of the sediment have been measured by James (2015) and show a variety of sediment classes (Figure 3.5).



(a) Bed substrates of Baie Orientale and Baie de l'Embouchure (sediment in yellow and rocky platforms in lila) (b) Marine ecosystems of Baie Orientale and Baie de l'Embouchure (seagrass meadows in green and Coral reefs in red)

Figure 3.4: Bed substrates and marine ecosystems in Saint Martin bays (AGRNSM, 2009a).

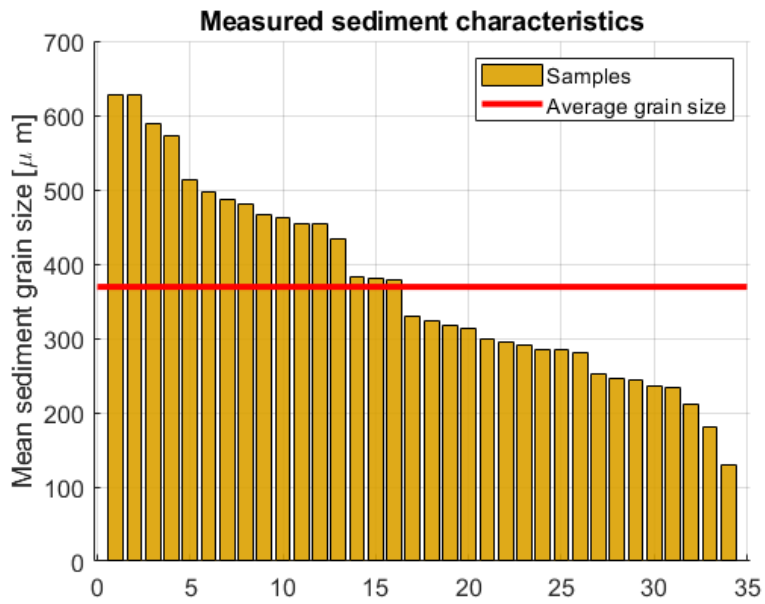
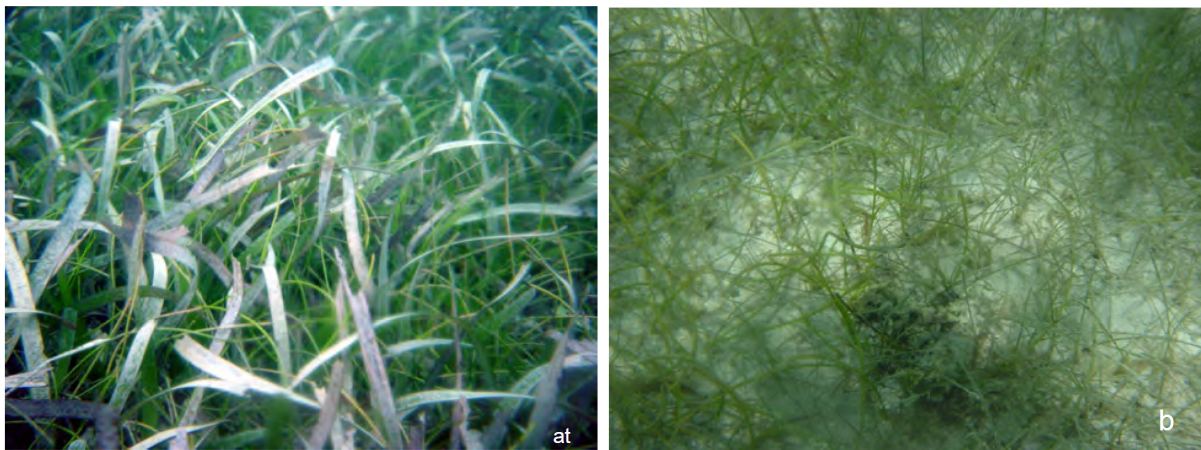


Figure 3.5: Mean sediment mean grain size measurements show a variety of sediment classes.

3.5. Presence of ecosystems

The coasts of both Baie Orientale and Baie de l'Embouchure accommodate seagrass meadows in the vicinity of the sandy beaches (Figure 3.4b). The seagrass meadows are present in the sheltered bays protected from the incoming waves by the coral reefs. Baie de l'Embouchure is fully sheltered by the barrier reefs, whilst Baie Orientale shows a breach of the reef halfway the bay. Coral reefs are declining and the poor development of the coral reef around the island could potentially be caused by the destructive impact of hurricanes, soft and sandy beds, and excessive sedimentation (Bouchon et al., 2000; AGRNSM, 2009b).

The seagrass species that are encountered in Baie Orientale and Baie de l'Embouchure are *Thalassia testudinum*, *Syringodium filiforme*, and *Halodule wrightii* (Figure 3.6). The different seagrass species are distributed over the bathymetry. The species *H. wrightii* can be typically found at the shores. *T. testudinum* are predominantly present in the bays and are located between a depth of 1 to 12 m. From a depth of 12 to 20 m, sparse meadows of *S. filiforme* can be detected (AGRNSM, 2018; Bouchon et al., 1995). But also mixtures of the species *T. testudinum* and *S. filiforme* are encountered.



(a) Dense *T. testudinum* (thick) and *S. filiforme* (thin)

(b) Sparse meadow of *H. wrightii* with sandy bed

Figure 3.6: Seagrass species in Baie de l'Embouchure. Adopted from S. Chauvaud as cited in AGRNSM (2009b).

4

Methodology

This chapter describes the technical design of the research. A description of the research strategy is given in Section 4.1. In Section 4.2, an overview is given of the utilized Delft3D-FM software. The (adapted) model setup of the hydrodynamic and morphodynamic modules are outlined in Section 4.3 and 4.4, respectively. A morphological sensitivity analysis has been performed and the results are summarized in Section 4.5. The constructed model is validated in Section 4.6. Lastly, the two base cases and alternative simulations and scenarios used for the investigation, are introduced in Section 4.7.

4.1. Research strategy

This study aims to provide a better understanding of the role of seagrass ecosystems in coastal bays by assessing the impact on the morphodynamic behavior. In order to achieve this, an existing hydrodynamic model (Delft3D Flexible Mesh) has been extended to include morphodynamics. For this purpose, the reliability of the bed shear stress has been improved.

Two different bays have been investigated, Baie Orientale and Baie de l'Embouchure (St. Martin), which represent a partially exposed and fully sheltered bay, respectively. Both regular wave conditions and extreme storm conditions have been investigated to understand the consequences of seagrass loss on coastal erosion for different environmental climates. The environmental conditions and the state of the seagrass have been altered to assess the effectiveness of the sediment stabilization role by seagrass. Moreover, the seagrass and reef ecosystem interdependencies have been assessed by comparing the erosion control provided by both ecosystems in the presence and absence of the other ecosystem. Finally, the stabilization role of seagrass has been explored for future sea-level rise and climate change.

4.2. Model description

The hydrodynamic behavior of the coastal bays is simulated with Delft3D Flexible Mesh software developed at Deltares (Deltares, 2019a). This process-based model software is based on numerical discretizations of the Navier-Stokes equations and incorporated in two separate modules, D-Flow and D-waves. By incorporating transport phenomena for sediment it is possible to study the morphological behavior of the bays. This module is called D-Morphology and is coupled to the hydrodynamic module. The seagrass ecosystems are represented with a vegetation roughness that attenuates the flow and as a sink of the wave energy. The coral reefs are incorporated as bathymetric structures. Appendix B can be consulted, for a detailed description of the different modules and incorporation of the vegetation.

4.3. Adaptations of hydrodynamic model

The hydrodynamic model has been constructed by Keyzer (2018). An overview of the important aspects of the model setup is given in Appendix C. In this section, the adaptations of the hydrodynamic setup are indicated.

4.3.1. Bed shear stress

The analysis of the bed shear stress resulted in two adaptations of the former hydrodynamic model. Firstly, the friction of the reefs has been set equal to the alluvial bed friction. Secondly, the wave set-up has been activated in the Wave module. The detailed analysis of the bed shear stress can be consulted in Appendix D.

4.3.2. Ecosystems

A spatially varying vegetation field has been imposed to represent the seagrass meadows (Figure 4.1). The characteristics of the seagrass have been restricted to a singular vegetation class to simplify the analysis. Based on measurements of James (2015) and data of AGRNSM (2009b), the characteristics of the predominately present species (*T. Testudinum*) have been adopted and are summarized in Table 4.1.

The coral reefs have been included as bathymetric structures with the same friction as the bed. Therefore, the roughness represented by the reefs is only influenced by the water depth on top of the reefs.

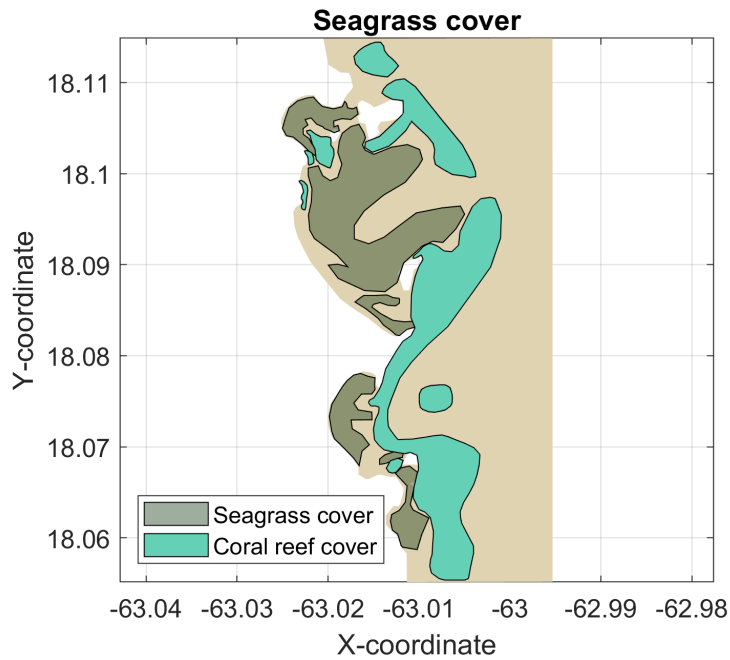


Figure 4.1: Seagrass and reef cover.

| Characteristic | Value |
|-------------------|--------------------------|
| Vegetation height | 29.5 cm |
| Leaf diameter | 1.1 cm |
| Shoot density | 800 stems/m ² |

Table 4.1: Vegetation characteristics of singular seagrass class.

4.4. Morphological model setup

The hydrodynamic model has been extended to include the morphological development of the coastal bays. In this section, the setup of the morphological module is described.

4.4.1. Morphological settings

Sediment characteristics

A uniform sediment class for the morphological model was adopted. The data of the sediment characteristics were obtained from measurements performed by James (2015). The averaged sediment characteristics were adopted and are shown in Table 4.2. The porosity (ϕ) was estimated (35%) and chosen close to the upper limit of sand since the porosity is inversely related to the sediment density (Das, 2013). This was found to be consistent with data of Valdés and Real (1994, Table 1, Arena values between 30-40%), whereby the type of sediment is similar to the sediment in St. Martin. The sediment settling velocity (w_s) was calculated with the Van Rijn formulation (Equation A.8).

| Characteristic | D_{50} [μm] | ρ_s [kg/m^3] | ρ_{bulk} [kg/m^3] | ϕ [%] | w_s [cm/s] |
|----------------|----------------------------|-------------------------------------|--|------------|--------------------------------|
| Value | 350 | 2200 | 1400 | 35 | 4.2 |

Table 4.2: Sediment characteristics of the average sediment class.

Spatial sediment availability

A spatial sediment cover has been set up (Figure 4.2) to match the observed sediment presence (Figure 3.4a). A layer thickness of 5m was assumed to prevent full erosion and bare spots.

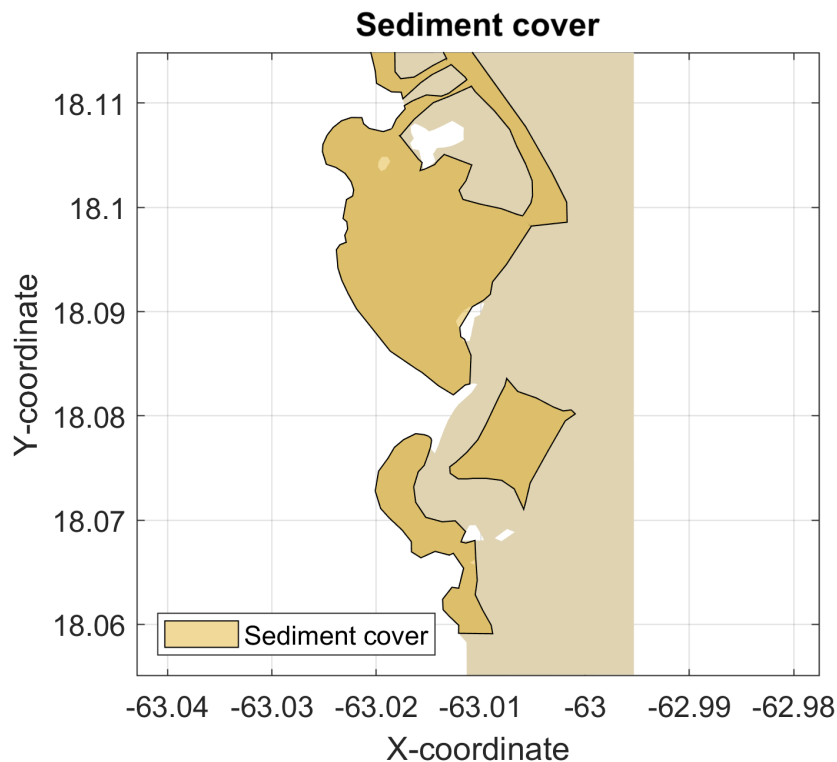


Figure 4.2: Initial spatial sediment cover.

Miscellaneous settings

Some miscellaneous settings of the model setup are summarized below:

- Gravitational bed slope effects have been included with the Bagnold formulation.
- Baie Orientale and Baie de l'Embouchure are considered to form coastal cells without external sinks. The internal sediment source from the reefs and calcifying macro-algae have not been included.
- A morphological up-scaling factor of 50 has been used for the regular wave climate simulation. The morphological up-scaling factor is set to 1 for the extreme storm event simulation.
- A morphological spin-up time of two hours has been adopted to assure that any initial hydrodynamic instabilities affect the morphological development.
- A flux limiter has been adopted (monotone central) since the sediment concentration is a conserved quantity and prevents unrealistic results (e.g. negative concentrations).

4.4.2. Sediment transport formulation

A variety of sediment transport formulations are available in Delft3D-FM. Both the impacts of the flow and waves need to be incorporated in the bed-load and suspended-load transport. Therefore, the formulation of Van Rijn (1993) and Bijker (1971) were considered and further analyzed. In Appendix A.2 brief descriptions of these transport formulations are given.

The van Rijn formulation leads to very dynamic development with many morphological changes, especially near the shore (Figure 4.3). Although this could be calibrated, the patterns of morphological changes show discrepancies with reality. For instance, a lot of sediment accumulates at the headland between Baie Orientale and Baie de l'Embouchure. This might be a direct consequence of the fact that the suspended-load transport only incorporates the wave influences and direction.

The Bijker formulation is a more robust formulation, specifically developed for applications in coastal areas. This formulation shows a more credible development of the morphology that does not show a large accumulation at the headland. This formulation incorporates both influences of the flows and waves on the suspended-load transport. Based on these preliminary results, the Bijker formulation was adopted as the final formulation.

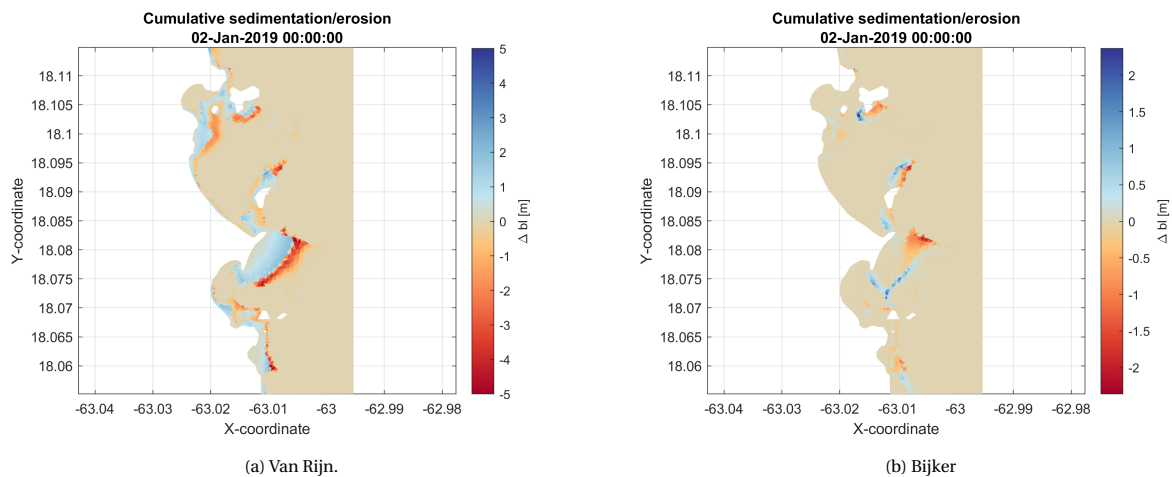


Figure 4.3: Analysis of sediment transport formulations. The morphological changes after 50 days are shown. The van Rijn formulation leads to large sediment accumulation towards the headland, which is not observed in reality.

4.5. Sensitivity analysis

The wave conditions and sediment characteristics have been included in a sensitivity analysis to assess the impact of the morphological changes. The main findings are included in this section and the detailed sensitivity analysis is given in Appendix E.

Waveform and wave energy

The amount of erosion under varying wave conditions is shown in Figure 4.4 for both the regular wave climate and extreme storm event cases. Considering the storm duration, the erosion is quite considerable. However, the regular wave conditions are normative regarding the morphological development on the longer timescales. The erosion increases for higher waves since more wave energy is present to initiate the sediment's motion, suspension and the increased flow velocities lead to more transport of these particles. Furthermore, the longer waves propagate relatively further towards the shore which leads to more wave energy in front and beyond the reefs. This also increases the flow velocities and sediment transport. This effect is more noticeable for the higher waves.

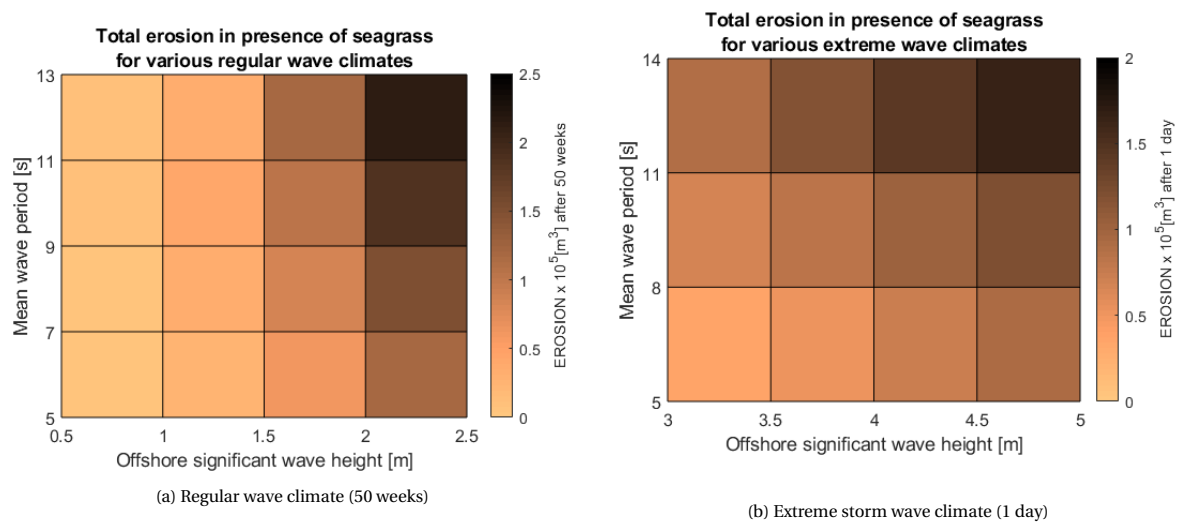


Figure 4.4: Morphological sensitivity to the wave conditions. Considering the storm duration, the amount of erosion is much larger compared to the regular wave conditions. Two erosion gradients are visible in which the higher and longer waves increase the erosion.

Wave direction

The uniformity of the waves, especially the wave direction, is reflected in the sediment fluxes. The pattern of the morphological changes is therefore amplified during the simulation period. In reality, it is expected that the dynamic wave climate (i.e. varying magnitude and direction), would smoothen the uniform pattern of the sediment fluxes.

Sediment characteristics

Differences in the sediment characteristics are expected to influence the rates of sediment transport, type of transport and how far the sediment is transported.

4.6. Model validation

The available data was used to validate the model, both quantitatively and qualitatively. The technical validation and justification of the use of the hydrodynamic model are described by Keyzer (2018). Since a few adaptations were carried out and the model applications for this research include now the sediment dynamics, the hydrodynamic and morphological behavior have been validated.

4.6.1. Validation of hydrodynamics

Measurements of the water depth and wave height performed by James (2015) were used to validate the hydrodynamic model. Two measurement sites are located in Baie l'Embouchure and one in Baie Orientale (Figure 4.5). It has been tried to match the tidal phase with data of the tidal amplitude in Saint Barthelemy during the period of September 2015 (TIDES4FISHING, 2015). It has been found that the main tidal components are represented and the minor differences in the signal might be caused by the simplification of the constructed tide. The ranges of the water depth and significant wave height for the measurements and model output shown in Table 4.3 & 4.4.



Figure 4.5: Locations of measurements performed by James (2015) used for validation (V1-V3). Observation points (O1-O4) have been marked used to assess the model output of the erosion rates. Lastly, a cross-section (A-A') is indicated. Adopted from (Google Maps, 2019).

The simulated water depth matches the measured values for Baie Orientale (V3), whilst the water depths in Baie de l'Embouchure (V1 & V2) show differences between 20 and 35cm.

| Validation point | wd_{model} [cm] | wd_{meas} [cm] |
|------------------|-------------------|------------------|
| V1 | 50-70 | 15-38 |
| V2 | 78-95 | 58-72 |
| V3 | 100-130 | 98-122 |

Table 4.3: Validation of water depth. Ranges of water depth of the model output and measurements of James (2015)

The wave height measurements were found to be generally consistent with the simulated wave height. Especially the wave signal in the southern location in Baie de l'Embouchure (V2) shows a nice fit. The wave height is overestimated ($\approx 10\text{cm}$) in the northern location of Baie de l'Embouchure (V1) and might be a direct consequence of the corresponding water depth overestimation. Whilst, the wave height is slightly underestimated ($\approx 15\text{cm}$) in Baie Orientale (V3), despite the consistent water depths.

| Validation point | $H_{s,model}$ [cm] | $H_{s,meas}$ [cm] |
|------------------|--------------------|-------------------|
| V1 | 5-17 | 21-27 |
| V2 | 10-18 | 5-19 |
| V3 | 11-19 | 15-47 |

Table 4.4: Validation of wave height. Ranges of significant wave height of the model output and measurements of James (2015).

The bed shear stress is found credible in contrast to the output of the former hydrodynamic model, which produced unreliably large bed shear stresses. The total bed shear stress is dominated by the influences of the waves which is coherent with the fact that this coastal system is dominated by waves and to a lesser extent influenced by the tide. The bed shear stresses remain, therefore, low in the sheltered bays due to sheltered conditions. Whilst, at the reefs, larger values of the bed shear stress can be observed (\approx up to 17 Pa). The coral reefs induce an abrupt change in the bathymetry, and results in the predominant surf-breaking of the waves.

Overall, the magnitude of the wave height is considered to be correct in which the influences of the main tidal constituents are also represented. The small differences can be attributed to discrepancies with the hydrodynamic and/or weather conditions. Moreover, errors in the bathymetry in the bays, but especially at the reefs, are also expected to influence the propagation of wave energy. The bed shear stress has been improved and found to be credible. Therefore, the constructed hydrodynamic model is found valid for the purpose of this research and will be used to expand to a morphodynamic model.

4.6.2. Validation of morphology

The historical morphological development of Baie Orientale and Baie de L'Embouchure (Figure 4.7) are used to qualitatively validate the simulated development (Figure 4.6). The similarities of this qualitative validation are outlined below:

- The morphological changes remain limited and no significant changes of the shorelines are observed. This can also be expected based on the smaller swell waves. But also due to the sheltered conditions, the morphological changes remain limited which is consistent with the observed development.
- The coastal headland between Baie Orientale and Baie de l'Embouchure does not show any significant accretion or erosion. Although sediment is available in front of the headland, this sediment is transported in south-northwards directions, dependent on the wave direction, in the simulation.
- A southward sediment transport flux is visible in the model output below Baie l'Embouchure. This might explain the deficit of sediment at the coast of Baie Lucas, beneath Baie de l'Embouchure.
- The model shows a small sediment flux northwards, in the northern part of Baie Orientale. Only through this small passage or the reef gap halfway the bay sediment can be transported. The spatial presence of sediment (Figure 3.4a) might also indicate a sediment flux from the bay towards the reef gap.
- The coastline does not significantly regress or transgress during the simulated extreme storm event. Also from satellite images, it can not be concluded that the coastline did either regress or transgress significantly during Hurricane Irma. Irma caused beach overwash (in combination with the transport of lots of

debris). However, this can not be observed in the model since this process can only be simulated with a land-based model.

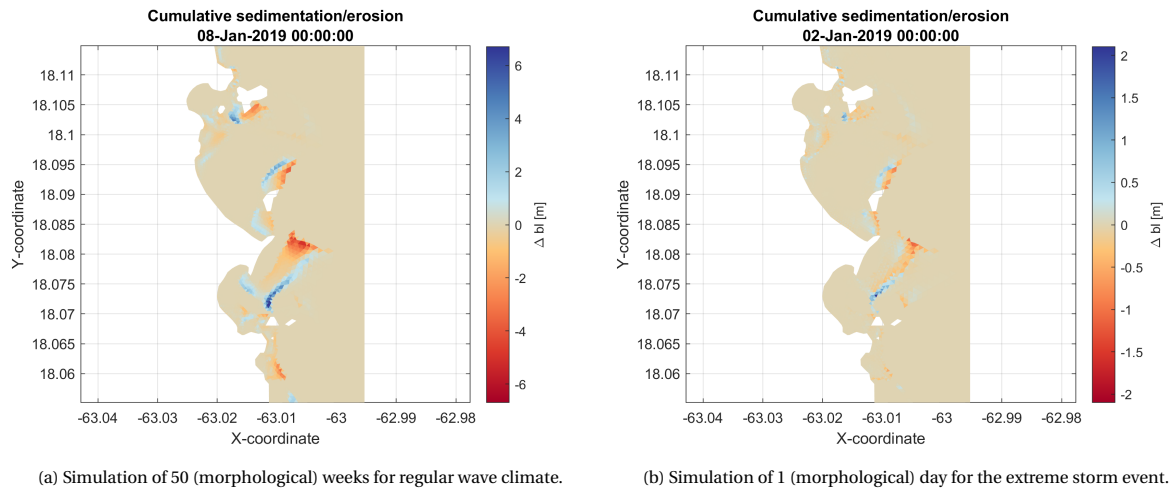


Figure 4.6: Morphological development for base cases.



Figure 4.7: Observed development of Saint Martin coastal bays (Google Earth Engine, 2019)

A small data-set of shear velocities at which sediment particles are entrained (James, 2015) is used to quanti-

tatively validate the morphodynamic model. The threshold velocities were measured with an uni-directional flow field flume. An in-situ flume was placed at the bottom of the coast inside Baie de l'Embouchure on top of both vegetated and unvegetated areas. This data is compared with the simulated shear velocity. Although, in reality, it is expected that the turbulent flow and vorticity of the flow will result in more suspension of the sediment particles compared to the uni-directional flume measurements. Other field flume experiments, at a site in Bonaire with an oscillatory flow, showed that the required shear velocities to move sediment are indeed lower (R.K. James, Personal communication, July 8, 2019).

| Case | Unvegetated bed | Vegetated bed |
|----------------------|-----------------|---------------|
| Baie de l'Embouchure | 0.15-0.23 | 1 |
| Bonaire | 0.10 | 0.15-0.20 |

Table 4.5: Measurements of critical shear velocities [m/s].

Two dominant sediment fluxes can be observed in the shallow regions (Figure 4.8). The shear velocity at the unvegetated bed is approximately 0.09-0.10m/s which is close to the values in Table 4.5. The sediment flux at the vegetated bed is smaller than the sediment flux at the unvegetated. Whilst, the shear velocities are slightly larger in the vegetated bed (0.10-0.11m/s) and comparable with the measurements in Bonaire. Therefore, it can be concluded that the required shear velocity to suspend sediments is larger for vegetated beds compared to unvegetated beds and is consistent with the findings of James (2015).

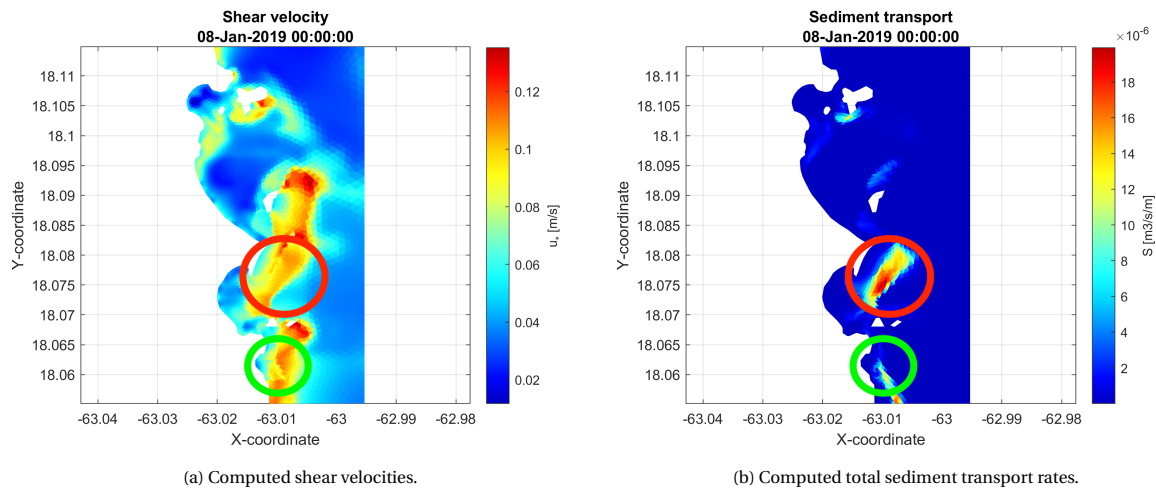


Figure 4.8: Sediment transport and shear velocities. Two dominant sediment fluxes can be observed in the shallow regions. The vegetated bed is indicated with the green circle and the unvegetated bed with the red circle.

To overcome the problematic difficulty of simulating both the changes of the hydrodynamic and morphological behavior with different time-scales, a morphological up-scaling factor has been adopted. With this technique, the differences in both time scales are efficiently utilized. Otherwise, the computational effort becomes too large and makes it unfeasible to simulate the entire morphological period. When the MORF factor is chosen too large, the extrapolated bathymetry might not be representative anymore for the actual bathymetry. Therefore, the MORF factor has been validated by comparing a simulation of one day (MORF=50) with a simulation of 50 days (MORF=1). From Figure 4.9 it can be concluded that both simulations yield the same result and justify the use of a MORF factor of 50.

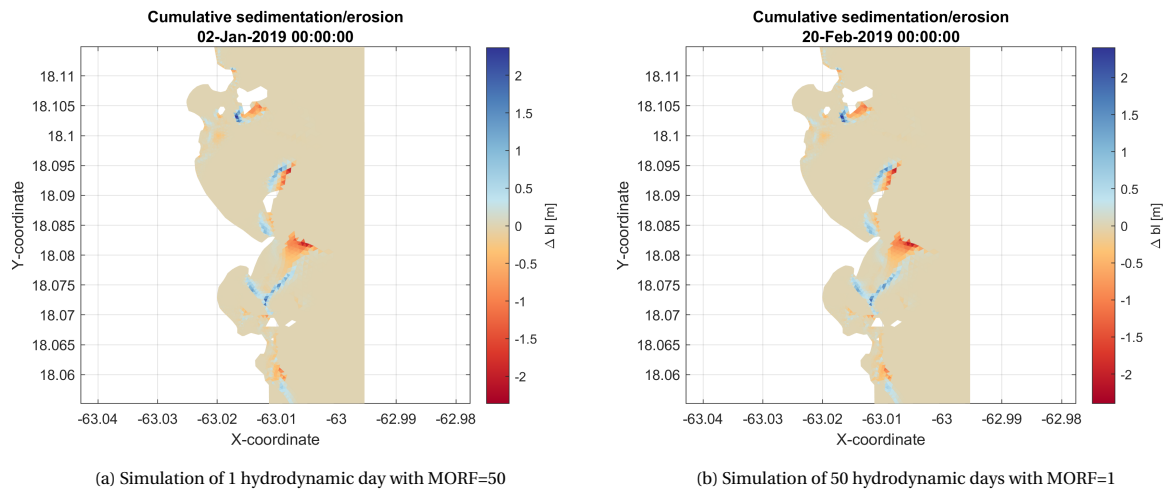


Figure 4.9: Verification of morphological up-scaling factor.

The findings of the historical coastal development, measurements of the critical shear velocities and the technical assessment of the morphological up-scaling factor, lead to a morphodynamic model which can be considered to be qualitatively valid. The sediment transport rates and quantitative values of the morphological changes are expected to not match the reality precisely. This is a direct consequence of the adopted hydrodynamic and morphological simplifications, but also the lack of data that is needed for proper quantitative calibration of the model.

4.7. Simulations and scenarios

Various alternative simulations and scenarios have been analyzed besides the base cases of the regular wave climate and extreme storm event. Simulations have been run to assess the stabilization role of seagrass under different wave conditions. Besides, the vegetation height and spatial distribution of seagrass have been adapted in separate simulations. Moreover, simulations have been set up to analyze the interaction between seagrass meadows and coral reefs. Lastly, future scenarios have been constructed, which include the sea-level rise and consequences of climate change, to analyze the future role of the seagrass.

4.7.1. Simulations base cases

The hydrodynamic model setup, shown in Appendix C is used to simulate the regular swell wave climate. Moreover, an extreme storm event simulation has been set up with a duration of one day. Hereafter, both base cases are referred to as the regular (swell) wave climate and extreme storm event.

Mainly three components differentiate an extreme storm event from a regular wave climate which are the storm surge, extreme wind velocities, and high wave energy. The storm waves are typically high, short-crested waves with increased irregularity. The differences between both simulations are summarized in Table 4.6.

The environmental conditions were chosen similar to the conditions during Hurricane Irma (2017) and based on the numerical results of a Global Forecast System and a WAVEWATCH III model (Beccario, C, 2019). During Irma, which can be considered to be a rare event, the wind velocities reached high magnitudes. To prevent an overestimation of the wind force since the wind is imposed uniformly and stationary, a smaller wind velocity was chosen. The storm surge has been estimated as 0.5m.

| Simulation | wl [MWL+m] | U_{10} [m/s] | H_s [m], T_m [s], θ [°] |
|------------------------------|------------|----------------|------------------------------------|
| Regular (swell) wave climate | 0 | 5 | 1.5, 9, 10 |
| Extreme storm event | 0.5 | 15 | 4.0, 14, 20 |

Table 4.6: Environmental conditions of the two base cases. The differences of the two simulations are the storm surge (wl), wind velocity (U_{10}) and wave climate: wave height (H_s), mean period (T_m) and directional spreading (θ).

4.7.2. Simulations seagrass effectiveness

Impact of seagrass for various wave conditions

The wave height and period for both base case simulations have been varied to assess under which wave conditions the stabilization role of seagrass is more prominent.

Impact of seagrass for different vegetation heights

The distribution of the seagrass over the water depth is an important characteristic regarding the hydrodynamic attenuation. Therefore, different simulations have been carried out in which the vegetation height has been varied uniformly.

Impact of seagrass for different spatial distributions

Three different simulations have been assessed in which the spatial seagrass cover has been altered. The different covers of the seagrass meadows are shown in Figure 4.10.

The seagrass meadows in Baie Orientale and Baie de l'Embouchure are present between water depths of 1-12m. In the first simulation, it is chosen to remove the shallow seagrass meadows located between 1 and 3m. With a vegetation height of 30cm, the relative vegetation height reaches now 10% at most for the shallowest boundaries.

To determine the effectiveness of the current spatial distribution, the seagrass has been expanded towards a deeper region in front of the reef-gap in Baie Orientale. Moreover, the impact of a full seagrass cover inside the bays is assessed.

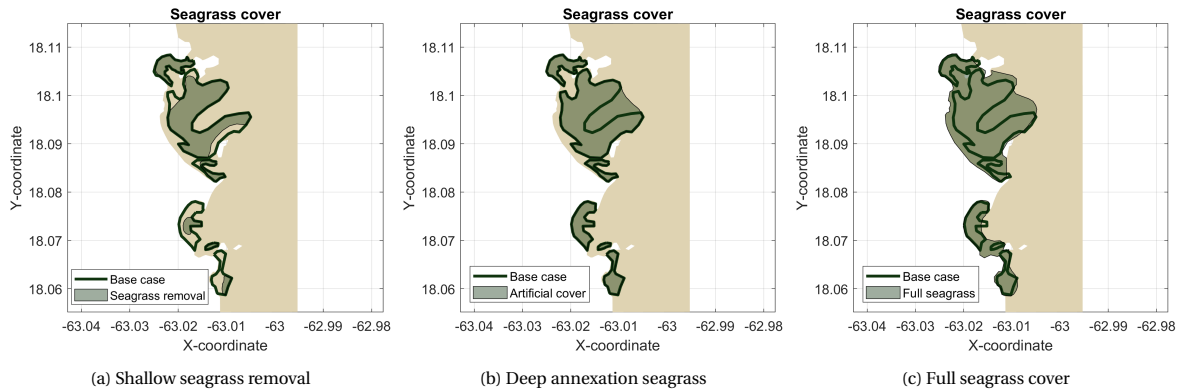


Figure 4.10: Different spatial seagrass covers.

4.7.3. Simulations seagrass-reef interaction

The reefs predominantly dissipate the wave energy and hence provide a sheltering function. To assess the influences of the reefs and their impact on the stabilization role of the seagrass meadows, the bathymetric reef structures have been removed. A synthetic bathymetry has been created and is shown in Figure 4.11.

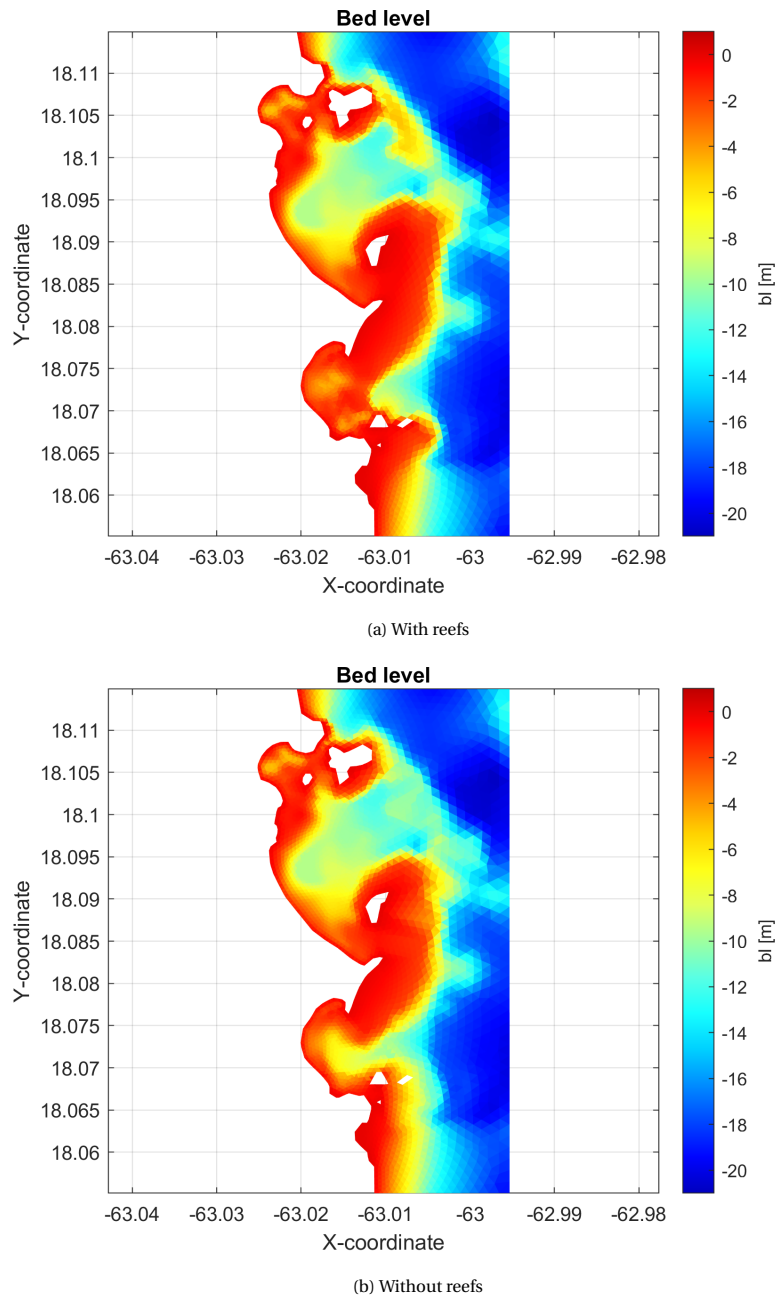


Figure 4.11: Bathymetry with and without reef structures.

4.7.4. Future scenarios

The development of the morphology and marine ecosystems remains uncertain. To assess the future stabilization role of seagrass, two scenarios have set up in which a sea-level rise has been imposed. The water level increase has been chosen as 87cm and is an approximation of the sea-level rise in 2100 in Puerto Rico under the RCP8.5 (Jevrejeva et al., 2016). This is also in line with predictions of IPCC (2014) as shown in Figure 2.11. The regular swell wave climate has been considered for the future scenarios.

In the first scenario, referred to as the catch up scenario, the bays, seagrass, and coral reefs remain similar to the present state. The seagrass meadows are located in between the 1m and 12m depth ranges (AGRNSM, 2009b). Therefore, the spatial seagrass cover for the catch up scenario has been reduced. The deeper parts of the meadows that would have surpassed the depth limit of 12m under sea-level rise have been removed (Figure 4.12b). Other than that, no changes have been applied to the seagrass meadows. It is assumed that the habitat, between the depth limits, remains favorable and leads to the same characteristics as the current seagrass. Note that the new opportunities for habitat extension have not been considered.

In the second scenario (called keep up), the bathymetry of the bays has also been increased with 87cm. It has been assumed that enough sediment from offshore will act as a source for the inner bays and would not significantly change the offshore bathymetry. Moreover, the seagrass meadows and coral reefs also follow the sea-level rise. The adapted bathymetry for the keep up scenario is shown in Figure 4.12a.

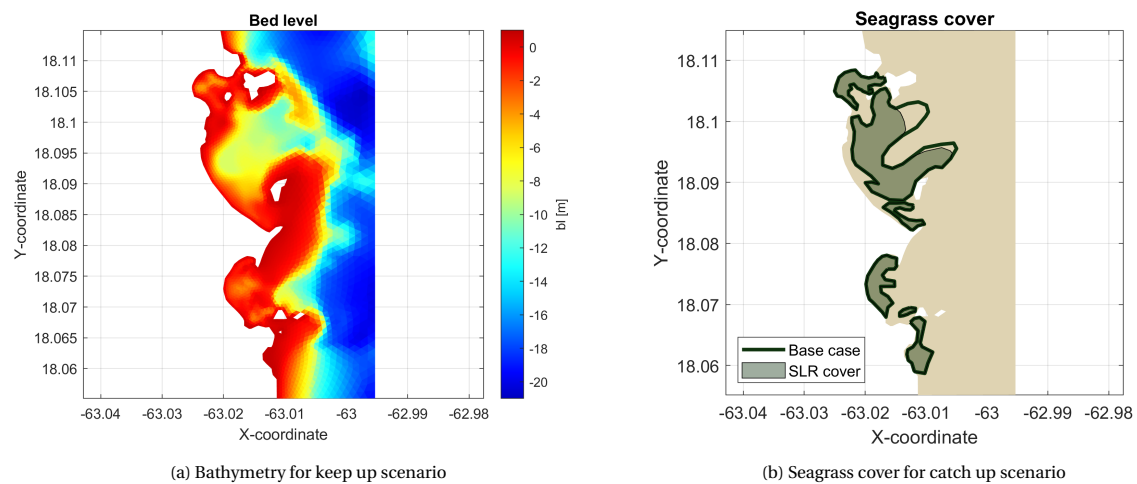


Figure 4.12: Bathymetry (keep up) and seagrass cover (catch up) for future scenarios.

5

Morphodynamic behavior of coastal bays

In this chapter, the morphodynamic behavior for the simulations of the regular wave climate and extreme storm event (in the presence of seagrass) are described. At first, the hydrodynamic behavior is treated in Section 5.1. The hydrodynamic behavior is investigated by looking at the patterns of the waves, flows and related components. In Section 5.2, the cumulative changes in the morphological development of the coastal bays are described.

5.1. Hydrodynamic behavior of bays

5.1.1. Hydrodynamics under regular wave climate

Transformation of wave energy

The presence of reefs and the influences on the transformation of the wave energy characterize the tropical sheltered bays (Figure 5.1a). The bathymetry influences the incoming waves which shoal towards the reefs. When the reefs are reached, most of the wave energy is dissipated on top of the reefs (up to 85 % of the wave height). The bays are, therefore, mostly sheltered from the incoming waves, except for one region in Baie Orientale. This region is exposed due to the absence of any reef structures and increases the wave energy locally. The wave-induced orbital velocities are highest in the shallow regions with high wave energy (Figure 5.1c).

Reef-induced circulation flows

A few circulation flows in the bays can be recognized (Figure 5.1b). These flows are induced by the breaking waves on top of the reefs. The decreased wave-induced radiation stresses generate a pressure gradient that drives a flow. The flow circulates in the bay and continuity of mass requires the flow to leave towards the ocean. A large circulation flow is present in Baie Orientale and multiple minor flows can be found in Baie de l'Embouchure. The circulation flow in Baie Orientale is somewhat smaller in magnitude and shifts slightly towards the ocean in comparison with the former hydrodynamic model of Keyzer (2018). This might be a direct consequence of the adoption of a smaller reef roughness since the surface roughness enhances the circulation flow.

Total bed shear stress

The bed shear stress is found to be highest in regions where a lot of wave energy is present and resembles the pattern of the wave-induced orbital velocities (Figure 5.1d & 5.1c). The wave transformation on top of the reefs results in the highest bed shear stresses. The bed shear stress is much smaller in the sheltered bays. However, the bed shear stress increases nearby the shore where the final wave energy is dissipated. The bed shear stresses are especially large in the exposed region which is a direct consequence of the higher wave energy. This is another indication that the bed shear stress is dominated by the influences of the waves. This can also be concluded from the bed shear stress components as shown in Appendix D (Figure D.5).

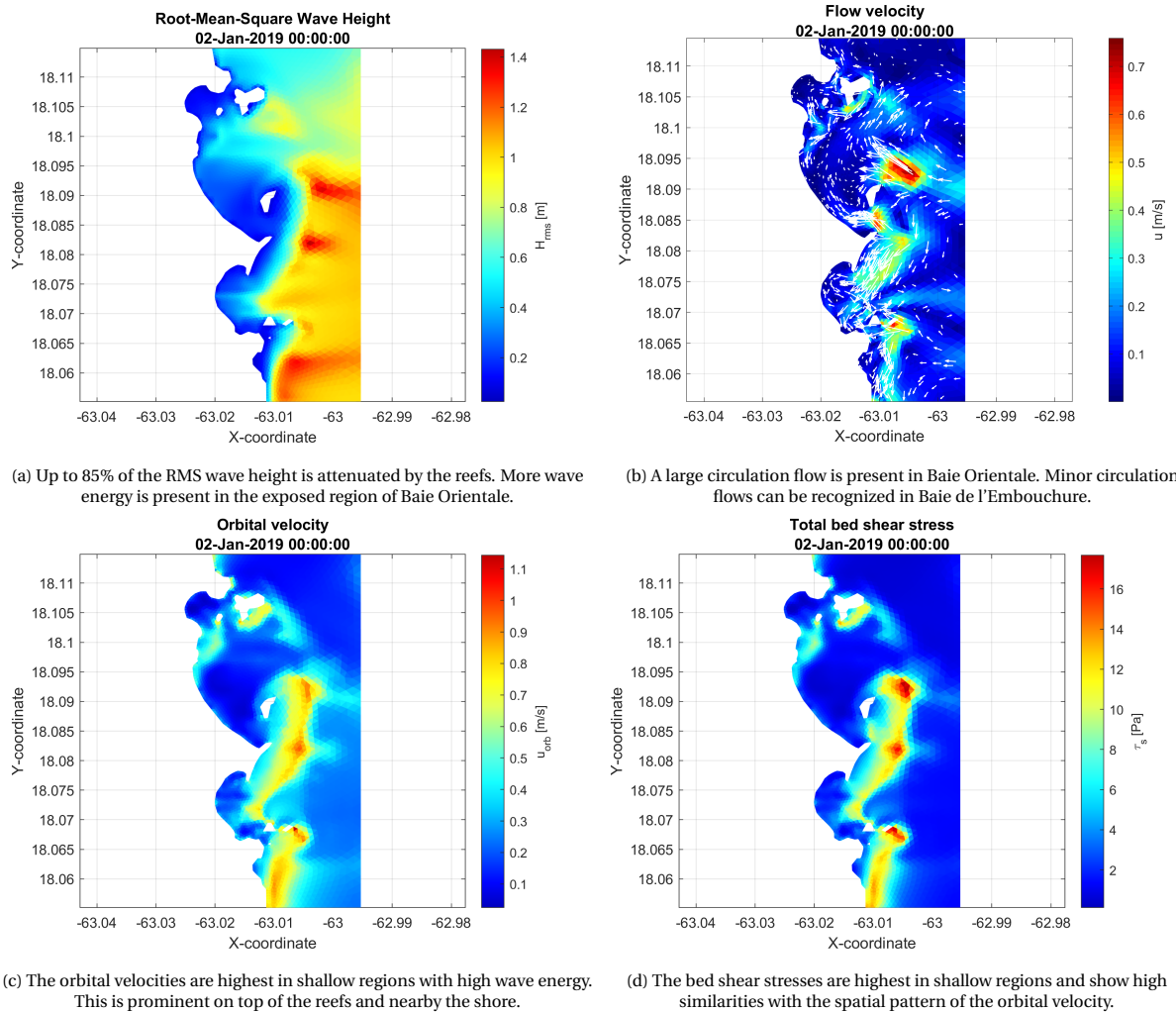


Figure 5.1: Hydrodynamic behavior of coastal bays under regular wave climate.

5.1.2. Hydrodynamics under extreme storm event

The altered hydrodynamic behavior under the extreme storm conditions relative to the regular wave climate is summarized in Figure 5.2. An extreme storm has typically higher and shorter waves. Steeper waves break in an earlier stage, nevertheless still more wave energy propagates inside the sheltered bays compared to regular wave conditions. The increased wave energy strengthens the circulation flows inside the bays and shifts the flows towards the shore. Moreover, the magnitude of the orbital velocity and bed shears stress increase significantly in the shallow regions. Besides the significant increases of the hydrodynamic forces, the storm conditions also raise the water level (Figure 5.3). The increased wind velocity is an additional source for the wave energy and contributes to the wave set-up. The storm surge increases the water level and reduces the depth-induced wave breaking on top of the reefs. This also allows more wave energy to propagate inside the sheltered bays and increases the wave-induced set-up.

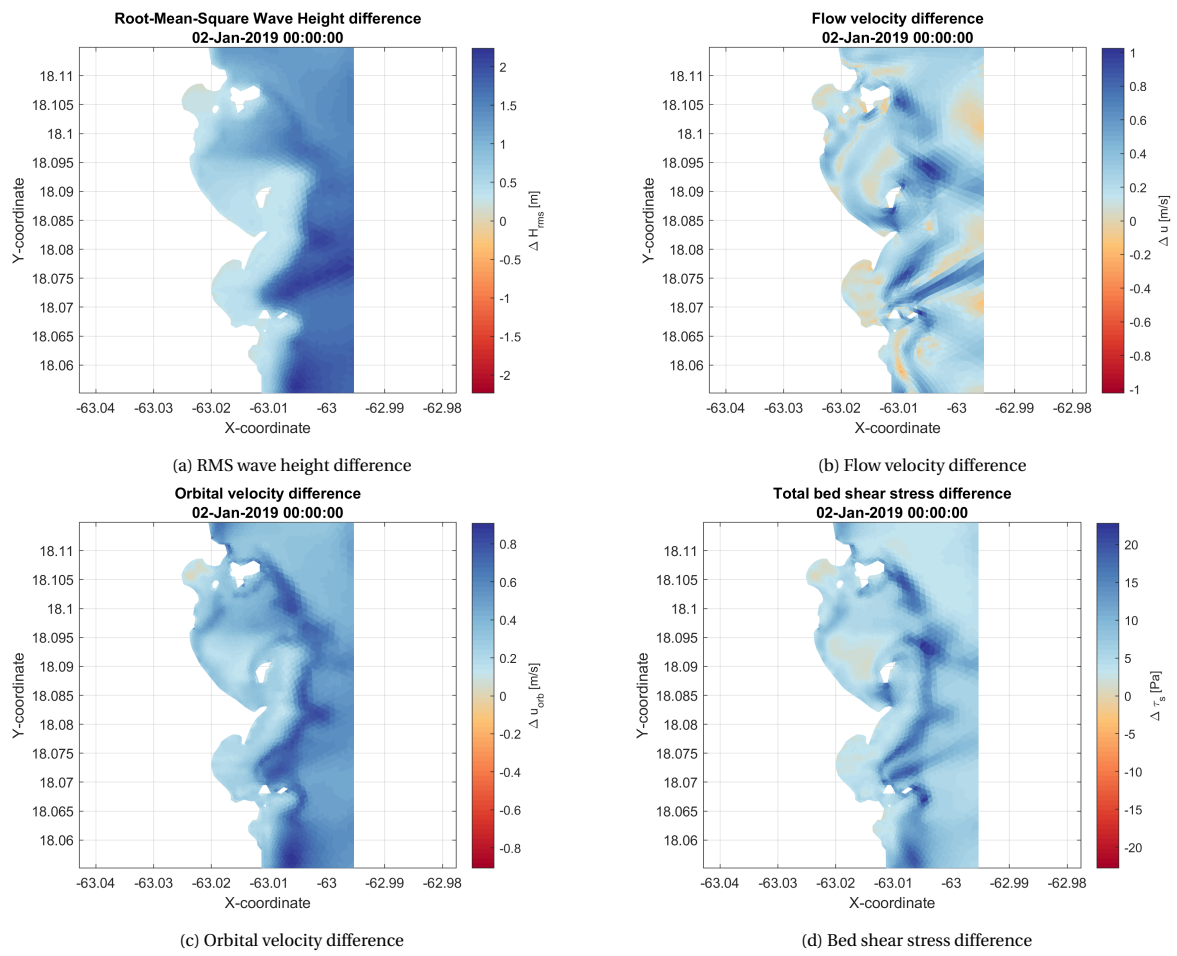


Figure 5.2: Increase of hydrodynamic forces during the extreme storm event compared to the regular wave climate.

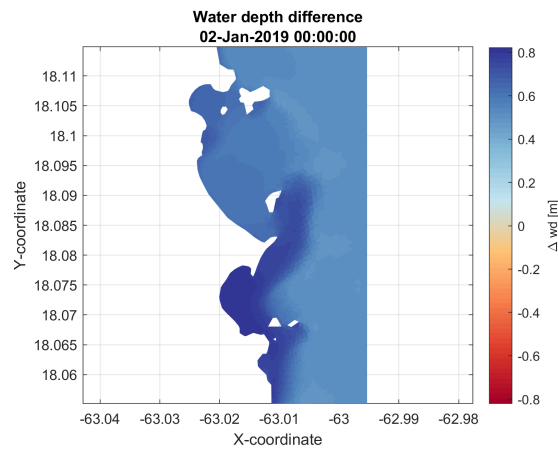


Figure 5.3: Water depth increase during the extreme storm event compared to the regular wave climate.

5.2. Morphological behavior of bays

5.2.1. Morphology under regular wave climate

The beaches of Baie Orientale and Baie de l'Embouchure do not show significant regression after 50 weeks (Figure 5.4). The waves are attenuated by the reefs to such an extent that the bed shear stresses are not large enough to cause significant regression of the beaches. Only the northern part of the beach of Baie Orientale shows minor erosion (Figure 5.5a).

The erosion inside the bays is largest in shallow regions and most prominent in the exposed area of Baie Orientale compared to the sheltered areas (Figure 5.5a & 5.5b). The sediment in the exposed region is transported by a current along the shore which flows towards the south. Another erosion/accumulation pattern can be found in Baie Orientale in which two converging flows around Caye Verte cause a dominant sediment flux towards the shore. In both cases, the sediment remains inside the bay. However, the return current in Baie Orientale causes some sediment to leave the bay through the reef gap.

The area in front of the headland shows the most morphological changes. A large southward sediment flux can be observed that is caused by the large bed shear stresses and a strong flow. This flux partially acts as a source of sediment for Baie de l'Embouchure which accumulates at the northern end of the bay. This fully sheltered bay shows minor erosion compared to Baie Orientale. A southward erosion flux can be found in the region between Baie de l'Embouchure and the neighboring Baie Lucas.

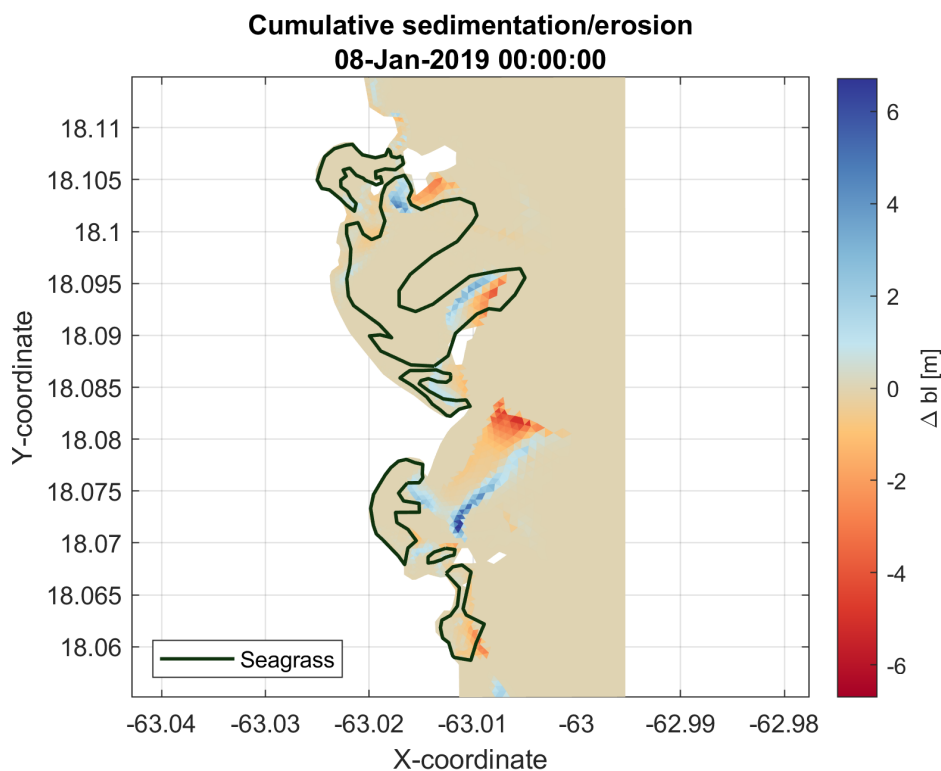


Figure 5.4: Morphological changes in the coastal domain under regular wave climate after a morphological period of 50 weeks. More morphological activity is present in the exposed area of Baie Orientale. Around Caye Verte sediment is transported towards the shore. Furthermore, the high bed shear stresses and southward flows also lead two southward sediment fluxes in front of the headland and between Baie de l'Embouchure and Baie Lucas.

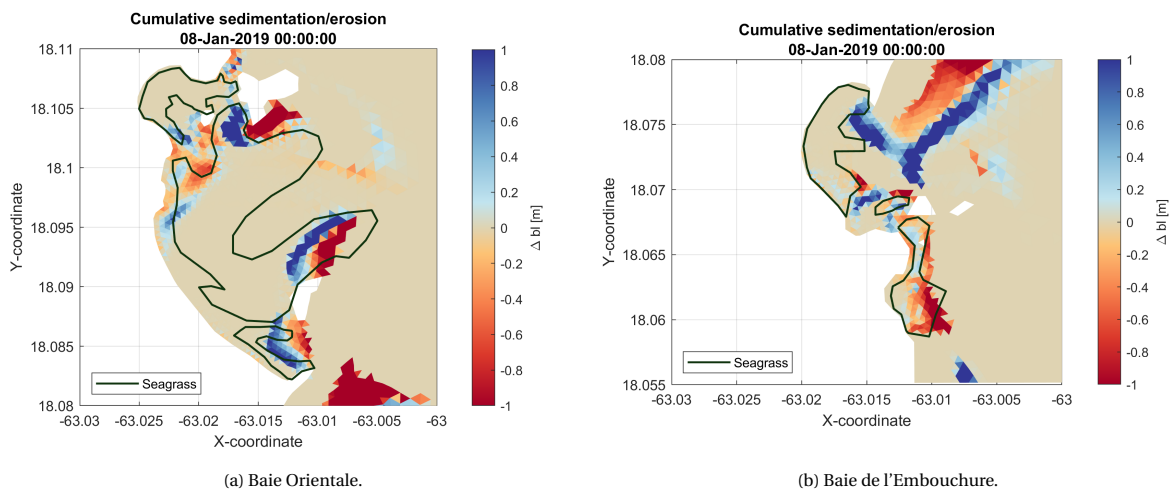


Figure 5.5: Morphological changes in coastal bays after a morphological period of 50 weeks. The northern part of the beach in Baie Orientale leads to some minor erosion. Other parts and Baie de l'Embouchure are more resilient.

A cross-shore morphological development in the exposed region of Baie Orientale is shown in Figure 5.6. The profile reveals a steep front from 0 to 500m, which is typical for a regular swell wave environment. Another slope can be found from 1.1 to 1.6 km. In between, the profile has a much lower slope. Note that the seagrass is present from 0-0.5km and close to 1-1.5km. Between these ranges, the profile is steeper than the part in the middle and might indicate the historical sediment stabilization by the seagrass meadows. Sediment is transported towards the shore in which the second part of the steep front (200-500m) generally steepens over time. This sediment accumulates in the first part of the steep front (0-200m). No other significant changes in the profile are noticeable further offshore.

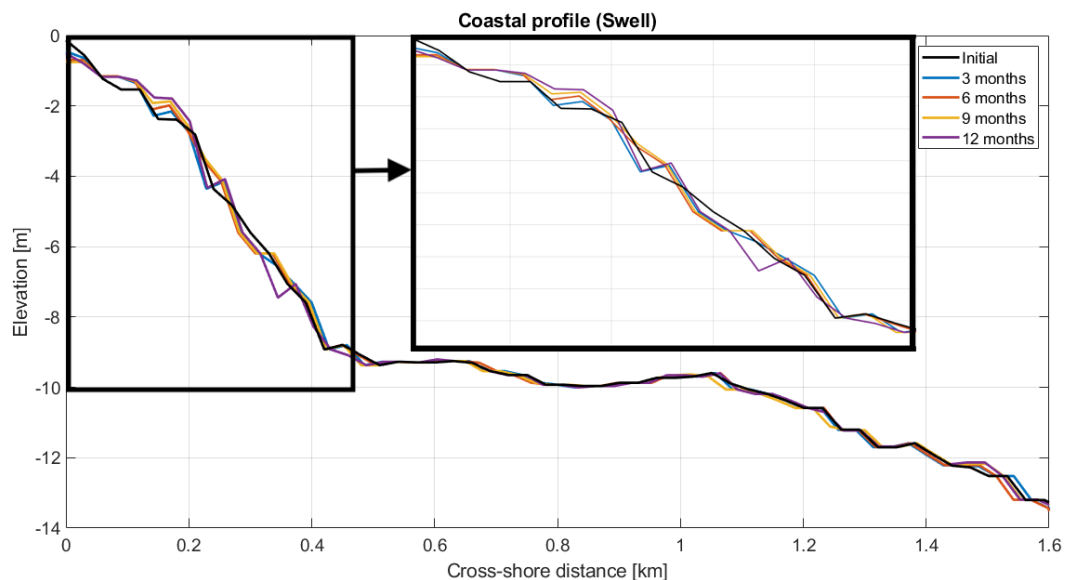


Figure 5.6: Development of coastal profile A-A' (as indicated in Figure 4.5) under regular swell wave climate. The profile steepens between 200-500m, in which sediment is transported towards the shore and accumulates between 0-200m.

5.2.2. Morphology under extreme storm event

The spatial patterns of the sediment fluxes under extreme storm conditions (Figure 5.7a & 5.7b) are similar to the changes under the regular wave conditions (Figure 5.5a & 5.5b). However, the changes inside the bays under regular wave conditions are not noticeable after one day and almost negligible. Whereas the erosion rates increase considerably under extreme storm conditions (Figure 5.7). The difference in the amount of erosion is one order of magnitude. The morphological changes are noticeable in Baie Orientale, whereas Baie de l'Embouchure shows to be resilient. The sediment transport is observable in the exposed region of Baie Orientale and around Caye Verte. The beach does not show any significant regression.

The storm period is, however, too small to cause catastrophic morphological changes. The total amount of erosion is about 10% of the erosion under the regular wave climate (after 50 weeks). Therefore, when longer timescales (i.e. months to years) are considered together with the return period of such an extreme storm event, it can be concluded that the regular wave climate is normative in shaping the morphodynamics of the bays.

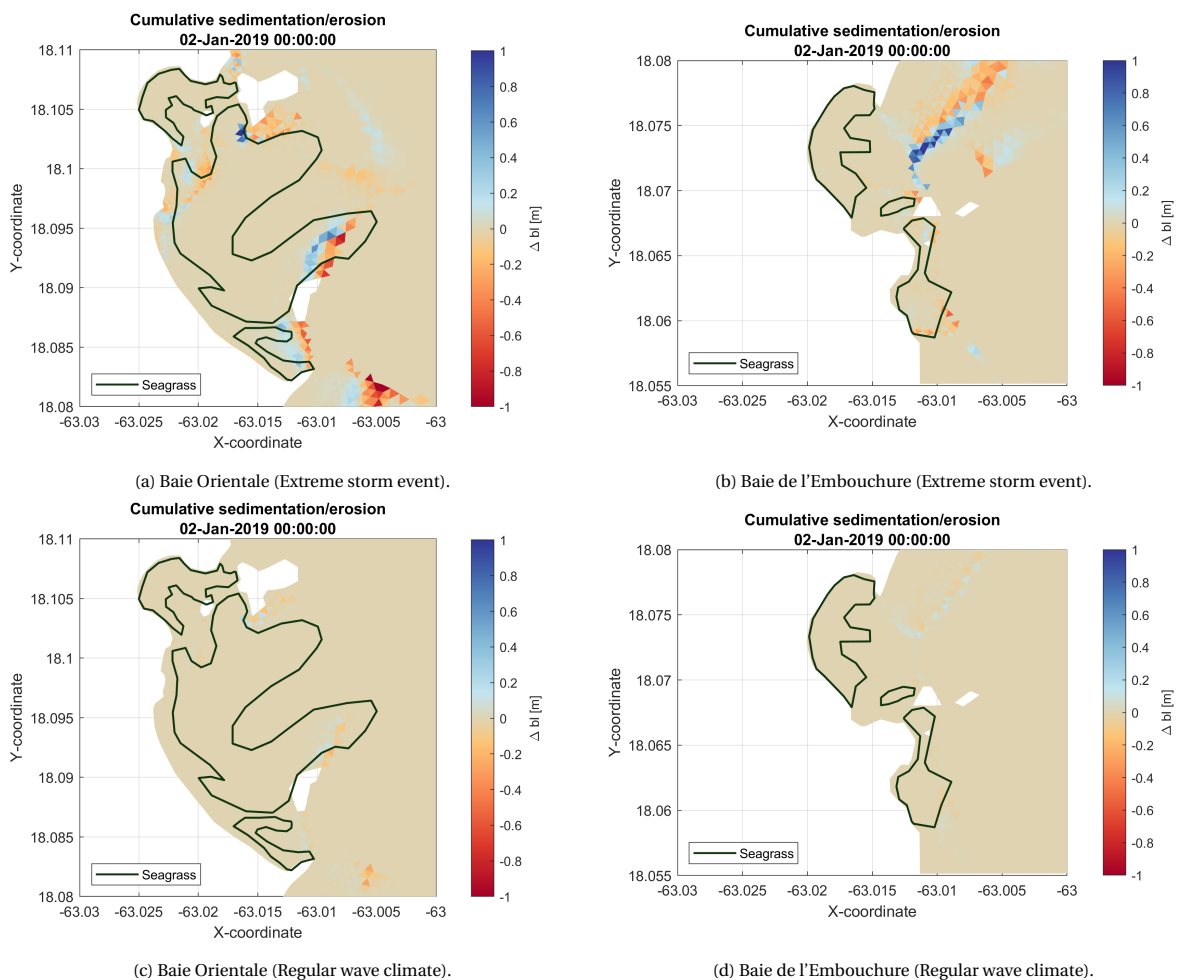


Figure 5.7: Morphological changes in coastal bays under regular swell wave climate & extreme storm event after 1 day. The storm causes much more sediment transport compared to the regular wave climate. However, when the longer timescales (i.e. months to years) are considered and the return period of such an extreme event, the morphological development under the regular wave climate is normative.e.

The coastal erosion under the extreme storm conditions has been visualized in Figure 5.8 by means of the development of the coastal profile. Furthermore, the development under the regular wave conditions after one day is shown.

The shore shows some erosion under the extreme storm conditions and is slightly smaller under regular wave conditions (Figure 5.8). Furthermore, during the storm, cross-shore transport of sediments takes place in which probably a few sand bars can be recognized. The general pattern is that some part of the coastal profile erodes and is transported offshore. Whereas, the regular swell waves tend to slow this offshore transport down or even transport the sediment towards the shore which leads to the steepening of the profile.

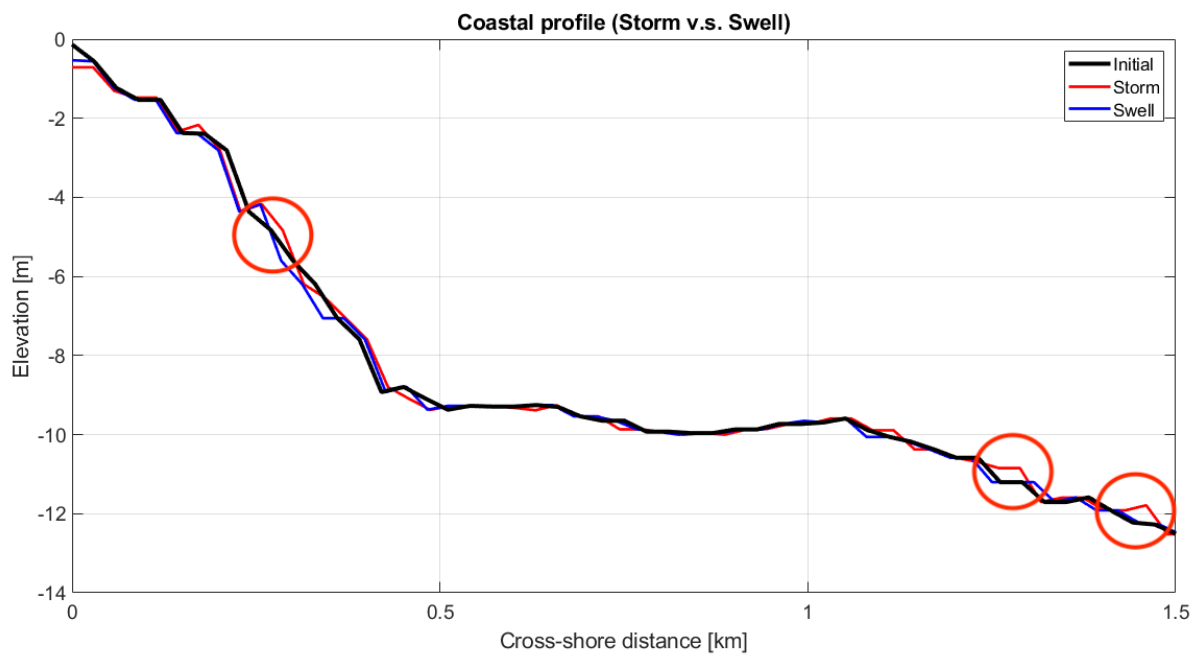


Figure 5.8: Development of coastal profile A-A' (as indicated in Figure 4.5) under extreme storm and regular wave conditions. A minor beach regression can be observed. Moreover, the cross-shore transport of sediment can be observed that is directed offshore under the storm conditions (indicated with red circles).

6

Role of seagrass

The impact of seagrass on the hydrodynamic attenuation and sediment stabilization are treated in Section 6.1 and 6.2, respectively. In these sections, the role of the seagrass meadows has been assessed for both the regular wave climate and extreme storm event. Alternative scenarios have been investigated in Section 6.3 to assess under which environmental conditions and seagrass distributions the sediment stabilization is most effective. Thereafter, the interaction between seagrass and reef ecosystems is analyzed in Section 6.4. Lastly, in Section 6.5, future scenarios have been studied to assess the evolution spectrum of the seagrass's role due to climate change and the consequences to the morphological development of the bays.

6.1. Hydrodynamic attenuation by seagrass

The spatially-averaged attenuation of the hydrodynamic forces due to the presence of seagrass has been calculated and shown in Figure 6.1. The flows are most attenuated by the seagrass, whilst the wave energy is least attenuated. The bed shear stress is affected by both the flows and waves and the reduction of the bed shear stress is, therefore, larger than the wave attenuation. The attenuation of the flow velocities and bed shear stress could have a significant impact on sediment stabilization. Both components are important with regard to the dynamics of sediment, which is very sensitive to the hydrodynamic forces.

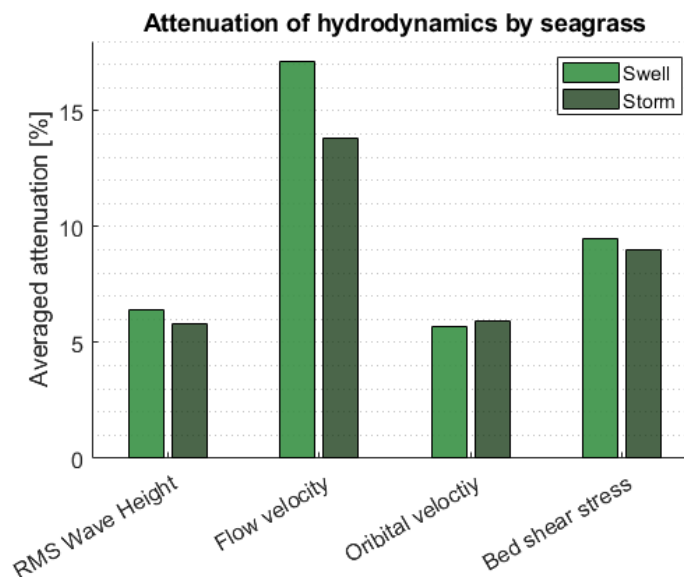


Figure 6.1: Spatially-averaged seagrass attenuation. The flows are most attenuated by the seagrass and the wave energy to a lesser extent. The impact of the seagrass is slightly smaller under extreme storm conditions, except for the orbital velocities.

It can also be observed that the impact of the seagrass on the hydrodynamic attenuation is slightly smaller during the extreme storm event compared to the regular swell wave climate. An exception is the attenuation of the orbital velocities. The decay of the wave-induced water motions is larger under the extreme storm conditions due to the increased water depth. This results in a relatively larger impact of the seagrass on the attenuation of the wave-induced orbital velocities. The spatial attenuation patterns of the hydrodynamic forces are similar for both the regular swell wave climate and extreme storm event and are shown in Appendix F. Moreover, a more detailed analysis of the hydrodynamic attenuation and results of a sensitivity analysis regarding the vegetation characteristics are further described.

6.2. Sediment stabilization by seagrass

The relative sediment stabilization due to the presence of seagrass is shown in Figure 6.2. The seagrass meadows effectively reduce the erosion in the shallow regions in both bays. Some shallow spots can be even observed in which the sediment is fully stabilized. The erosion in the deeper regions is reduced less effectively.

The sediment flux around Caye Verte is, for instance, significantly reduced by the seagrass. Likewise, the southward sediment flux beneath Baie de l'Embouchure is effectively reduced. Furthermore, the minor regression of both beaches is almost fully stabilized by the seagrass meadows. However, the impact of the seagrass on the erosion in the deeper and exposed part of Baie Orientale is less significant. The seagrass meadows reduce the sediment fluxes in this region, but this is rather limited in terms of the magnitude and area that is affected by the seagrass.

The sediment stabilization by seagrass is substantial if the total stabilized volume of sediment is considered. The total amount of erosion in the absence of the seagrass is reduced by 28.4% in the presence of the seagrass.

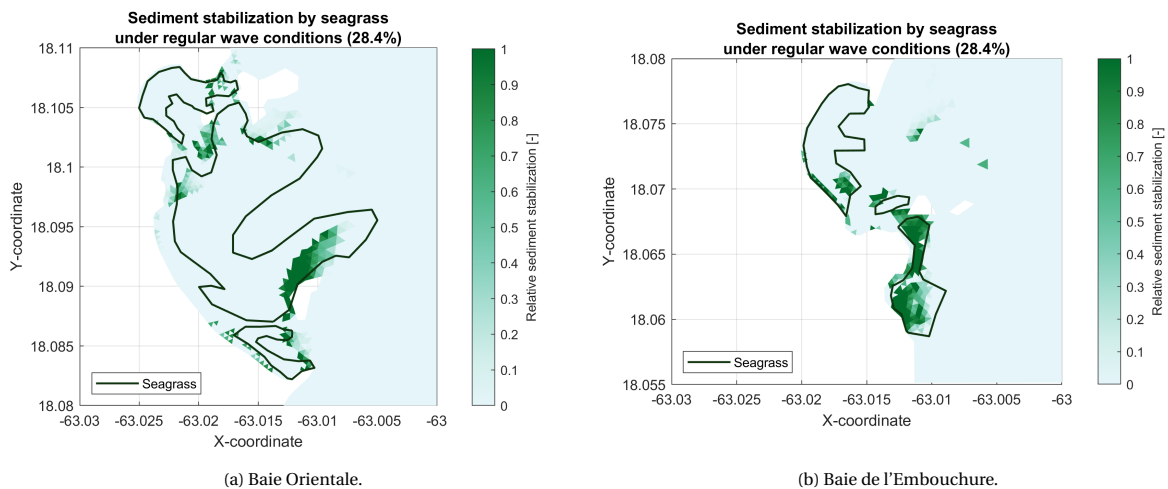


Figure 6.2: Relative impact of seagrass on sediment stabilization under regular swell conditions. The total sediment stabilization is 28.4%.

The sediment stabilization under the extreme storm conditions is shown in Figure 6.3. Since the timescales are different, the amount of erosion differs compared to the simulation with the regular wave climate. However, when the relative changes are considered it can be observed that the impact of the seagrass on the total amount of sediment stabilization slightly reduces under the extreme storm conditions and equals 23.1%.

The reduced stabilization is a direct consequence of the altered hydrodynamics during the extreme storm

event. In Section 5.1 it has been shown that all components that characterize a storm event do increase the water level. This decreases the relative vegetation height and hence the impact on the hydrodynamic attenuation (Section 6.1) and sediment stabilization. Taking into account that the impact of the seagrass is most effective in the shallow regions, even a small water depth increase could be significant.

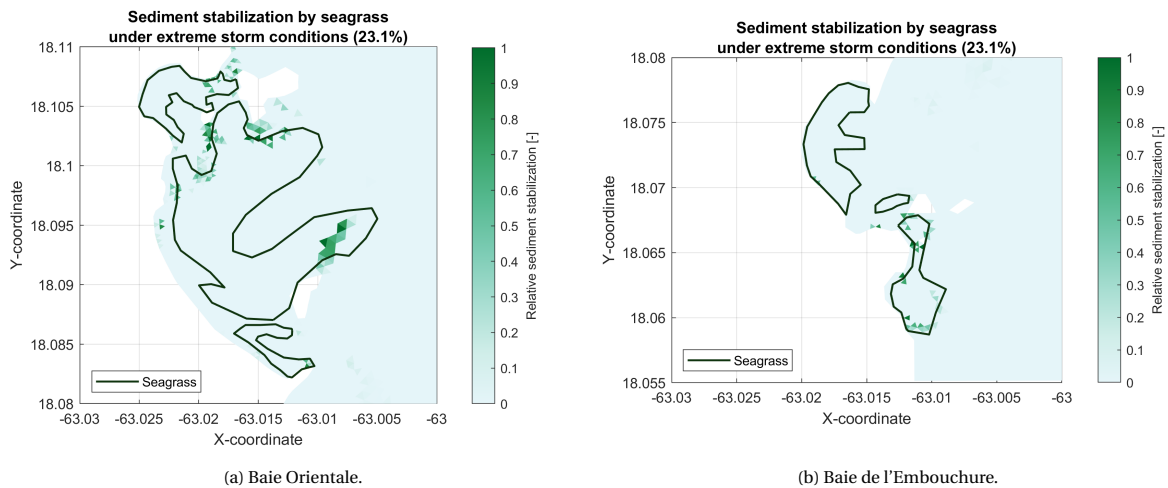


Figure 6.3: Relative impact of seagrass on sediment stabilization under extreme storm conditions. The total sediment stabilization is slightly less significant during an extreme storm event and equals 23.1%. This reduction can be attributed to the increased water levels.

6.3. Effectiveness seagrass

In Section 6.2 it has been found that the sediment stabilization by seagrass is especially effective in the shallow regions. Moreover, the sediment stabilization reduces under extreme storm conditions. Therefore, the effectiveness of the seagrass on sediment stabilization is investigated in this section for various wave conditions, vegetation heights, and spatial distributions of the meadows.

6.3.1. Impact of seagrass for various wave conditions

The sediment stabilization under varying wave conditions has been assessed for both the regular wave climate and extreme storm event cases. The seagrass impact on the total sediment stabilization under various wave conditions is shown in Figure 6.4 for both cases. It can be observed that the sediment stabilization reduces with increasing wave energy. Furthermore, the stabilization increases generally for the longer waves, with an exception of the mildest waves.

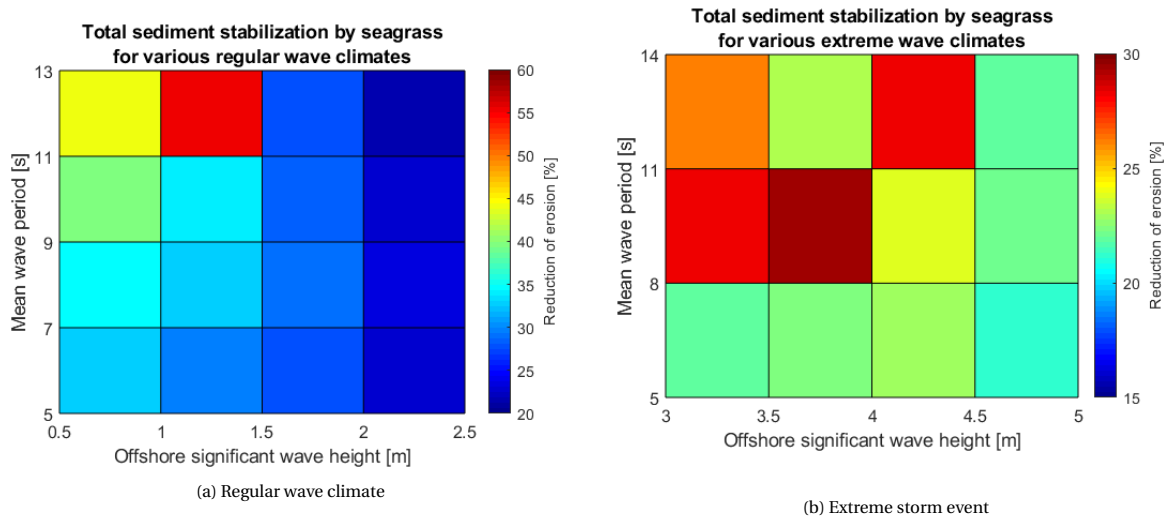


Figure 6.4: Impact of seagrass on total sediment stabilization under varying wave conditions. The stabilization of seagrass reduces with increasing wave energy, primarily due to the increased wave set-up and bed shear stresses. Moreover, the sediment is typically more effectively stabilized for longer waves. Except for the mildest waves, in which the increased water levels seem to dominate and reduce the impact of the seagrass.

The sediment stabilization by seagrass decreases with increasing wave energy primarily due to the increased water levels and bed shear stresses. The increased wave set-up is especially noticeable in Baie de l'Embouchure due to the confined nature of the bay (Figure 6.5a). Whereas the size of Baie Orientale is much larger and hence the wave set-up is less significant.

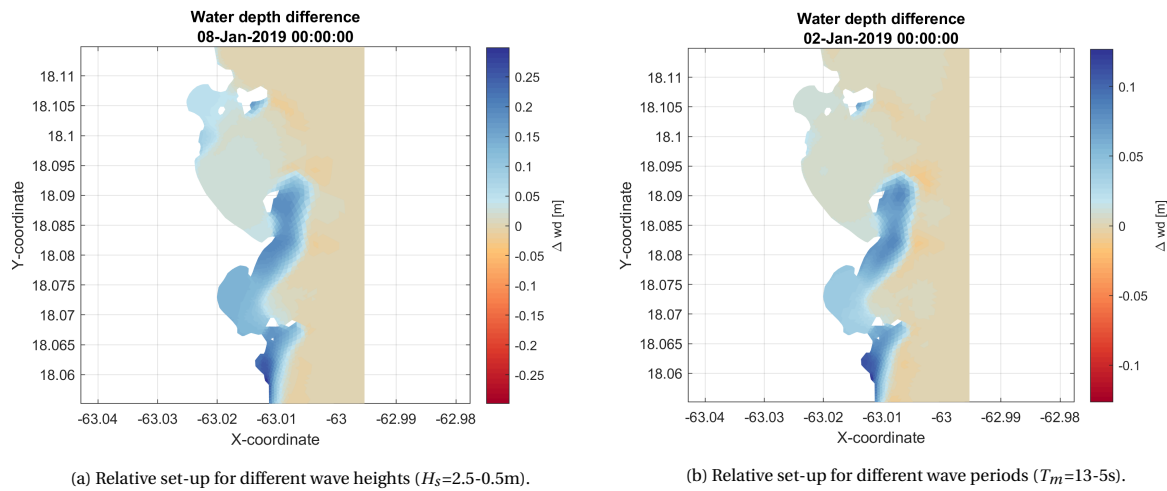


Figure 6.5: Wave-induced set-up. The higher and longer waves cause a significant increase of the water level.

Although the longer waves also cause a slightly larger wave set-up (Figure 6.5b), the sediment stabilization is typically larger for longer waves. The wave-induced oscillatory water motions are prolonged and the boundary layer is able to grow larger (as explained in Section A.1). This decreases the vertical velocity gradients and bed shear stresses (Figure 6.6). The shear exerted by the seagrass is thus relatively larger and leads to more effective

sediment stabilization. However, in Figure 6.4 also exceptions can be found for the mildest waves for both simulations. For these mildest waves, it seems that the increased water levels and corresponding increased wave-induced bed shear stresses seem to dominate which reduces the impact of the seagrass.

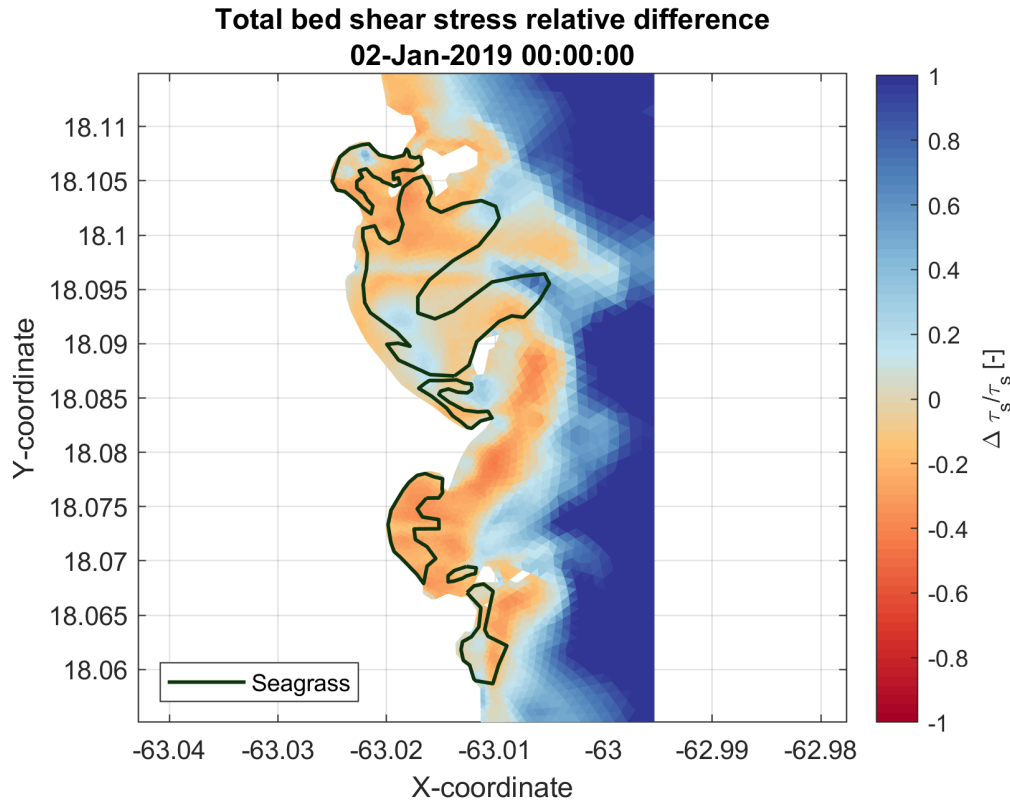


Figure 6.6: Effect of wave period on bed shear stress. The normalized values of the differences of the bed shear stress are shown. The bed shear stresses generally decrease inside the bays (indicated with red) for a larger wave period ($T_m = 13s$) compared to a smaller wave period ($T_m = 5s$). Note that the bed shear stresses increase outside the bays for the longer waves since more wave energy is present compared to the shorter waves and therefore dominates the bed shear stress (increase instead of decrease).

6.3.2. Impact of seagrass for different vegetation heights

The vegetation height has been uniformly varied in different simulations to assess under which vegetation height the sediment stabilization starts to become effective. The outcome of the different vegetation heights on the total sediment stabilization is shown in Figure 6.7.

The stabilization role of seagrass increases almost linearly for smaller heights ($\leq 5\text{cm}$) after which the stabilization increases with a reduced rate (concave downward) for larger vegetation heights. The decline of the stabilization increases thus for smaller vegetation heights. The sediment stabilization could be regarded as insignificant when the vegetation height is smaller than 5 cm. In this case, less than 6% of the total erosion is stabilized by the seagrass. However, this threshold is only useful regarding the impact on the total erosion in these specific coastal bays.

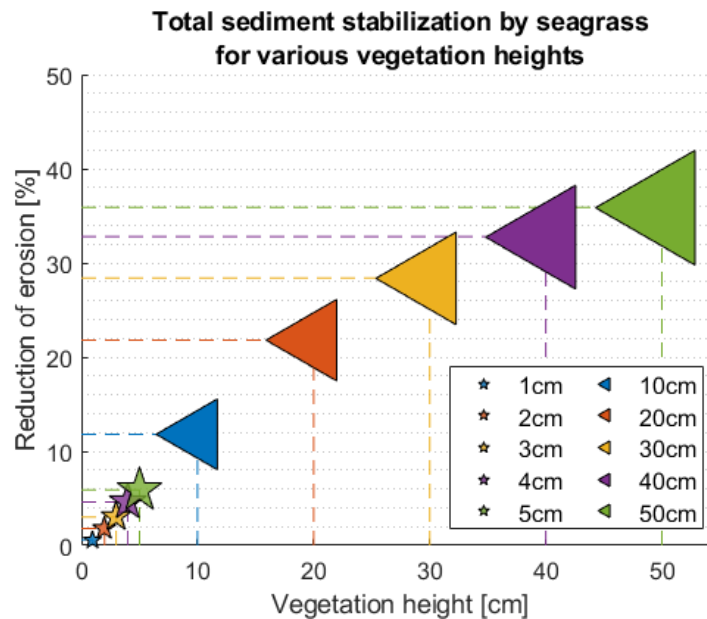


Figure 6.7: Impact of vegetation height on total sediment stabilization. The seagrass impact increases almost linearly for smaller heights (≤ 5 cm) after which the impact for the larger vegetation heights increases with a reduced rate. The reduction of the erosion could be regarded as insignificant when the vegetation height is smaller than 5 cm ($< 6\%$).

In Figure 6.8a it can be observed that the sediment stabilization by seagrass is most effective around Caye Verte (indicated with the red circle) and between Baie de l'Embouchure and Baie Lucas (indicated with the green circle). The relative vegetation height in this regions are, therefore, further assessed and shown in Figure 6.8b. The seagrass meadows of 10cm have a relative vegetation height of 4-12% around Caye Verte and 10-20% between Baie de l'Embouchure and Baie Lucas. Therefore, the impact of the vegetation starts to become significant ($> 11.8\%$) from a relative vegetation height of approximately 10%.

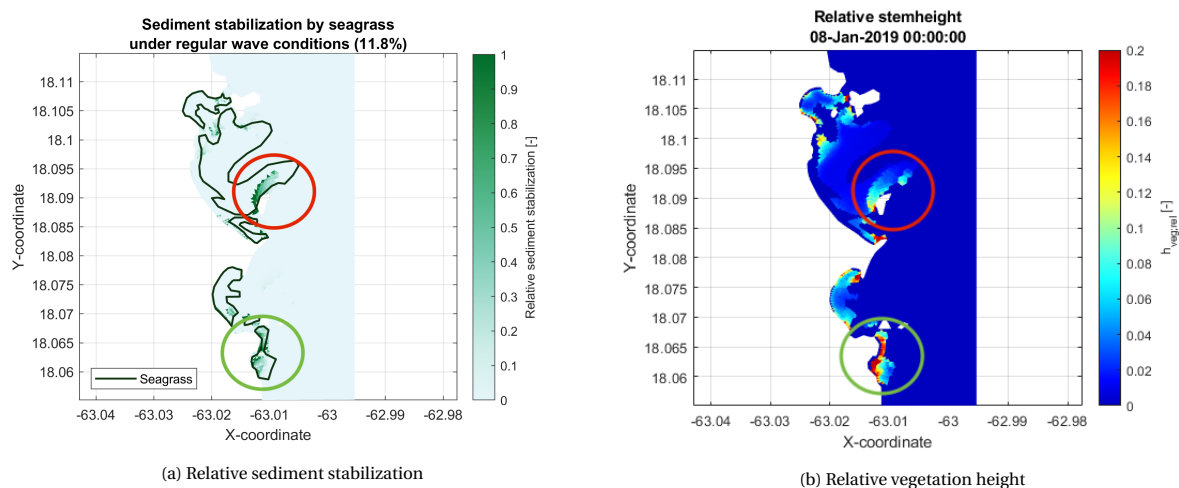


Figure 6.8: Relative sediment stabilization and vegetation height for a vegetation height of 10 cm. The impact of the seagrass on sediment stabilization starts to become significant ($> 11.8\%$) from a relative vegetation height of approximately 10%.

6.3.3. Impact of seagrass for different spatial distributions

The impact of different spatial distributions of seagrass meadows (as defined in Section 4.7) on the sediment stabilization is shown in Figure 6.9. These results further emphasize the importance of the presence of seagrass meadows in the shallow regions. The seagrass removal (between 1-3m) limits the relative vegetation height and equals at most 10% of the water depth. This small reduction of the seagrass cover in the foreshore approximately halves the total sediment stabilization. This again shows the significance of the vegetation height and the seagrass presence in the shallow foreshore. Furthermore, the current seagrass distribution did evolve to a state which is already quite effective compared to the impact of the full seagrass cover. However, if the seagrass meadows are able to expand, especially towards the shore, the sediment stabilization could increase significantly. An extension towards the deeper parts does not result in a significant increase.

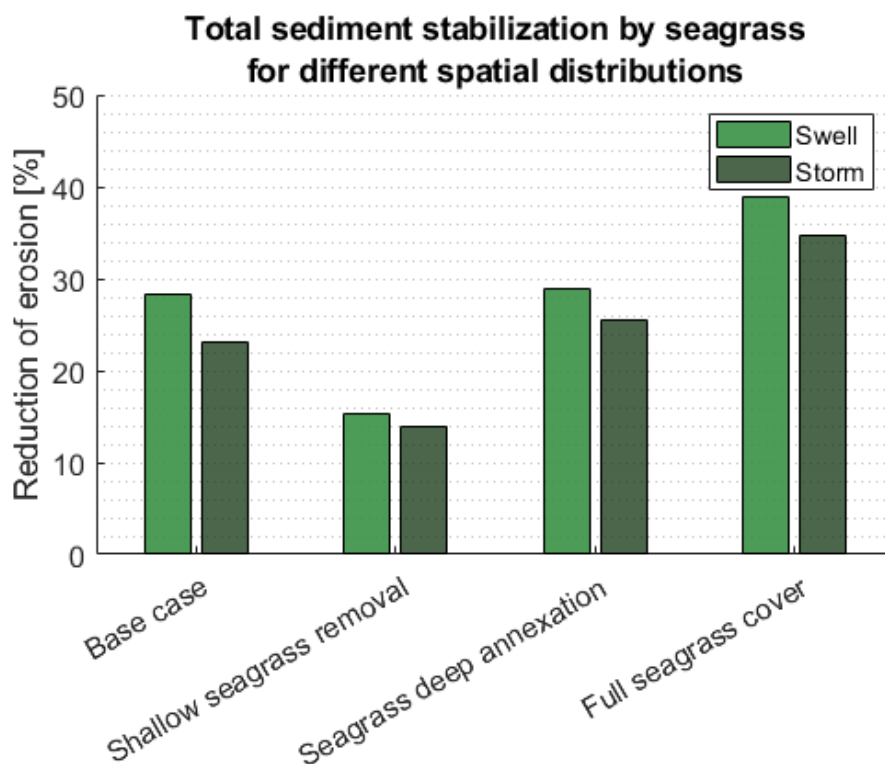


Figure 6.9: Impact of different spatial distributions of seagrass meadows on sediment stabilization. The impact of the different seagrass covers on the erosion control further emphasizes the importance of the presence of the seagrass meadows in the shallow regions.

6.4. Seagrass and reef interaction

The propagation of wave energy towards the bays results in a wave set-up which has been found to reduce the stabilization role of seagrass quite substantially. Furthermore, the reefs are found to predominantly dissipate the wave energy which reduces the water levels and bed shear stresses inside the sheltered bays. Therefore, the influence of the reefs on the stabilization role of seagrass is investigated in this section with a simulation in which the reefs have been removed (as described in Section 4.7). Besides, the erosion control provided by the reefs is also investigated in the presence and absence of the seagrass meadows.

The impacts of both ecosystems on the sediment stabilization in the presence and absence of the other ecosystem are shown in Figure 6.10 for both the regular wave conditions and extreme storm conditions. The results reveal interactions between the seagrass and reef ecosystems that reinforces the stabilization of sediments provided by the individual ecosystems.

The stabilization role of seagrass is indeed higher in the presence of the reefs and reduces quite significantly in absence of the reefs (by 17%). Moreover, the erosion control provided by the reefs also increases in the presence of the seagrass meadows which is partially caused by the seagrass-induced subtle water level set-up and reduced bed shear stresses. It must also be noted that the impact of the reefs is larger under extreme storm conditions compared to the regular swell conditions. The collective stabilization of the erosion by both ecosystems is substantial and approximately halves the total erosion.

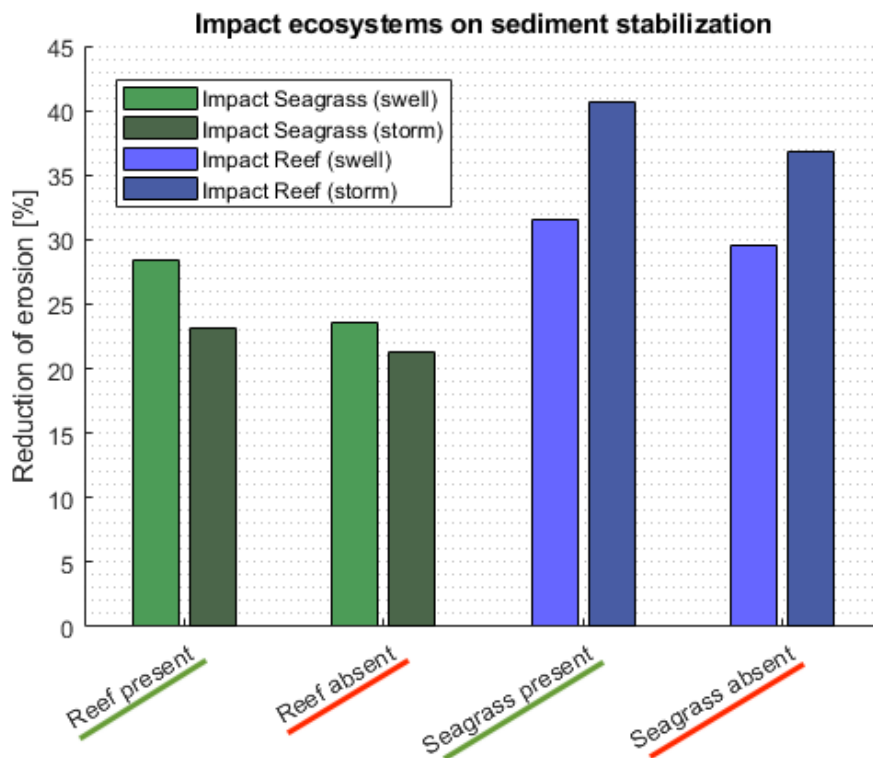


Figure 6.10: Impact ecosystems and inter-ecosystem interactions on sediment stabilization. The individual impacts of the seagrass and reef ecosystems are reinforced in the presence of the other ecosystem. The seagrass meadows are more effective under the smaller and longer wave conditions (swell), whereas the reefs are more dominant in the dissipation of the higher and shorter (storm) waves.

6.5. Future role of seagrass

The role of seagrass on sediment stabilization under sea-level rise has been explored with two scenarios (as defined in Section 4.7).

The morphological changes under the keep up scenario are almost similar to the present base case scenario of the regular swell wave climate. The total erosion increases with 5% for the keep up scenario. The increased erosion under the catch up scenario is more significant and equals 15%. Especially the southern parts of both beaches show a substantial regression (Figure 6.11).

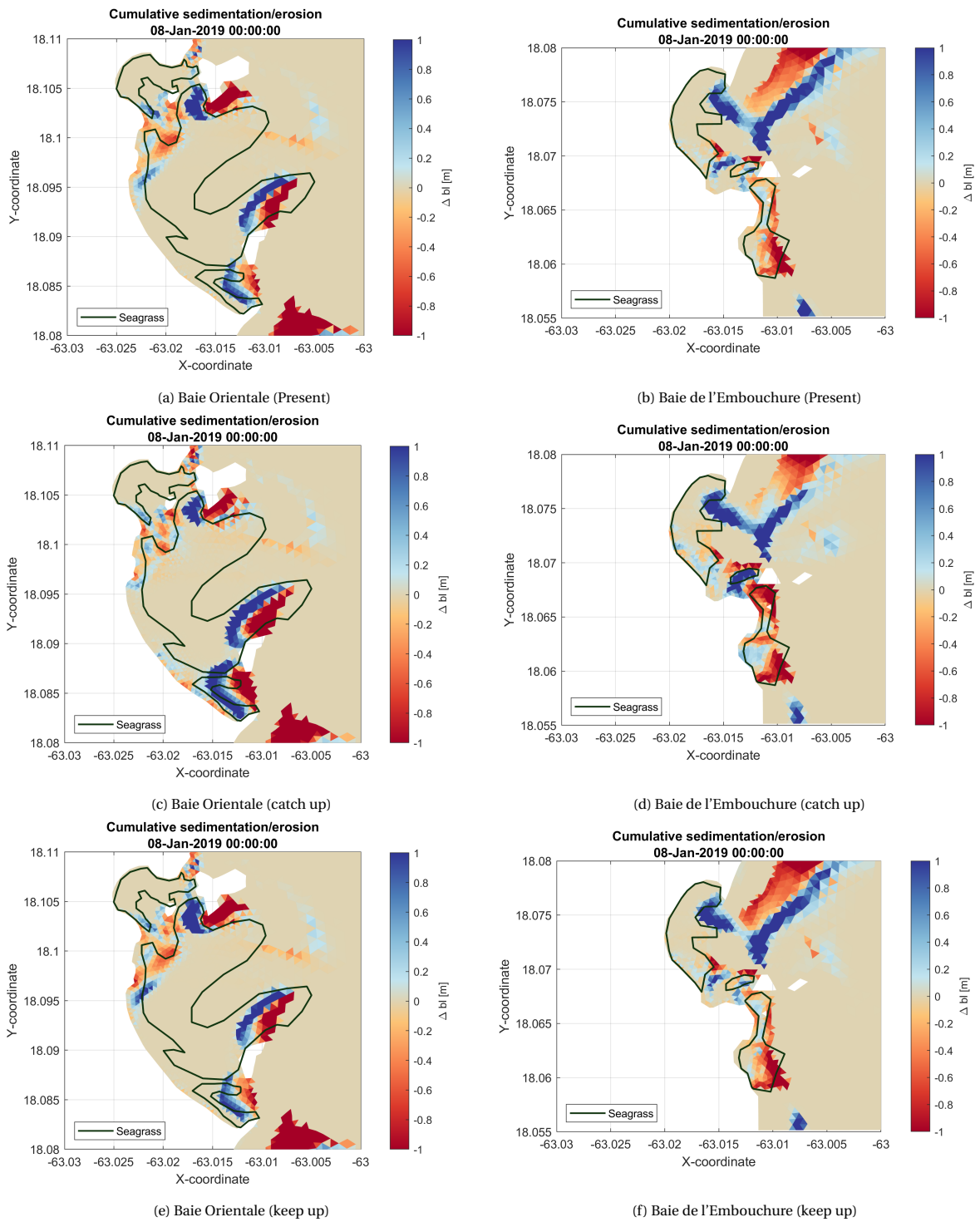


Figure 6.11: Morphological development for the climate change scenarios. The erosion under the catch up scenario increases significantly and the southern parts of both beaches show a regression. The increased erosion under the keep up is not as significant.

Whilst the erosion increases due to the higher hydrodynamic forces, the stabilization role of seagrass reduces for both sea-level rise scenarios. The relative reduction of the sediment stabilization under the catch up scenario is significant and equals 15%. Whilst, the sediment stabilization for the keep up scenario almost remains the same (relative reduction of 1%).

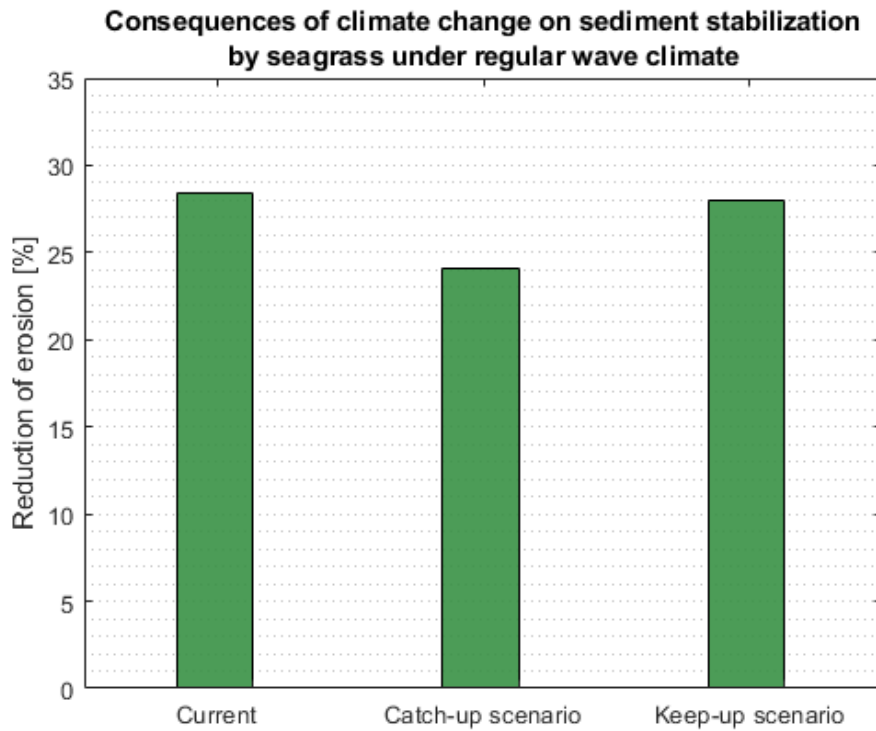


Figure 6.12: Stabilization role of seagrass under climate change. The sediment stabilization by seagrass reduces for both sea-level rise scenarios. The reduction is substantial for the catch up scenario and insignificant for the keep up scenario.

7

Discussion

Some aspects of this research need to be reflected before a conclusion can be drawn. A reflection of the model setup is treated in Section 7.1. The results of this study are also linked to findings of different researches, to check the consistency of the outcomes and to relate the relevance of the findings with practice. The significance of seagrass ecosystems in the foreshore is highlighted in Section 7.2. In Section 7.3, attention is drawn to the inter-ecosystem interactions between seagrass and reefs. Finally, the findings of the future role of seagrass are discussed in Section 7.4.

7.1. Model setup

7.1.1. Morphodynamic development

The hydrodynamic and morphological conditions in the model setup have been simplified for the sake of simplicity and analysis of the results. However, a distorted disequilibrium can be expected when disturbances on the hydrodynamic and/or morphological conditions are imposed that differ from reality. The morphodynamic disequilibrium leads especially in the beginning stage of the simulations to large morphological changes and reduces over time (Figure 7.1).

It has been decided to force the model with a stationary wave climate. This reflects on the pattern of the morphological changes and mainly affects where the erosion takes places and in which direction the sediment is transported. In reality, the wave climate is irregular that varies in time (i.e. varying waveform, wave height, and direction). The discrepancies of the wave conditions have a significant influence on the sediment transport. For instance, the wave directions over an entire year vary between the ESE and ENE sectors in Saint Martin (AGRNSM, 2009b) which does not enlarge the monotone sediment fluxes but rather would reduce the net fluxes.

The morphological changes in the coastal bays are of a monotonic character. The erosion is amplified over time, as a consequence of the applied simplifications of the model setup and imposed disturbances. The simulated erosion might not be representative of reality for which the net morphological changes are expected to be smaller. Therefore, the focus in this research is of a qualitative nature in which the conclusions are not based on the representation of the absolute quantities of erosion. But rather, a qualitative analysis is performed on the relative differences of the erosion to assess the role of the seagrass meadows on coastal erosion.

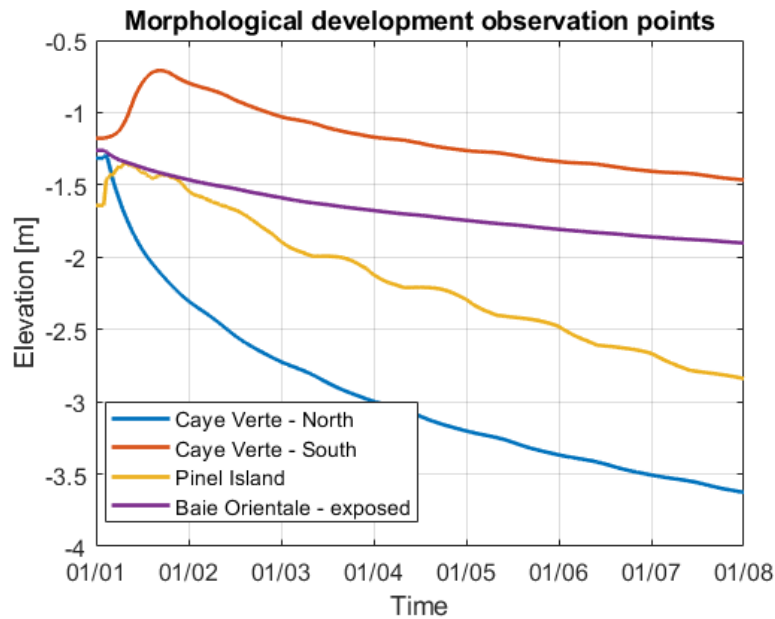


Figure 7.1: Morphological development of observation points (O1-O4, as indicated in Figure 4.5). The erosion rates are especially high in the beginning stage when the disequilibrium is largest and reduce over time.

7.1.2. Vegetation formulation

It has been found that reefs predominately dissipate the wave energy, whilst the seagrass meadows attenuate the waves to a lesser extent. Coral reefs dissipate high wave forces by depth-induced wave breaking and the reef friction (Ferrario et al., 2014), whereas seagrass meadows only attenuate the hydrodynamic energy via the exerted drag which depends on the leaf structure and stem density (Gillis et al., 2014).

Laboratory flume experiments have shown that the flow attenuation and dissipation of wave energy by seagrass are highly influenced by the relative vegetation height, whereas the shoot density is found to be not as significant (M. S. Fonseca & Cahalan, 1992; M. S. Fonseca & Fisher, 1986; M. Fonseca et al., 1982). The relevance of the relative vegetation height is consistent with the findings of this research (Section 6.3). It has been found that the attenuation of the flows is particularly sensitive to vegetation height and to a lesser extent to the vegetation density. The wave attenuation is also found to be sensitive to the vegetation height but to a lesser extent compared to the flow velocities, and almost equally important as the vegetation density.

It is a possibility that the hydrodynamic sensitivity to the vegetation density might be overestimated. The drag coefficients are used as calibration parameters and imposed as constant values in the formulations of the vegetation. Whereas, in reality, the spatial arrangement and a higher vegetation density might lower the drag exerted by vegetation as a consequence of the lowered turbulent motions and dissipation through the vegetation (P. M. J. Herman, personal communication, July 5, 2019).

The sediment stabilization by seagrass is reflected through the attenuation of the flow and waves. The decline of the sediment stabilization increases for smaller vegetation heights and highlights the relevance of the vegetation height. This is in line with the formulation of the vegetation roughness in which the logarithmic part of the formulation becomes dominant for the larger vegetation heights (Equation 2.5). Another experimental study not only emphasizes the importance of the vegetation height regarding the immobilization of sediment but also the belowground biomass (Christianen et al., 2013).

Another limitation is the representation of the vegetation as rigid cylinders. The flexible nature of seagrass reduces the drag, whereas it increases for stiffer species (Bouma et al., 2005). The leaves bend as a consequence of the flows and waves which decreases the vegetation area for drag and introduces lift forces. But the swaying movement of the vegetation may also cause additional resistance. However, this limitation is considered to be of less relevance. The genetic formulation of the vegetation resistance yields a reasonable fit with data from laboratory flume experiments, which include flexible vegetation types as well (Baptist et al., 2007).

7.2. Effectiveness seagrass

The seagrass meadows have been found to effectively counter the erosion in the shallow regions, whereas the erosion is reduced less effectively in the deeper regions. The sediment stabilization does also vary under different wave conditions since the wave climate has a strong influence on the water level in the sheltered bays.

The significance of the seagrass in the shallow regions is also consistent with the findings of another experimental research (James et al., 2019). A mobile flume is used in this study to assess the impact of seagrass on sediment stabilization in Baie de l'Embouchure. James et al. (2019) emphasize the relevance of the sediment stabilization by seagrass in the foreshore as well and suggest that seagrass might be an effective solution for maintaining tropical beaches worldwide.

7.3. Seagrass and reef interaction

Gillis et al. (2014) state the potential for reciprocal connections among marine coastal ecosystems through long-distance interactions. Interactions between seagrass and wave action are important in shaping the spatial distribution of seagrass meadows (Van Der Heide et al., 2010). The physical protection from high wave energy by coral reefs provides a sheltering function and facilitate the habitat of seagrass meadows (Saunders et al., 2014). Vice versa, seagrass ecosystems provide an important reciprocal service to the corals by acting as a buffer against excessive sediment and nutrients fluxes towards the reefs (F. T. Short & Short, 1984; Rogers, 1990). It has been shown that isolated reefs have a decreased algal biomass, in contrast to reefs that are located in the proximity of seagrass habitats (Gillis et al., 2014). A loss of seagrass meadows is therefore expected to cause a decrease in calcification rates of corals (Gillis et al., 2014).

This study shows that the sediment stabilization by seagrass is substantially affected by the wave set-up. Furthermore, it has been found that reefs predominantly dissipate wave energy. To assess the relevance of the reefs and their influences on the stabilizing role of seagrass, the bathymetric reef structures have been removed. It might be expected that the accompanied morphological disturbances would lead to a larger disequilibrium. The absolute quantities of the erosion might, therefore, be overestimated, as treated in Section 7.1. However, the relative differences of the erosion have been analyzed which reveals an interesting inter-ecosystem enhancement of erosion control.

From the results in Section 6.4, it can be inferred that reefs positively influence the sediment stabilization by seagrass due to the reduced water levels, wave motions and bed shear stresses inside the sheltered bays. Furthermore, the reduction of the erosion by reefs is also strengthened by the presence of seagrass meadows due to the subtle seagrass-induced water level set-up and lowered bed shear stresses. This shows that the interactions between seagrass and coral reefs are not only beneficial for the ecosystems themselves but also contribute to coastal resilience.

7.4. Future role of seagrass

This study shows that the stabilization role of seagrass is likely to reduce considerably due to climate change. Whilst, the coastal erosion, and beach regression will increase when the bays, seagrass, and coral reefs are not able to keep up with sea-level rise. When the bays and ecosystems are able to keep up with sea-level rise, the increased erosion and reduction of the seagrass impact are limited. However, the keep up scenario might be unlikely due to the expected increased deterioration of coral reefs as a consequence of the higher frequency of bleaching events and the limited adaptation time reefs will have (Hoegh-Guldberg et al., 2007). A limitation is that the dynamic evolution of the seagrass meadows has not been taken into account explicitly in the defined future scenarios. This adds to the uncertainty of the future development of the coastal bays.

Seagrass ecosystems are endangered e.g. by direct human interventions. An example is the physical removal of seagrass beds for purposes of the tourism industry. Seagrass beds are regarded to be unsightly and often sandy beaches with turquoise, clear waters are preferred. Based on the results of this study, this can be expected to be harmful to the shores on the longer timescales. This is only based on loss of the sediment stabilization and does not involve any harm that yields from the loss of other seagrass ecosystem services. A few practical cases that show (potential) causes and consequences of the loss of seagrass are summarized below:

- The seagrass meadows have been actively removed by hotel owners in Mauritius. A monitoring campaign revealed that the suspension of sediment particles increased in a pleasant swimming zone where the seagrass had been removed. This resulted in more destabilization of the seabed compared to an undisturbed area (Daby, 2003).
- Even if the seagrass meadows are not physically removed, seagrass could be lost. When a marine protected area is open for educational tourism (to foster environmental educational), this still could lead to degradation of the seagrass beds (Herrera-Silveira et al., 2010). There are evident differences in vegetation fields between a heavily visited and unvisited location in Costa Occidental de Isla Mujeres, Pjunta Cancún y punta Nizuc (Mexican Caribbean). The visited locations show sparser and shorter vegetation fields with reduced growth rates of *T. Testudinum* and are likely due to the harmful impacts of inexperienced and careless snorkelers.
- The seagrass in Saint Martin are protected (AGRNSM, 2009b), however, even good willing human interventions could potentially lead to unintended loss of seagrass. The sea turtles in the French Caribbean are conserved and protected from extinction since 1991 (AGRNSM, 2016). If a monitoring program of the population dynamics of such species is not carefully carried out, this could result in over-protection and cause an overabundance of the protected species (Gortázar et al., 2016). This would lead to excessive grazing of the seagrass and could possibly distort the ecosystem balance which will violate both the seagrass meadows and the population of the protected turtles.
- Seagrass beds were damaged by propellers of motorboats in Florida. Full recovery of the *T. Testudinum* meadows would require an average of 3.5-4.1 years (Davenport & Davenport, 2006; Dawes et al., 1997).

8

Conclusion and recommendations

The conclusion of this research is presented in Section 8.1. Thereafter, recommendations of opportunities for further model extensions, research and managing coastal bays are given in Section 8.2.

8.1. Conclusion

The presence of (barrier) reefs characterizes tropical sheltered bays. Reefs highly affect the wave field and initiate flows that circulate in the bays. It is shown that the bed shear stress is dominated by the waves and to a lesser extent by the flows. The coastal erosion is, therefore, more prominent in the exposed region, whereas the more sheltered areas are found to be more resilient. The erosion takes place in shallow waters but remains limited under regular swell conditions. The increased wave energy, during an extreme storm event, increases the erosion rates considerably. However, the regular swell conditions are normative in shaping the morphological development of both these coastal bays when longer timescales are considered.

The hydrodynamic attenuation and sediment stabilization by seagrass are found to be strongly influenced by the vegetation height and location of the meadows. The seagrass counters erosion most effectively in the foreshore and much less in deeper regions. Removal of seagrass in the foreshore (between 1-3m) halves the sediment stabilization. In contrast, the sediment stabilization increases if the meadows are able to spread especially towards the shore.

The impact of the seagrass on sediment stabilization is also affected to a great extent by the wave climate. The stabilization typically decreases for higher and shorter (storm) waves, primarily due to the increased wave set-up and bed shear stress. Whereas, the stabilization increases for smaller and longer (swell) waves. The sediment stabilization offered by seagrass varies between 17.1% and 59.8%.

The long-distance interactions between seagrass meadows and coral reefs have led to their mutual coexistence. These interactions are found to be beneficial for the erosion control of the coastal bays. Reefs reinforce the sediment stabilization provided by seagrass and vice versa. The dissipation of wave energy on top of the reefs fosters the sediment stabilization by seagrass. Moreover, the impact of reefs on sediment stabilization also increases in the presence of the seagrass meadows due to the additional drag exerted by the seagrass. The seagrass meadows are typically more effective under swell waves, whereas the reefs are more dominant in the dissipation of the higher and shorter storm waves. The coexistence of seagrass meadows and coral reefs can thus be regarded as ideal regarding the coastal erosion, apart from all other ecological benefits.

The tropical sheltered bays are expected to be vulnerable to rapidly rising sea levels. The present stabilization role of the seagrass on the sediments has been found to be quite significant. However, the impact of the seagrass on sediment stabilization will reduce considerably when the bays, seagrass and reef ecosystems are not able to keep up with sea-level rise. Increased erosion and beach regression are likely to occur as a consequence

of the higher wave energy inside the sheltered bays and reduced sediment stabilization by seagrass.

On a concluding note, the hydrodynamic attenuation and sediment stabilization provided by seagrass meadows are significant. The impact of seagrass is most effective in shallow and sheltered regions under typically smaller and longer (swell) waves. Whilst, coral reefs are more dominant in attenuating the higher and shorter (storm) waves. Seagrass and reef ecosystems form thus an ideal synergy in which the stabilization of sediments by the individual ecosystems is facilitated, reinforced, and complemented by the proximate presence of the other ecosystem. Seagrass meadows effectively stabilize the erosion in the foreshore and the impact could increase if the seagrass meadows would extend towards the shore. However, these tropical coastal bays and ecosystems are vulnerable and might be threatened by the rising sea levels and climate change. The sediment stabilization by seagrass might be weakened and will lead to increased coastal erosion.

8.2. Recommendations

Recommendations for model extensions and possibilities for innovative research applications of the current biogeomorphic model are indicated in this section. Moreover, practical suggestions for managing coastal bays are highlighted.

8.2.1. Model extensions

Additional seagrass processes that are known to affect the hydrodynamics and/or morphology could be added:

- **The bed stiffness** is increased by the seagrass roots, whereas a bare bed is looser and easier to erode. The strengthening of the bed relates therefore to the belowground biomass of seagrass which has been found to have a major effect on the immobilization of sediment (Christianen et al., 2013).
- **The complex turbulent interplay** between the flow and vegetation is not taken into account in the adopted formulation of the vegetation roughness (Baptist et al., 2007). The turbulent water motions are found to be especially large at the canopy-water interface (Gambi et al., 1990). Turbulence affects the drag exerted by seagrass and the transport of sediments. The exerted vegetation resistance on flows and waves is typically a three-dimensional problem due to the vertical heterogeneity of vegetation. Therefore, a three-dimensional model could be adopted, in which the depth-averaged vegetation roughness could be exchanged with a so-called rigid rod formulation Deltares (2019b). The rigid rod formulation represents the vertical variations inside the vegetation layer. This might also solve for deficiency of the representation of the vegetation drag and its dependencies with the vegetation shoot density and turbulence. However, this extension would also lead to a more sophisticated model that is computationally expensive. It has to be investigated whether such a model is feasible to run for large coastal areas.

Baie Orientale and Baie de l'Embouchure were used to study the sediment stabilization role of seagrass. A precise model setup of the case study area was therefore of less priority. The objective was not to simulate the actual quantities of the morphological changes in the two bays, but rather to qualitatively assess the relative changes under different environmental conditions and scenarios. However, it is recommended to further improve the model accuracy if this model is going to be used to obtain more precise quantitative results. The model setup should match reality even better regarding the local hydrodynamic and morphological conditions. The diversity of the state of seagrass meadows and coral reefs should also be elaborated in the model setup. Regarding the reefs, further investigation is a necessity to correctly incorporate the increased rugosity of the reefs.

8.2.2. Innovative research applications

A follow-up of this research could be to investigate the development of seagrass meadows with the use of a Dynamic Vegetation Module (DVM):

- A logistic growth formulation has been found to describe the spatial growth of *Spartina anglica* well for the coastal salt marsh in the Westerschelde, Netherlands (Temmerman et al., 2007). The development of the seagrass meadows is simulated by allowing the seagrass to grow in the number of stems per unit area. This logistic growth formulation does implicitly include several ecological stages and processes:
 - A slow growth rate at the beginning stage of the vegetation's lifetime.
 - A growth rate that is related to the state of the vegetation.
 - A stabilized growth limit induced by the carrying capacity, self-shading effects, and grazing.
- To provide more accurate predictions, the reciprocal impacts of the hydrodynamics and morphology on seagrass ecosystems should also be incorporated in the DVM. Some relations that affect the seagrass are:
 - Light is a crucial source of energy needed for the photosynthesis of seagrass. The surface light irradiance does penetrate through the water to the seagrass. The light is thereby weakened and imposes a lower depth limit to seagrass (Duarte, 1991). The light attenuation also depends on the suspended (sediment) concentrations (Carr et al., 2010).
 - The physical impact of waves imposes an upper depth limit (M. A. Hemminga & Duarte, 2000, P.16).
 - Burial and erosion of vegetated beds limit the vegetation presence (Cabaço et al., 2008).
- The impacts of extreme storm conditions on seagrass damage and recovery could be studied with the DVM. For this purpose, also the lateral seagrass colonization and longitudinal rhizome elongation could be included.

An important factor in the development of coastal bays is the response of coral reefs to climate change and how this is going to affect the seagrass meadows. It is recommended to further assess the interactions between seagrass and reef ecosystems. Improvements in the scenarios of reef evolution would enhance the predictions of the state of seagrass and coastal bays. For this reason, a Dynamic Coral Reef Module could be constructed to simulate the growth of coral reefs and could be linked to the current biogeomorphic model.

8.2.3. Managing coastal bays

The synergy between seagrass and reefs regarding erosion control emphasizes that the state and responses of both ecosystems are of importance for the future of tropical sheltered bays. Seagrass and reef ecosystems can be viewed as self-organized by the long-distance interactions and form an intertwined network (van de Koppel et al., 2015). These coastal (eco)systems should therefore not be managed in isolation. The integrated marine ecosystem services might even be a sustainable and ecological alternative for conventional coastal defense strategies against coastal hazards and climate change (Temmerman et al., 2013).

However, the indicated significance of the sediment stabilization offered by seagrass is an alarming message if seagrass meadows continue to vanish. It is, therefore, important to identify the aspects that contribute to the damage of seagrass meadows. Monitoring of the seagrass meadows is a necessity to understand the current state and development of seagrass (Unsworth et al., 2019). Besides, effort needs to be made to restore damaged seagrass meadows and could be reinforced with artificial seagrass to rehabilitate the damaged meadows (Talbot & Wilkinson, 2001). Above all, the lack of awareness and attention on the value of the seagrass ecosystem services (Unsworth et al., 2019) should be addressed. Proportionate regulations need to be asserted to stop the decline of seagrass ecosystems. This should prevent human activities that degrade seagrass ecosystems, such as the removal of seagrass meadows in touristic coastal areas. An example of a recent movement that tries to raise awareness about the values of the seagrass ecosystems is the #ProtectMaldivesSeagrass campaign. This campaign endeavors to protect the seagrass meadows, which have been actively removed around the low-lying islands of the Maldives by many resorts (Blue Marine Foundation, 2019).

Bibliography

- AGRNSM. (2009a). *Illustrations Cartographiques*. Plan de gestion 2010-2015.
- AGRNSM. (2009b). *PLAN DE GESTION DE LA RÉSERVE NATURELLE NATIONALE DE L'ÎLE DE SAINT-MARTIN ET DES SITES DU CONSERVATOIRE DE L'ESPACE LITTORAL ET DES RIVAGES LACUSTRES*. Plan de gestion 2010-2015.
- AGRNSM. (2016). *La terre ne nous appartient pas, ce sont nos enfants qui nous la prêtent*. Le Journal DE LA RÉSERVE NATURELLE DE SAINT-MARTIN.
- AGRNSM. (2018). *Partie B - Gestion de la RNN*. Plan de gestion 2018-2027.
- Ateweberhan, M., Feary, D. A., Keshavmurthy, S., Chen, A., Schleyer, M. H., & Sheppard, C. R. (2013). Climate change impacts on coral reefs: synergies with local effects, possibilities for acclimation, and management implications. *Marine pollution bulletin*, 74(2), 526–539.
- Balke, T., Herman, P. M., & Bouma, T. J. (2014). Critical transitions in disturbance-driven ecosystems: identifying windows of opportunity for recovery. *Journal of Ecology*, 102(3), 700–708.
- Baptist, M., Babovic, V., Rodríguez Uthurburu, J., Keijzer, M., Uittenbogaard, R., Mynett, A., & Verwey, A. (2007). On inducing equations for vegetation resistance. *Journal of Hydraulic Research*, 45(4), 435–450.
- Barbier, E. B., Hacker, S. D., Kennedy, C., Koch, E. W., Stier, A. C., & Silliman, B. R. (2011). The value of estuarine and coastal ecosystem services. *Ecological monographs*, 81(2), 169–193.
- Beccario, C. (2019). *A visualization of global weather conditions forecast by supercomputers updated every three hours*. Retrieved 2019-09-10, from <https://earth.nullschool.net/about.html>
- Bijker, E. (1992). Mechanics of sediment transport by the combination of waves and current. *Design and Reliability of Coastal Structures, short course during the 23rd ICCE in Venice*.
- Blue Marine Foundation. (2019). *THE MALDIVES RESILIENT REEFS PROJECT #ProtectMaldivesSeagrass*. Retrieved 2019-10-06, from <http://www.maldivesresilientreefs.com/campaigns/seagrass/>
- Bosboom, J., & Stive, M. J. (2015). *Coastal dynamics i*. Delft Academic Press.
- Bouchon, C., Bouchon-Navaro, Y., Brugneaux, S., & Mazeas, F. (2000). L'état des récifs coralliens dans les antilles françaises. martinique, guadeloupe, saint barthélemy et saint martin. *Rapport IFRECOR*.
- Bouchon, C., Bouchon-Navaro, Y., & Louis, M. (1995). Les biocénoses marines côtières de l'île de saint-martin. *Étude scientifique pour la création d'une réserve naturelle. Rapport UAG*.
- Bouma, T., De Vries, M., Low, E., Peralta, G., Tánzos, I. v., van de Koppel, J., & Herman, P. M. J. (2005). Trade-offs related to ecosystem engineering: A case study on stiffness of emerging macrophytes. *Ecology*, 86(8), 2187–2199.
- Cabaço, S., Santos, R., & Duarte, C. M. (2008). The impact of sediment burial and erosion on seagrasses: a review. *Estuarine, Coastal and Shelf Science*, 79(3), 354–366.

- Carr, J., D'odorico, P., McGlathery, K., & Wiberg, P. (2010). Stability and bistability of seagrass ecosystems in shallow coastal lagoons: Role of feedbacks with sediment resuspension and light attenuation. *Journal of Geophysical Research: Biogeosciences*, 115(G3).
- Central Intelligence Agency [US]. (2018). *The World Factbook: Saint Martin*. Retrieved 2019-01-15, from <https://www.cia.gov/library/publications/the-world-factbook/geos/rn.html>
- Christianen, M. J., van Belzen, J., Herman, P. M., van Katwijk, M. M., Lamers, L. P., van Leent, P. J., & Bouma, T. J. (2013). Low-canopy seagrass beds still provide important coastal protection services. *PloS one*, 8(5), e62413.
- Costanza, R., d'Arge, R., De Groot, R., Farber, S., Grasso, M., Hannon, B., ... others (1997). The value of the world's ecosystem services and natural capital. *nature*, 387(6630), 253.
- Cox, P. M., Betts, R. A., Jones, C. D., Spall, S. A., & Totterdell, I. J. (2000). Acceleration of global warming due to carbon-cycle feedbacks in a coupled climate model. *Nature*, 408(6809), 184.
- Daby, D. (2003). Effects of seagrass bed removal for tourism purposes in a mauritian bay. *Environmental Pollution*, 125(3), 313–324.
- Dalrymple, R. A., Kirby, J. T., & Hwang, P. A. (1984). Wave diffraction due to areas of energy dissipation. *Journal of Waterway, Port, Coastal, and Ocean Engineering*, 110(1), 67–79.
- Das, B. M. (2013). *Advanced soil mechanics*. Crc Press.
- Davenport, J., & Davenport, J. L. (2006). The impact of tourism and personal leisure transport on coastal environments: a review. *Estuarine, Coastal and Shelf Science*, 67(1-2), 280–292.
- Dawes, C. J., Andorfer, J., Rose, C., Uranowski, C., & Ehringer, N. (1997). Regrowth of the seagrass *thalassia testudinum* into propeller scars. *Aquatic Botany*, 59(1-2), 139–155.
- Deltares. (2019a). *Delft3d flexible mesh suite*. Retrieved 15-04-2019, from <https://www.deltares.nl/en/software/delft3d-flexible-mesh-suite/>
- Deltares. (2019b). D-FLOW Flexible Mesh User Manual. *Delft, the Netherlands*.
- Deltares. (2019c). D-Morphology Flexible Mesh User Manual. *Delft, the Netherlands*.
- Deltares. (2019d). D-Waves Flexible Mesh User Manual. *Delft, the Netherlands*.
- Dewsbury, B. M., Bhat, M., & Fourqurean, J. W. (2016). A review of seagrass economic valuations: Gaps and progress in valuation approaches. *Ecosystem Services*, 18, 68–77.
- Duarte, C. M. (1991). Seagrass depth limits. *Aquatic botany*, 40(4), 363–377.
- Duarte, C. M. (2002). The future of seagrass meadows. *Environmental conservation*, 29(2), 192–206.
- Duarte, C. M., & Chiscano, C. L. (1999). Seagrass biomass and production: a reassessment. *Aquatic botany*, 65(1-4), 159–174.
- Duarte, C. M., Dennison, W. C., Orth, R. J., & Carruthers, T. J. (2008). The charisma of coastal ecosystems: addressing the imbalance. *Estuaries and coasts*, 31(2), 233–238.
- Dunton, K. (1994). Seasonal growth and biomass of the subtropical seagrass *halodule wrightii* in relation to continuous measurements of underwater irradiance. *Marine Biology*, 120(3), 479–489.

- Dutch Caribbean Nature Alliance. (n.d.-a). *Coral reefs*. Retrieved 2019-02-04, from <https://www.dcnanature.org/nature/ecosystems/coral-reefs/>
- Dutch Caribbean Nature Alliance. (n.d.-b). *Seagrass beds*. Retrieved 2019-02-04, from <https://www.dcnanature.org/nature/ecosystems/seagrass-beds/>
- Dutch Caribbean Nature Alliance. (2017). *BioNews 7 - St. Maarten: Impact Hurricane Irma on Nature*. Retrieved 2019-02-06, from <https://www.dcnanature.org/wp-content/uploads/2017/11/BioNews-2017-Issue7-Online2.pdf>
- Elliff, C. I., & Silva, I. R. (2017). Coral reefs as the first line of defense: Shoreline protection in face of climate change. *Marine environmental research*, 127, 148–154.
- Ettema, R. (2006). Hunter rouse—his work in retrospect. *Journal of Hydraulic Engineering*, 132(12), 1248–1258.
- Ferrario, F., Beck, M. W., Storlazzi, C. D., Micheli, F., Shepard, C. C., & Airoidi, L. (2014). The effectiveness of coral reefs for coastal hazard risk reduction and adaptation. *Nature communications*, 5, 3794.
- Fonseca, M., Fisher, J., Zieman, J., & Thayer, G. (1982). Influence of the seagrass, *zostera marina* L., on current flow. *Estuarine, Coastal and Shelf Science*, 15(4), 351–364.
- Fonseca, M. S., & Cahalan, J. A. (1992). A preliminary evaluation of wave attenuation by four species of seagrass. *Estuarine, Coastal and Shelf Science*, 35(6), 565–576.
- Fonseca, M. S., & Fisher, J. S. (1986). A comparison of canopy friction and sediment movement between four species of seagrass with reference to their ecology and restoration. *Marine Ecology Progress Series*, 29(1).
- Fourqurean, J. W., & Robblee, M. B. (1999). Florida bay: a history of recent ecological changes. *Estuaries*, 22(2), 345–357.
- Fredse, J. (1984). Turbulent boundary layer in wave-current interaction. *Journal of Hydraulic Engineering ASCE*, 110(HY), 1103–1120.
- Gaba, E. (2015). *Saint-martin island topographic map*. Retrieved from https://commons.wikimedia.org/wiki/File:Saint-Martin_Island_topographic_map-en.svg (File: Saint-Martin Island topographic map-en.svg)
- Gacia, E., Granata, T., & Duarte, C. (1999). An approach to measurement of particle flux and sediment retention within seagrass (*posidonia oceanica*) meadows. *Aquatic Botany*, 65(1-4), 255–268.
- Gambi, M. C., Nowell, A. R., & Jumars, P. A. (1990). Flume observations on flow dynamics in *zostera marina* (eelgrass) beds. *Marine ecology progress series. Oldendorf*, 61(1), 159–169.
- Gillis, L., Bouma, T., Jones, C., Van Katwijk, M., Nagelkerken, I., Jeuken, C., ... Ziegler, A. (2014). Potential for landscape-scale positive interactions among tropical marine ecosystems. *Marine Ecology Progress Series*, 503, 289–303.
- Google Earth. (2014). *Saint Martin*. Retrieved 2019-10-04, from <https://www.google.nl/intl/nl/earth/>
- Google Earth Engine. (2019). *Timelapse Saint Martin*. Retrieved 2019-05-22, from <https://earthengine.google.com/timelapse/>
- Google Maps. (2019). *Baie Orientale and baie de l'Embouchure, Sint Maarten*. Retrieved 2019-06-13, from <https://www.google.nl/maps/place/Sint+Maarten>

- Gortázar, C., Ruiz-Fons, J., & Höfle, U. (2016). Infections shared with wildlife: an updated perspective. *European Journal of Wildlife Research*, 62(5), 511–525.
- Graus, R. R., & Macintyre, I. G. (1998). Global warming and the future of caribbean coral reefs. *Carbonates and Evaporites*, 13(1), 43.
- Harley, C. D. G., Hughes, A. R., Kristin, M., Miner, B. G., Sorte, C. J. B., & Carol, S. (2006). REVIEWS AND The impacts of climate change in coastal marine systems. *Ecology Letters*, 228–241. doi: 10.1111/j.1461-0248.2005.00871.x
- Hasselmann, K., Barnett, T., Bouws, E., Carlson, H., Cartwright, D., Enke, K., . . . others (1973). Measurements of wind-wave growth and swell decay during the joint north sea wave project (jonswap). *Ergänzungsheft 8-12*.
- Hemminga, M., & Nieuwenhuize, J. (1990). Seagrass wrack-induced dune formation on a tropical coast (banc d'arguin, mauritania). *Estuarine, Coastal and Shelf Science*, 31(4), 499–502.
- Hemminga, M. A., & Duarte, C. M. (2000). *Seagrass ecology*. Cambridge University Press.
- Herrera-Silveira, J. A., Cebrian, J., Hauxwell, J., Ramirez-Ramirez, J., & Ralph, P. (2010). Evidence of negative impacts of ecological tourism on turtlegrass (*thalassia testudinum*) beds in a marine protected area of the mexican caribbean. *Aquatic Ecology*, 44(1), 23–31.
- Hoegh-Guldberg, O. (1999, 01). Climate change, coral bleaching and the future of the world's coral reefs. *Marine and Freshwater Research*, 50. doi: 10.1071/MF99078
- Hoegh-Guldberg, O., Mumby, P. J., Hooten, A. J., Steneck, R. S., Greenfield, P., Gomez, E., . . . others (2007). Coral reefs under rapid climate change and ocean acidification. *science*, 318(5857), 1737–1742.
- Hoffman, J. S., Keyes, D. L., & Titus, J. G. (1983). *Projecting future sea level rise: methodology, estimates to the year 2100, and research needs*. Strategic Studies Staff, Office of Policy Analysis, Office of Policy and . . .
- Holthuijsen, L. H. (2010). *Waves in oceanic and coastal waters*. Cambridge University Press.
- IPCC. (2014). Climate change 2014: Synthesis Report. *Contribution of Working Group I, II and III to the Fifth Assessment Report of the Intergovernmental Panel on Climate Change, [Core Writing Team, R.K. Pachauri and L.A. Meyer (eds.)]*. IPCC, Geneva, Switzerland, 151 pp.
- James, R. K. (2015). *SXM Measurements*. (Unpublished raw data).
- James, R. K., Silva, R., van Tussenbroek, B. I., Escudero-Castillo, M., Mariño-Tapia, I., Dijkstra, H. A., . . . others (2019). Maintaining tropical beaches with seagrass and algae: a promising alternative to engineering solutions. *BioScience*, 69(2), 136–142.
- Jevrejeva, S., Jackson, L. P., Riva, R. E., Grinsted, A., & Moore, J. C. (2016). Coastal sea level rise with warming above 2 c. *Proceedings of the National Academy of Sciences*, 113(47), 13342–13347.
- Keyzer, L. (2018). *Predicting the impact of sea-level rise in Baie Orientale and Baie de L'Embouchure, Saint Martin*. (Master's thesis, Delft University of Technology). doi: uuid:7b21cf31-0c1d-43a6-86ed-b28249646bfa
- Koch, E. W., Ackerman, J. D., Verduin, J., & van Keulen, M. (2007). Fluid dynamics in seagrass ecology—from molecules to ecosystems. In *Seagrasses: Biology, ecology and conservation* (pp. 193–225). Springer.
- Koch, E. W., Sanford, L. P., Chen, S.-N., Shafer, D. J., & Smith, J. M. (2006). *Waves in seagrass systems: review and technical recommendations* (Tech. Rep.). MARYLAND UNIV CAMBRIDGE CENTER FOR ENVIRONMENTAL SCIENCE.

- Lotze, H. K., Lenihan, H. S., Bourque, B. J., Bradbury, R. H., Cooke, R. G., Kay, M. C., ... Jackson, J. B. (2006). Depletion, degradation, and recovery potential of estuaries and coastal seas. *Science*, 312(5781), 1806–1809.
- Lowe, R. J., Falter, J. L., Monismith, S. G., & Atkinson, M. J. (2009). Wave-driven circulation of a coastal reef-lagoon system. *Journal of Physical Oceanography*, 39(4), 873–893.
- Martin, C. M. (2019). *Tea tree turtle grass camo yoga leggings*. Retrieved 2019-10-15, from https://www.ohanacreationsfl.com/uploads/1/1/9/9/119904017/s381127054836313247_p98_i5_w2560.png
- Mendez, F. J., & Losada, I. J. (2004). An empirical model to estimate the propagation of random breaking and nonbreaking waves over vegetation fields. *Coastal Engineering*, 51(2), 103–118.
- Nepf, H., & Vivoni, E. (2000). Flow structure in depth-limited, vegetated flow. *Journal of Geophysical Research: Oceans*, 105(C12), 28547–28557.
- Nicholls, R. J., & Cazenave, A. (2010). Sea-level rise and its impact on coastal zones. *science*, 328(5985), 1517–1520.
- Nikuradze, J. (1930). *Turbulente stromungen in nichtkreisformigen rohren'ing*. Arch.
- NIOZ. (2014). *SCENES: Stability of Caribbean coastal Ecosystem uNder future Extreme Sea level changes*. Retrieved 2019-01-15, from <https://www.nioz.nl/en/research/projects/4164-0>
- Nurse, L. A., McLean, R. F., Agard, J., Briguglio, L. P., Duvat-Magnan, V., Pelesikoti, N., ... Webb, A. (2014). *Small islands*. Cambridge University Press.
- Orth, R. J., Carruthers, T. J., Dennison, W. C., Duarte, C. M., Fourqurean, J. W., Heck, K. L., ... others (2006). A global crisis for seagrass ecosystems. *Bioscience*, 56(12), 987–996.
- Pandolfi, J. M., Connolly, S. R., Marshall, D. J., & Cohen, A. L. (2011). Projecting coral reef futures under global warming and ocean acidification. *science*, 333(6041), 418–422.
- Paul, M., & Amos, C. (2011). Spatial and seasonal variation in wave attenuation over *zostera noltii*. *Journal of Geophysical Research: Oceans*, 116(C8).
- Pietrzak, J. (2017). *An introduction to oceanography for civil and offshore engineers*. Draft Lecture notes CIE5317.
- Preen, A., Long, W. L., & Coles, R. (1995). Flood and cyclone related loss, and partial recovery, of more than 1000 km² of seagrass in hervey bay, queensland, australia. *Aquatic Botany*, 52(1-2), 3–17.
- Quataert, E., Storlazzi, C., Rooijen, A., Cheriton, O., & Dongeren, A. (2015). The influence of coral reefs and climate change on wave-driven flooding of tropical coastlines. *Geophysical Research Letters*, 42(15), 6407–6415.
- Rogers, C. S. (1990). Responses of coral reefs and reef organisms to sedimentation. *Marine ecology progress series. Oldendorf*, 62(1), 185–202.
- Rosaz, k., & Azzar, C. (2018). A year on, Caribbean islands bear scars of Hurricane Irma. *Phys.org - News and Articles on Science and Technology*. Retrieved 2019-02-06, from <https://phys.org/news/2018-09-year-caribbean-islands-scars-hurricane.html>
- Rouse, H. (1937). Modern conceptions of the mechanics of fluid turbulence. *Trans ASCE*, 102, 463–505.
- Ruggiero, P., Buijsman, M., Kaminsky, G. M., & Gelfenbaum, G. (2010). Modeling the effects of wave climate and sediment supply variability on large-scale shoreline change. *Marine Geology*, 273(1-4), 127–140.

- Saunders, M. I., Albert, S., Roelfsema, C. M., Leon, J. X., Woodroffe, C. D., Phinn, S. R., & Mumby, P. J. (2016). Tectonic subsidence provides insight into possible coral reef futures under rapid sea-level rise. *Coral Reefs*, 35(1), 155–167.
- Saunders, M. I., Leon, J. X., Callaghan, D. P., Roelfsema, C. M., Hamylton, S., Brown, C. J., ... Mumby, P. J. (2014). Interdependency of tropical marine ecosystems in response to climate change. *Nature Climate Change*, 4(8), 724–729. doi: 10.1038/nclimate2274
- Sheppard, C., Dixon, D. J., Gourlay, M., Sheppard, A., & Payet, R. (2005). Coral mortality increases wave energy reaching shores protected by reef flats: examples from the seychelles. *Estuarine, Coastal and Shelf Science*, 64(2-3), 223–234.
- Short, F., Carruthers, T., Dennison, W., & Waycott, M. (2007). Global seagrass distribution and diversity: a bioregional model. *Journal of Experimental Marine Biology and Ecology*, 350(1-2), 3–20.
- Short, F. T., & Neckles, H. A. (1999). The effects of global climate change on seagrasses. *Aquatic Botany*, 63(3-4), 169–196.
- Short, F. T., & Short, C. A. (1984). The seagrass filter: purification of estuarine and coastal waters. In *The estuary as a filter* (pp. 395–413). Elsevier.
- Smits, A. J. (2000). *A physical introduction to fluid mechanics*. Wiley.
- Soulsby, R. L., Hamm, L., Klopman, G., Myrhaug, D., Simons, R. R., & Thomas, G. P. (1993). Wave-current interaction within and outside the bottom boundary layer. *Coastal engineering*, 21(1-3), 41–69.
- Talbot, F., & Wilkinson, C. (2001). *Coral reefs, mangroves and seagrasses: A sourcebook for managers*. Australian Institute of Marine Science,.
- Temmerman, S., Bouma, T., Van de Koppel, J., Van der Wal, D., De Vries, M., & Herman, P. (2007). Vegetation causes channel erosion in a tidal landscape. *Geology*, 35(7), 631–634.
- Temmerman, S., Meire, P., Bouma, T. J., Herman, P. M., Ysebaert, T., & De Vriend, H. J. (2013). Ecosystem-based coastal defence in the face of global change. *Nature*, 504(7478), 79.
- TIDES4FISHING. (2015). *Tide time and charts for Gustavia (Saint Barthelemy)*. Retrieved 2019-04-30, from <https://tides4fishing.com/ci/lesser-antilles-and-virgin-islands/gustavia-saint-barthelemy>
- Tomasko, D., & Dawes, C. (1990). Influences of season and water depth on the clonal biology of the seagrass *Thalassia testudinum*. *Marine Biology*, 105(2), 345–351.
- Uijtewaal, W. (2018). *Turbulence in hydraulics*. Lecture notes CIE5312.
- Unsworth, R. K., Collier, C. J., Henderson, G. M., & McKenzie, L. J. (2012). Tropical seagrass meadows modify seawater carbon chemistry: implications for coral reefs impacted by ocean acidification. *Environmental Research Letters*, 7(2), 024026.
- Unsworth, R. K., McKenzie, L. J., Collier, C. J., Cullen-Unsworth, L. C., Duarte, C. M., Eklöf, J. S., ... Nordlund, L. M. (2019). Global challenges for seagrass conservation. *Ambio*, 48(8), 801–815.
- Valdés, D., & Real, E. (1994). Ammonium, nitrite, nitrate and phosphate fluxes across the sediment-water interface in a tropical lagoon. *ciencias Marinas*, 20(1), 65–80.

- van de Koppel, J., van der Heide, T., Altieri, A. H., Eriksson, B. K., Bouma, T. J., Olf, H., & Silliman, B. R. (2015). Long-distance interactions regulate the structure and resilience of coastal ecosystems. *Annual review of marine science*, 7, 139–158.
- Van Der Heide, T., Bouma, T. J., Van Nes, E. H., Van De Koppel, J., Scheffer, M., Roelofs, J. G., ... Smolders, A. J. (2010). Spatial self-organized patterning in seagrasses along a depth gradient of an intertidal ecosystem. *Ecology*, 91(2), 362–369.
- Van Rijn, L. C. (1993). *Principles of sediment transport in rivers, estuaries and coastal seas* (Vol. 1006). Aqua publications Amsterdam.
- Van Tussenbroek, B. I., Cortés, J., Collin, R., Fonseca, A. C., Gayle, P. M., Guzmán, H. M., ... others (2014). Caribbean-wide, long-term study of seagrass beds reveals local variations, shifts in community structure and occasional collapse. *PloS one*, 9(3), e90600.
- Verruijt, A., & Van Baars, S. (2007). *Soil mechanics*. VSSD Delft, the Netherlands.
- Waycott, M., Duarte, C. M., Carruthers, T. J. B., Orth, R. J., Dennison, W. C., Olyarnik, S., ... Williams, S. L. (2009). Accelerating loss of seagrasses across the globe threatens coastal ecosystems. *Proceedings of the National Academy of Sciences*, 1(19).
- Wild, C., Hoegh-Guldberg, O., Naumann, M. S., Colombo-Pallotta, M. F., Ateweberhan, M., Fitt, W. K., ... others (2011). Climate change impedes scleractinian corals as primary reef ecosystem engineers. *Marine and Freshwater Research*, 62(2), 205–215.
- Worm, B., Barbier, E. B., Beaumont, N., Duffy, J. E., Folke, C., Halpern, B. S., ... others (2006). Impacts of biodiversity loss on ocean ecosystem services. *science*, 314(5800), 787–790.
- Wright, L., & Short, A. D. (1984). Morphodynamic variability of surf zones and beaches: a synthesis. *Marine geology*, 56(1-4), 93–118.

A

Additional literature

This appendix includes additional literature findings that complement the literature study in Chapter 2.

A.1. Hydrodynamic behavior of coastal bays

Ocean waves are generated by wind and result in different wave climates. The wave climate of the Caribbean islands can be categorized as an East coast swell environment with seasonal variations. These waves result from far located storms generated at the Northern Atlantic Ocean. Due to the frequency-directional dispersion of waves, the irregular wave fields created locally at the storm site propagate and transform to regular swell waves (Holthuijsen, 2010, P. 175). Therefore, swell waves are typically continuous, long waves and are uniform in direction, shape and size (Bosboom & Stive, 2015, P.148-149).

Waves cause an oscillatory fluid motion associated with the motion of the water surface (Figure A.1). In deeper waters, the movement of water particles results in almost enclosed circles. The related vertical velocity profile shows a decay towards the bottom. In shallow waters, the movement of the particles could be described as elliptical paths that become flatter towards the bed. The velocity profile is uniform over the depth (Bosboom & Stive, 2015, P.178-180).

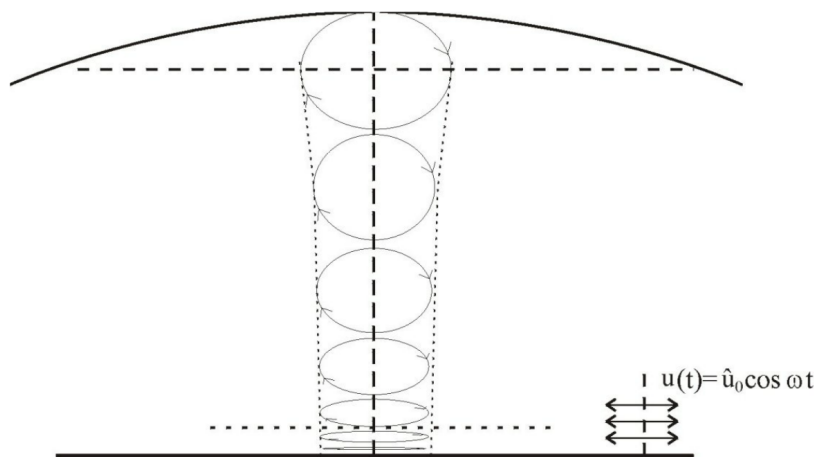


Figure A.1: Wave-induced orbital motion of fluid particles in intermediate to shallow water. The orbits of the particles are ellipsoids and become flatter towards the bed (Bosboom & Stive, 2015, P.178).

At the bed, a boundary layer can be found which forms the transition between the bed and the free stream velocity caused by the oscillatory wave motion (Figure A.2). The linear wave theory is not sufficient to describe

the fluid motion in this layer. The boundary layer is small (thickness δ order of a few centimeters) since the layer does not have sufficient time to develop due to the oscillatory behavior of the wave-induced currents. For waves with a larger wave period, the boundary layer grows slightly larger. The behavior of the horizontal flow velocities in this layer is different from velocities outside the boundary layer and are affected by the presence of the bed. Due to the bed friction, the flow velocities are reduced to zero (no-slip condition). Moreover, vorticity (rotation) is generated in this layer and the flow has, therefore, a turbulent character. A large velocity gradient can be found at the boundary layer which results in large shear stresses ($\tau \propto \frac{\partial u}{\partial z}$). Besides an oscillatory flow, waves induce a non-zero averaged flow called Longuet-Higgins streaming directed in the wave direction (Bosboom & Stive, 2015, P.181-183).

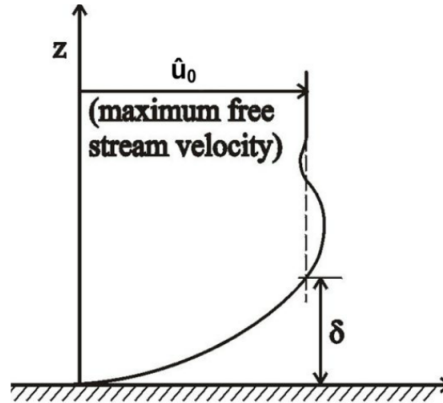


Figure A.2: Wave-induced velocity profile close to the boundary layer (Bosboom & Stive, 2015, P.181). The boundary layer is relatively small, since the layer does not have sufficient time to develop and gives rise to large bed shear stresses.

Likewise, flows experience friction by the bed. The resulting velocity profile for a fully rough bed is logarithmic (Figure A.3) as derived by Prandtl and Von Kármán:

$$u = \frac{u_*}{\kappa} \ln \left(\frac{z}{z_0} \right) \quad (\text{A.1})$$

where u_* represents the shear velocity, κ is the Von Kármán coefficient, and z_0 the roughness height. The roughness height can be expressed as $z_0 = k_s/30$, where k_s is the Nikuradse roughness height (Nikuradze, 1930). The roughness height can be related to the Chézy coefficient [$m^{1/2}s^{-1}$] with the White-Colebrook formula:

$$C = 18 \log \left(\frac{12R}{k_s} \right) \quad (\text{A.2})$$

where R is the hydraulic radius, which for wide-basin flows approximately equals the water depth (h). The Chézy coefficient can also be expressed in terms of the Manning roughness coefficient (n [$s/m^{1/3}$]) or the dimensionless friction factor, respectively:

$$C = \frac{\sqrt[6]{h}}{n} \quad (\text{A.3})$$

$$c_f = \frac{g}{C^2} \quad (\text{A.4})$$

Two layers can be distinguished in the boundary layer. The presence of the bed governs the flow in the inner layer, whilst the flow in the outer layer is governed by the whole flow geometry (Uijtewaal, 2018).

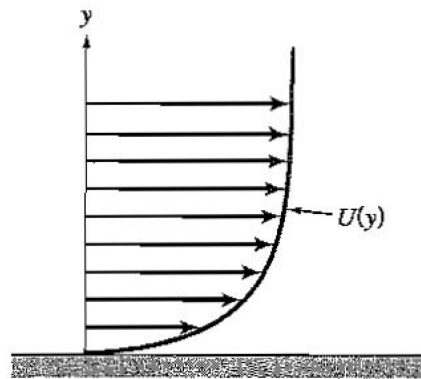


Figure A.3: Velocity profile of a confined flow by a solid and free surface (Smits, 2000). Turbulence is generated in the boundary layer due to the gradients of the velocity profile.

A.2. Morphological behavior of coastal bays

Bed-load transport

Bed-load transport is caused by the flow- and wave-induced bed shear stress. The combined water motion results in a shear stress which acts on the bed and forces sediment particles on the bed. Sediment will be set in motion when a certain threshold of the bed shear stress is exceeded (Bosboom & Stive, 2015, P.264-267). The forces on the sediment particles due to the water motion (Figure A.4) encompasses a drag force initiated by skin friction, a pressure difference around the sediment particle due to flow separation, and a lift force following from the Bernoulli principle (i.e. pressure difference due to contracting streamlines and increased flow velocities and flow separation). The resisting force is provided by gravity.

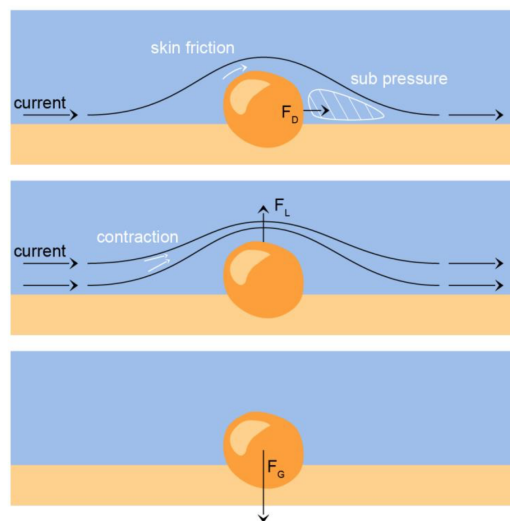


Figure A.4: Schematization of forces acting on an individual sediment particle in a stationary condition (Bosboom & Stive, 2015, P.264). The load forces are due to: the skin friction, a pressure gradient, and a lift force. The gravitational force is the resisting force.

A dimensionless constant, called the Shields parameter (θ_{cr}), can be deduced from the balance of forces. This constant is a valuable measure for the indication of the initiation of motion of sediment particles (Bosboom & Stive, 2015, P.265) and is defined as:

$$\theta_{cr} = \frac{\tau_{b,cr}}{(\rho_s - \rho_w)gD} \quad (\text{A.5})$$

where $(\rho_s - \rho_w)$ represents the submerged density of the sediment particles, g is the gravitational acceleration, and D is a characteristic measure for the diameter of the particles. The sediment density can be calculated if the porosity and the dry bulk density are known (Verruijt & Van Baars, 2007)[P.22]:

$$\rho_{s,dry} = (1 - n)\rho_s \quad (\text{A.6})$$

Suspended-load transport

Suspended-load transport occurs in the layer above the bed-load transport layer. The suspended sediment flux is computed as the product of the sediment concentration and the horizontal velocity (i.e. advective transport) and varies across the water depth. Turbulence affects the sediment concentration profile by the suspension of the sediment particles and tends to smoothen the concentration gradient out (Figure A.5). The turbulent fluxes increase with the intensity of the turbulent eddies and concentration gradients. It should be noted that the sediment particles do have a certain settling velocity and settle time and hence do not respond instantaneously to the hydrodynamic conditions (Bosboom & Stive, 2015, P.267-272).

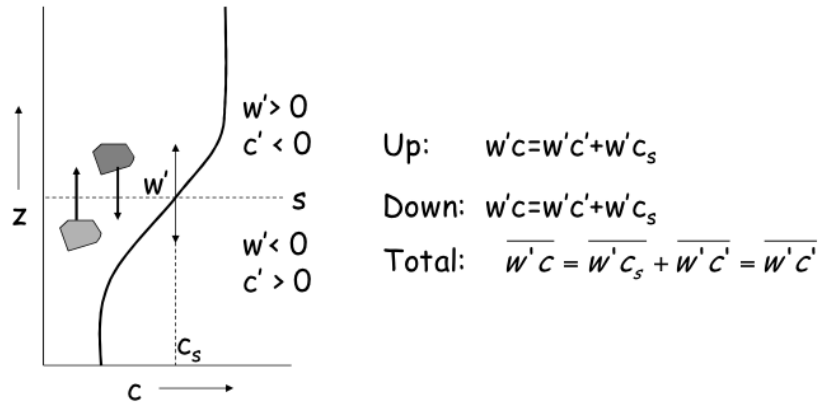
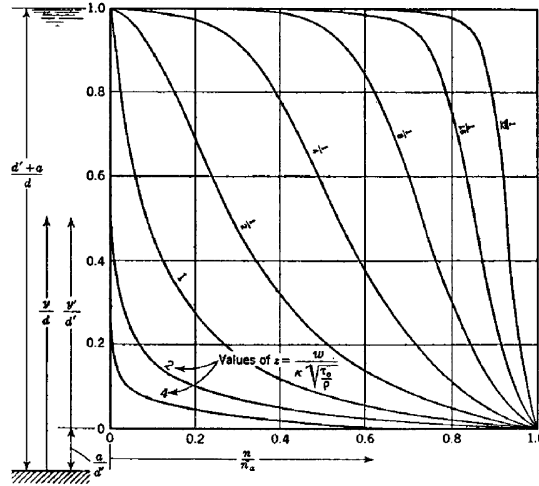


Figure A.5: Schematization turbulent suspension of an individual sediment particle (Uijttewaai, 2018, P.1-14). The turbulent character of the water motion tends to smoothen the sediment concentration gradient out.

The net turbulent diffusive transport causes sediment particles to move towards the surface and the gravitational force pulls the particles towards the bed. An equilibrium situation for uniform flow occurs when the turbulent flux equals the settling flux. The corresponding sediment concentration profile is characterized by a Rouse-profile and is based on the work of Rouse (1937):

$$c = c_a \left(\frac{a}{h-a} \frac{h-z}{z} \right)^\beta \quad (\text{A.7})$$

where c_a represents the near-bed concentration, a is the reference level of the determination of the near-bed concentration which depends on the bed topographic features of the bed, h the water depth and z the height w.r.t. the bed. The Rouse profile (Figure A.6) is affected by the sediment (w_s) and flow properties (u_*) and are expressed in the Rouse number: $\beta = \frac{w_s}{\kappa u_*}$. The shear velocity (u_*) is a fictitious velocity obtained by multiplying the actual velocity by the square root of the friction coefficient (c_f) or $u_* = \sqrt{\frac{\tau_b}{\rho}}$.



B

Delft3D-FM model description

The modules of Delft3D Flexible Mesh and incorporation of the vegetation are described in this section. D-FLOW has been officially released, whilst D-waves and D-Morphology are only available under beta conditions.

B.1. D-Flow

The D-Flow module solves the two- or three-dimensional unsteady, shallow-water equations (SWE). The shallow-water equations represent the free surface flows and are based on the the Navier-Stokes equations. The corresponding conservation of mass and momentum are given as:

$$\nabla \vec{u} = 0 \quad (\text{B.1})$$

$$\rho \left(\frac{\partial \vec{u}}{\partial t} + (\vec{u} \nabla \vec{u}) \right) = -\nabla \vec{p} + \mu \nabla^2 \vec{u} + \vec{k}_j \quad (\text{B.2})$$

where $\nabla = \left(\frac{\partial}{\partial x}, \frac{\partial}{\partial y}, \frac{\partial}{\partial z} \right)^T$, \vec{p} is the pressure, \vec{u} the three-dimensional velocity vector, μ the dynamic viscosity, and ρ the density of water. The term \vec{k}_j represents the different external forces (e.g. gravity, Coriolis, wave radiation stresses, etc).

The shallow-water equations are valid when the water depth is much smaller than the wavelength. Some other assumptions have been made to simplify the full Navier-Stokes equations:

- Incompressible fluid
- Hydrostatic pressure distribution
- Boussinesq approximation: horizontal density differences are small and negligible
- Eddy viscosity concept: turbulent motions are related to the mean flow

The depth-averaged shallow-water equations, implemented in Delft3D-FM, are given as (Deltare, 2019b):

$$\frac{\partial h}{\partial t} + \nabla \cdot (h \vec{u}) = 0 \quad (\text{B.3})$$

$$\frac{\partial h \vec{u}}{\partial t} + \nabla \cdot (h \vec{u} \vec{u}) = -gh \nabla \zeta + \nabla \cdot (\nu h (\nabla \vec{u} + \nabla \vec{u}^T)) + \frac{\vec{\tau}}{\rho} \quad (\text{B.4})$$

where $\nabla = \left(\frac{\partial}{\partial x}, \frac{\partial}{\partial y} \right)^T$, ζ is the water level, h the water depth, \vec{u} is the two-dimensional velocity vector, g the gravitational acceleration, ν the kinematic viscosity, ρ the density of water, and τ is the bottom friction. The

discretized partial differential equations, with the initial and boundary conditions, are solved on an unstructured finite volume grid. This grid is based on triangles of irregular sizes and is a main advantage of Delft3D-FM compared to its predecessor (Delft3D).

B.2. D-Waves

The D-Waves module is used to simulate the evolution of random, short-crested waves. D-Waves is based on the software of SWAN (Simulating WAVes Nearshore) and can be coupled to D-Flow by adding the radiation stresses as an external forcing term in the momentum equations. With D-Waves it is possible to compute the current- and depth-induced, refractive wave propagation for a given bathymetry, wind field, water level, and current field. Moreover, wave growth by wind, non-linear wave-wave interactions (triads and quadruplets) and dissipation (due to bottom friction, whitecapping, and depth-induced wave breaking) are incorporated (Deltares, 2019d). The SWAN model is based on the discrete spectral action balance equation, and is for Cartesian coordinates, given as (Hasselmann et al., 1973):

$$\frac{\partial N}{\partial t} + c_x \frac{\partial N}{\partial x} + c_y \frac{\partial N}{\partial y} + c_\sigma \frac{\partial N}{\partial \sigma} + c_\theta \frac{\partial N}{\partial \theta} = \frac{S}{\sigma} \quad (\text{B.5})$$

This balance equation describes the evolution in time (first term) and propagation (second and third terms) of the wave action ($N = \frac{E}{\sigma}$). The fourth term represents the current- and depth-induced shifting of the intrinsic frequency (σ). The wave refraction is represented by the fifth term. The right-hand side represents the sources and/or sinks to incorporate the effects of wave generation, dissipation, and non-linear wave-wave interactions.

B.3. D-Morphology

The dynamics of sediment is simulated with D-morphology (extension of D-Flow). This module incorporates the bed-load and suspended-load transport of non-cohesive sediments due to waves and currents. The elevation of the bed is updated at each computational time-step based on the fluxes of a grid cell (Deltares, 2019c). Since the morphological changes typically vary on a longer time scale compared to the hydrodynamic changes, a numerical technique can be applied in which the rate of the bed level changes is scaled up with a morphological time scale (MORF) factor.

Bed-load transport

The bed-load transport for non-cohesive sediment is simulated by calculating the magnitude and direction of the transport and corrected for the bed-slope effect, upwind bed composition, and sediment availability (Deltares, 2019c). The bed-load transport (S_b) of the Bijker formulation is given as (Bijker, 1992):

$$S_b = \underbrace{2D_{50} \frac{u}{C}}_{\text{Transport}} \underbrace{\sqrt{g} \exp\left[-0.27 \frac{\Delta D_{50} C^2}{\mu u^2}\right]}_{\text{stirring-up}} \quad (\text{B.6})$$

The median sediment grain size is represented with D_{50} , u is the flow velocity, C is the Chézy coefficient, Δ the relative density of the sediment, and μ a ripple factor to take the irregularities of the bed and turbulent motions into account.

Suspended-load transport

The transport of matter (e.q. sediment particles) for depth-averaged simulations is calculated with an advective and diffusive transport formulation (Deltares, 2019b):

$$\frac{\partial hc}{\partial t} + \nabla \cdot (h \vec{u} c) - \nabla \cdot (h \kappa \nabla c) = h s \quad (\text{B.7})$$

where h is the water depth, c is the concentration of the transported matter, \vec{u} the two-dimensional velocity vector, κ the diffusion coefficient, and s is a source term.

The suspended-load transport (S_s) of the Bijker formulation is defined as (Bijker, 1992):

$$S_s = \int_r^h c(z)u(z)dz = 1.83QS_b \quad (\text{B.8})$$

This advective type of transport takes place between a reference level (r) and the surface (h). The suspended-load is found to be (linearly) proportional to the bed-load transport, where Q represents the total Einstein integral term.

Sediment transfer fluxes

The sediment transfer between the bed and suspension layer (Figure B.1) is computed with the use of an erosive flux due to upward diffusion and a deposition flux due to the settling of sediments on the near-bottom layer:

$$-w_s c - \epsilon_z \frac{\partial c}{\partial z} = D - E \quad (\text{B.9})$$

where w_s is the settling velocity as formulated in Equation A.8, D is the sediment deposition rate, and E is the sediment erosion rate.

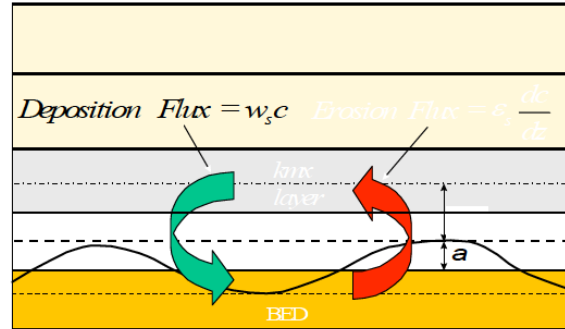


Figure B.1: Schematic representation of sediment transfer between the bed and suspension layer (Deltares, 2019c).

B.4. Vegetation formulation

Vegetation exerts a shear on the flow and can be characterized with a roughness coefficient. However, the bed friction will then be overestimated since the depth-averaged flow velocity is much higher than the flow velocity in the vegetation layer. The vegetation reduces and alters the flow distribution in which the flow through the vegetation is almost uniform and the flow above the vegetation is logarithmic (Deltares, 2019b). To also represent the altered flow distribution by the flow resistance, Delft3D-FM includes a vegetation formulation based on the work of Baptist et al. (2007). This formulation includes the contributions of both distinct flow regimes, within and outside the vegetation layer. The roughness in case of submerged vegetation is given in Equation 2.5. This roughness formulation takes both the alluvial bed roughness (C_b) and the flow resistance due to the vegetation (C_d) on a sub-grid level into account. However, in morphological computations, the resistance contribution of the vegetation should not be included in the bed friction terms that determine the sediment transport rates. Otherwise, the vegetation would lead to increased erosion, whereas in reality, the plant roots stabilize sediment.

To represent the dissipation of wave energy by vegetation a sink term is added in the spectral balance equation of the wave action (Equation B.5 & 2.6). The formulation of the wave dissipation of Mendez and Losada (2004) has been implemented in D-WAVES (Equation 2.7 & 2.8).

C

Hydrodynamic model setup by Keyzer

An outline of the hydrodynamic model setup constructed by Keyzer (2018) is given in this appendix. The work of Keyzer (2018) can be consulted for a more technical description of the hydrodynamic model.

C.1. Computational domain

The entire coastal domain and bathymetry can be seen in Figure C.1. Two computational domains can be distinguished. The domain used in the flow module is roughly 3 km by 6.5 km and includes both Baie Orientale and Baie de l'Embouchure. An unstructured grid is used for the flow domain that consists of irregular triangles. The main advantage is the varying grid size, which increases linearly from the shore towards the offshore boundary (from 50m to 150m). The larger, structured grid is used for the wave module. The domain has been chosen large enough to include the wave patterns around (Île Tintamarre) and to prevent any disturbance at the boundaries to affect the computations in the area of interest. The uniform grid size equals 0.001 deg ($\approx 110\text{m}$).

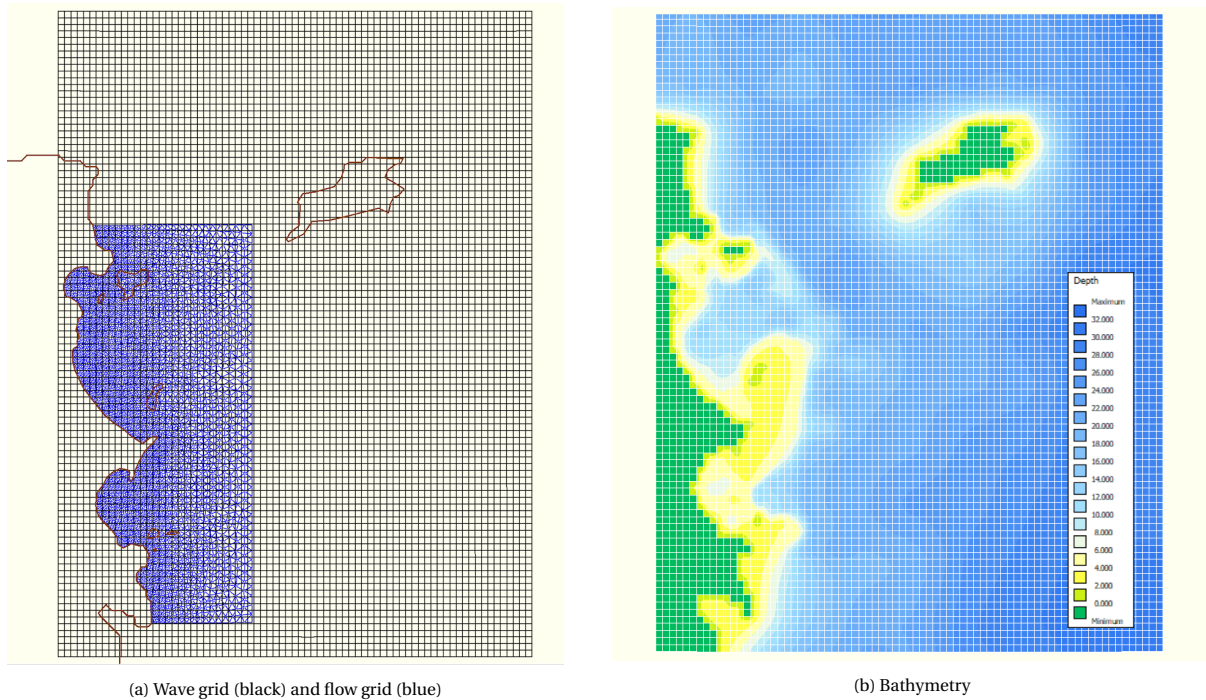


Figure C.1: Computational grids and bathymetry

C.2. Flow module setup

Boundary conditions

The constructed astronomic tidal signal contains three main tidal constituents as shown in Table C.1. This tidal signal is imposed at the eastern boundary (Figure C.2a), whilst the western boundary is a closed boundary. At the two lateral boundaries, a Neumann boundary condition has been imposed (Figure C.2b). In this manner, the water can move freely out of the domain and prevents that any external boundary effects occur.

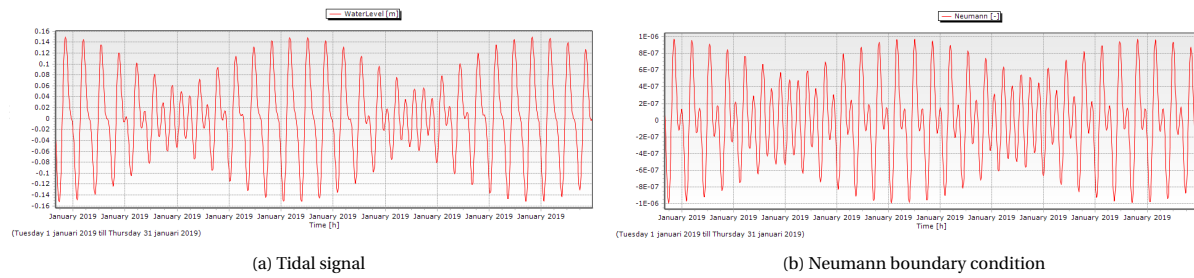


Figure C.2: Constructed tidal signal for one solar month.

| Constituents | Amplitude [cm] | Phase [°] |
|--|----------------|-----------|
| Principal Lunar Semi-diurnal (M2) | 5.9 | 222 |
| Principal Lunar Declinational Diurnal (O1) | 6.5 | 228 |
| Luni-Solar Declinational Diurnal (K1) | 5.0 | 357 |

Table C.1: Components of constructed astronomic tidal signal.

Bed roughness

A Manning value of $0.023 \text{ s}/\text{m}^{1/3}$ has been adopted for the bed roughness in the Flow module. The spatial varying Chèzy coefficient is indicated in Figure C.3.

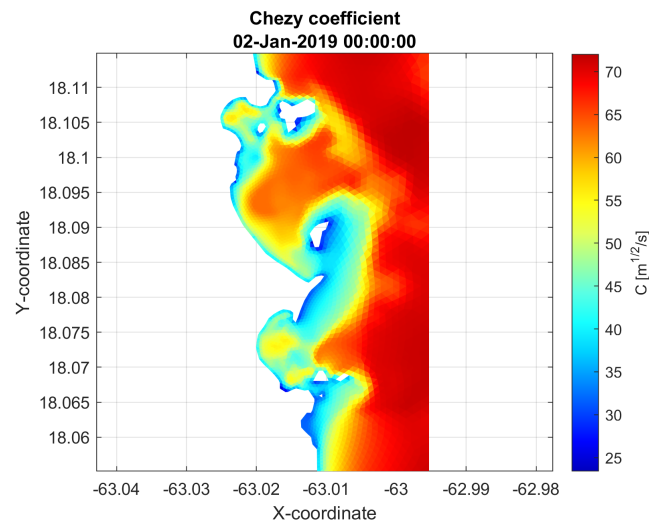


Figure C.3: Chèzy smoothness of the bed.

Vegetation

The vegetation drag coefficient is used as a calibration factor and not as an intrinsic characteristic of the vegetation. The drag does show vertical variations and the vegetation roots typically cause an increased drag at the bed. Based on the range of the drag coefficients over the water depth provided by Nepf and Vivoni (2000), a value of 1.0 has been adopted.

Wind

The winds vary in Gustavia (Figure 3.3) between the East-North-East and East-South-East sectors most of the time with an annually-averaged wind velocity of approximately 5m/s. Therefore, a steady and uniform wind field from the East has been imposed with a magnitude of 5 m/s.

C.3. Wave module setup

Boundary conditions

A JONSWAP wave energy density spectrum has been adopted to represent the wave climate in Saint Martin. A regular swell wave climate has been adopted in which the boundary conditions are stationary. The waves enter the domain from all three boundaries with a significant wave height of 1.5m and a wave period of 9s, coming from the East with a directional spreading of 10° . After the waves enter the domain the waves are affected by the following processes: shoaling, bed friction, depth-induced breaking, whitecapping, non-linear wave-wave interactions (Triads & Quadruplets), wind growth, diffraction, and refraction.

Bed roughness

In the wave module, only a constant roughness coefficient can be imposed. The JONSWAP friction coefficient was set to $0.038\text{m}^2/\text{s}^3$.

Vegetation

A bulk drag coefficient of 0.1 has been adopted for the attenuation of the wave energy. This value is consistent with the findings of Paul and Amos (2011), which shows that the bulk drag reaches a constant value of approximately 0.08 for turbulent motions.

Non-linear bed shear stress enhancement

The formulation of the friction model to represent the non-linear interactions of the current-induced and wave-induced bed shear stresses has been adopted as the FR84 formulation (Fredse, 1984). The corresponding Nikuradse wave-friction height (k_s) has been chosen as 0.01m.

D

Bed shear stress analysis

Keyzer (2018) performed an analysis to verify the bed shear stress since the output was found unreliable. A couple of issues have been indicated and are summarized in Table D.1. The correct computation of the bed shear stress is crucial regarding the simulation of sediment transport. Therefore, the total bed shear stress has been extensively investigated in this study. The issues have been resolved based on physical reasoning, fixing a software technical error and finding a work-around and are treated in Section D.1. The individual bed shear stress components have also been analyzed and the findings are summarized in Section D.2.

| Simulations | No vegetation | Vegetation |
|-------------|---------------|------------|
| Flow | Valid | Invalid |
| Flow-Wave | Invalid | Invalid |

Table D.1: Bed shear stress issues indicated by Keyzer (2018). The bed shear stresses has been found to be computed correctly only in a Flow-standalone simulation without vegetation.

D.1. Total bed shear stress

The different cases, for which the bed shear stress has been found to be invalid, are treated separately in this section.

Flow & Vegetation

Keyzer (2018) concluded that the reduction of the bed shear stress could only be attributed to the decreased flow velocities. The output of the roughness values remained constant irrespective of the presence of vegetation. Therefore, the bed shear stress was classified as falsely correct. However, after the software implementation and documentation were consulted it has been found that the alluvial roughness is outputted, which is used for the calculation of the bed shear stress. The physical explanation is that the resistance contribution by vegetation roots should not be used for the calculation of the bed shear stress that causes sediment transport. Otherwise, this would increase the bed shear stress and hence the sediment transport, whilst the vegetation is supposed to stabilize sediment. Therefore, it can be concluded that the bed shear stress for this case is not falsely, but correctly, computed.

Flow-Wave & Vegetation

The bed shear stress has been found to be unreliable and was not even close to the sum of the flow- and wave-induced components. But rather, the model output was surprisingly small and in each simulation equaled the flow-induced bed shear stress component (Figure D.1). A software technical error was found in the source code which caused this problem. The total bed shear stress was found to be computed at several subroutines and was eventually overwritten with the flow-induced bed shear stress component. This has been solved and a new software version has been made available.

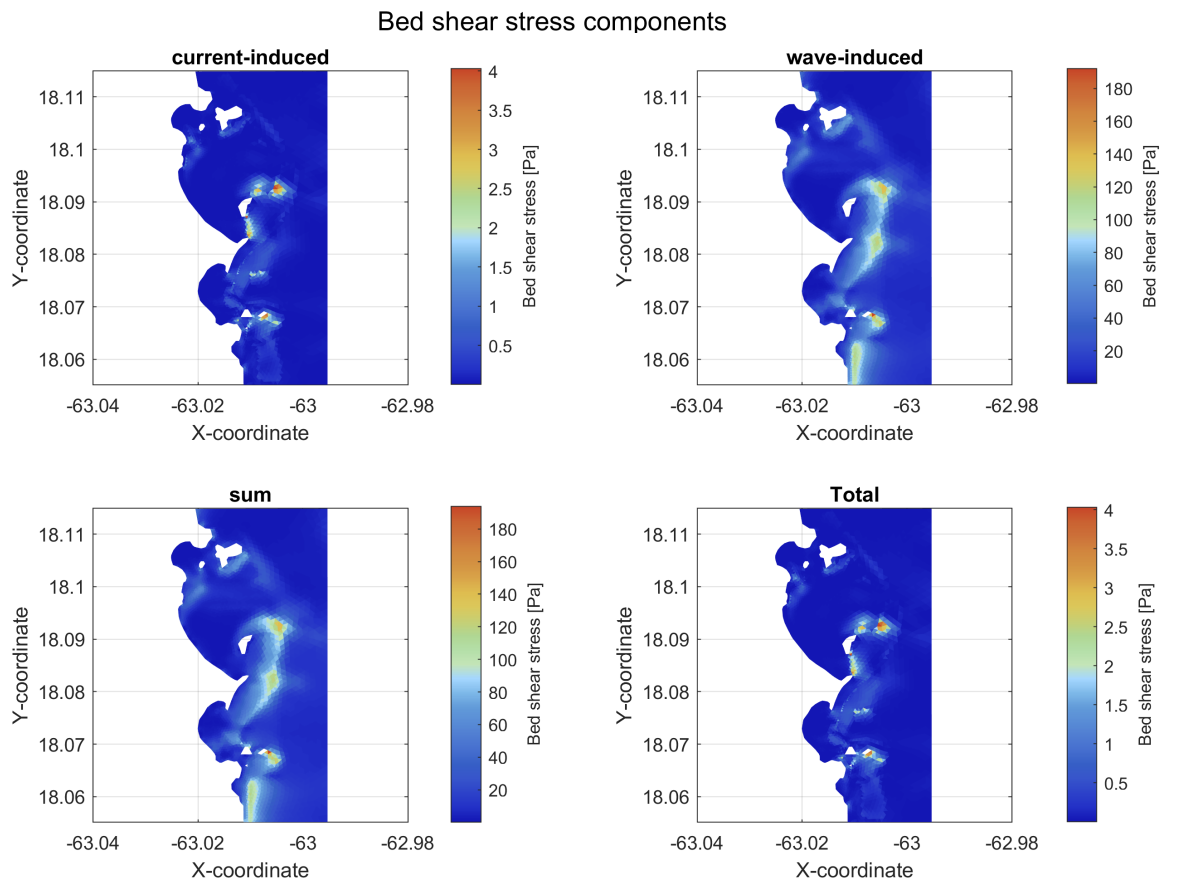


Figure D.1: Bed shear stress components for Flow-Wave & vegetation case. The total bed shear stress does exactly equal the current-induced component.

Flow-Wave & No Vegetation

The total bed shear stress model output was found to be unrealistically large, especially locally at the coral reefs. The spatial pattern shows discrepancies with the wave-induced orbital velocities and shows high similarities with the pattern of the roughness field of the reefs (Figure 4.1). The bed shear stresses are expected to increase locally at the reefs due to the high dissipation of wave energy, but the model output is considered to be too large (by one order of magnitude).

A simulation has been run in which the distinct reef friction field was disabled and surprisingly this resulted in a large reduction of the bed shear stress. Moreover, the spatial pattern of the bed shear stress resembles the orbital velocity pattern. Thereafter, the friction of the coral reefs was lowered in an attempt to decrease the spatial gradient of the roughness around the reefs. However, for substantial differences between the alluvial bed and reef roughness, the bed shear stress remained high and the spatial pattern still showed high similarities with the reef fields.

It has been concluded that the implementation of the distinct roughness field of the reefs is not reliable. The bed friction has, therefore, been adopted uniformly in the entire coastal domain. This might not represent the reality appropriately since coral reefs do have a higher roughness compared to the alluvial bed. However, this hydrodynamic setup is used for further analysis since the bed shear stress output is now more credible compared to the former hydrodynamic model (Figure D.2).

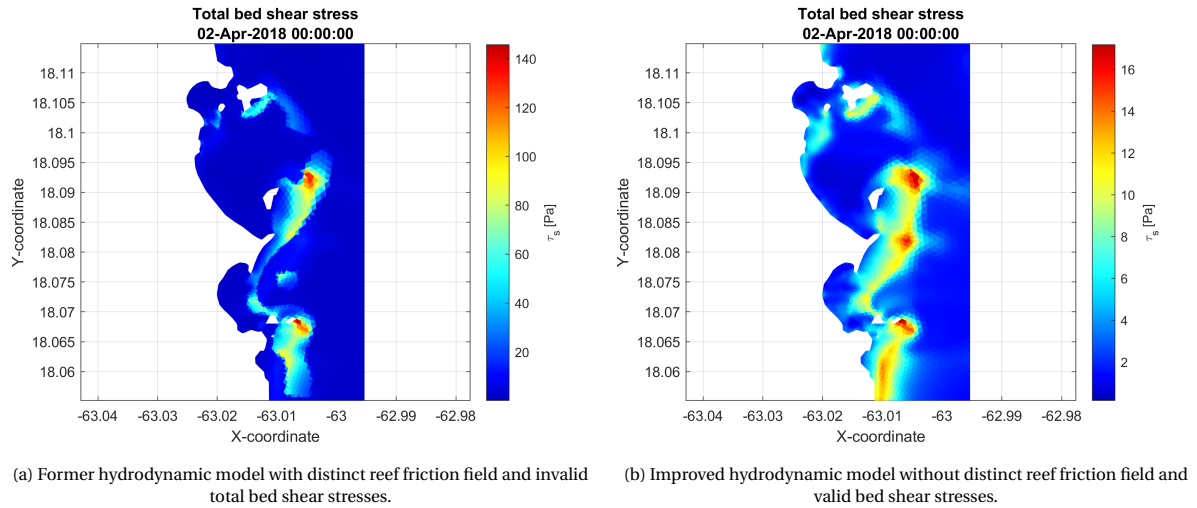


Figure D.2: Total bed shear stress for Flow-Wave & no vegetation case.

D.2. Individual components

The model output of the total bed shear stress has been found credible when no distinct reef friction field is included. However, the total bed shear stress is still smaller than the sum of the individual components. The individual bed shear stress components are calculated based on the model output of the hydrodynamic conditions. Since the maximum bed shear stress is outputted, the model output should at least equal the sum of the two individual components. Generally, the total bed shear stress is larger and the variations can be attributed to the non-linear enhancement of the bed shear stress as explained in 2.1.1.

The wave-induced bed shear stress is unrealistically large and has the same order of magnitude as the former incorrect total bed shear stress (Figure D.3). The wave-induced bed shear stress is calculated with the wave-induced orbital velocities (Equation 2.2). The orbital velocities show a decay from the surface towards the bottom. An increased water depth would, therefore, reduce the orbital velocities. Another simulation has been run in which the wave-induced set-up has been activated in D-Waves. The water level set-up is a characteristic of the coral reefs due to the energy transformation of the waves. Moreover, the friction induced by the reefs causes also a set-up, which currently is not taken into account.

Usually, the wave set-up is taken into account in the Flow-module in which the wave-induced radiation stresses are communicated with the Flow-module. However, in the D-Waves module, a separate wave set-up option is available. It is stated in the manual that this should be only activated in a wave standalone simulation or when the wave set-up is not explicitly computed in the Flow module (Deltares, 2019d).

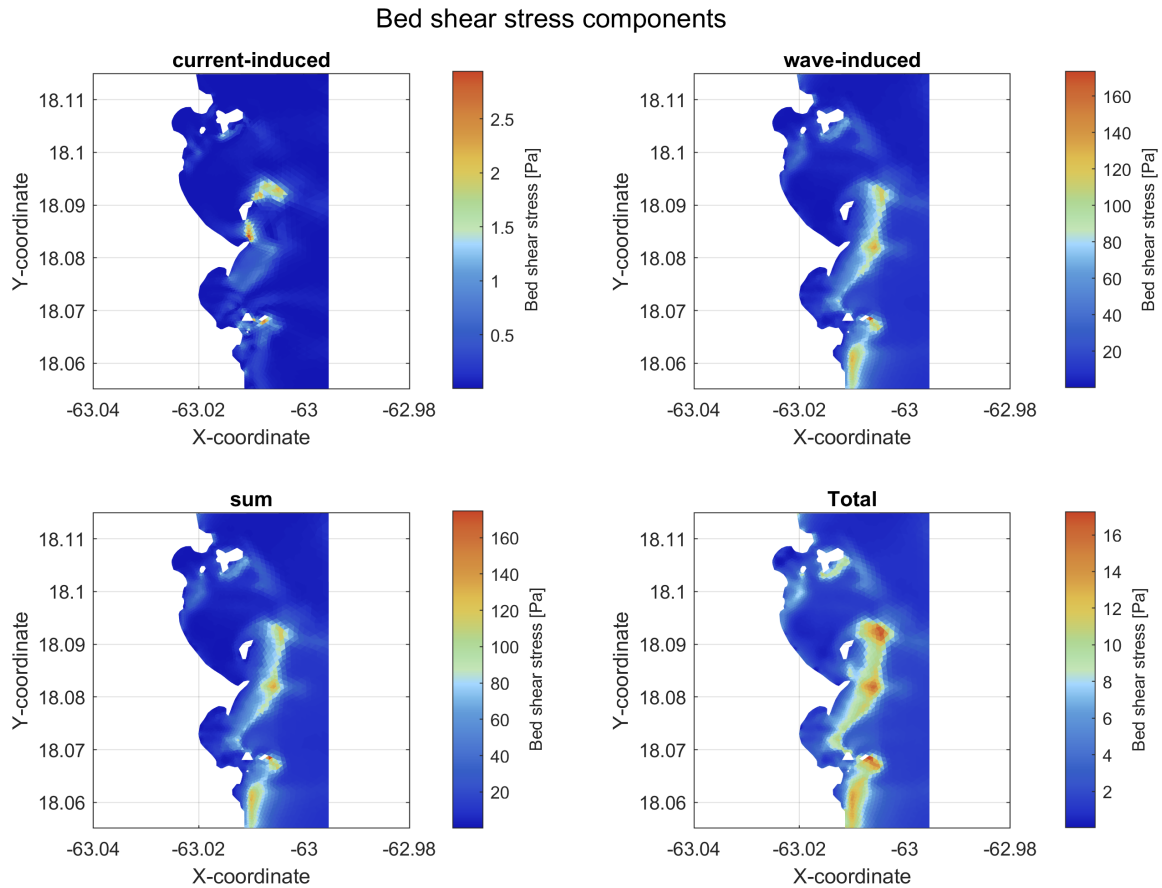


Figure D.3: Bed shear stress components for a simulation without distinct reef friction field. The wave-induced bed shear stress is calculated still incorrectly and is unrealistically large.

The orbital velocities indeed decrease on top of the reefs when the wave set-up is activated in D-Waves (Figure D.4). The total bed shear stress shows minor variations compared to the wave-induced bed shear stress. But more remarkable, is the large reduction of the wave-induced bed shear stress component (Figure D.5).

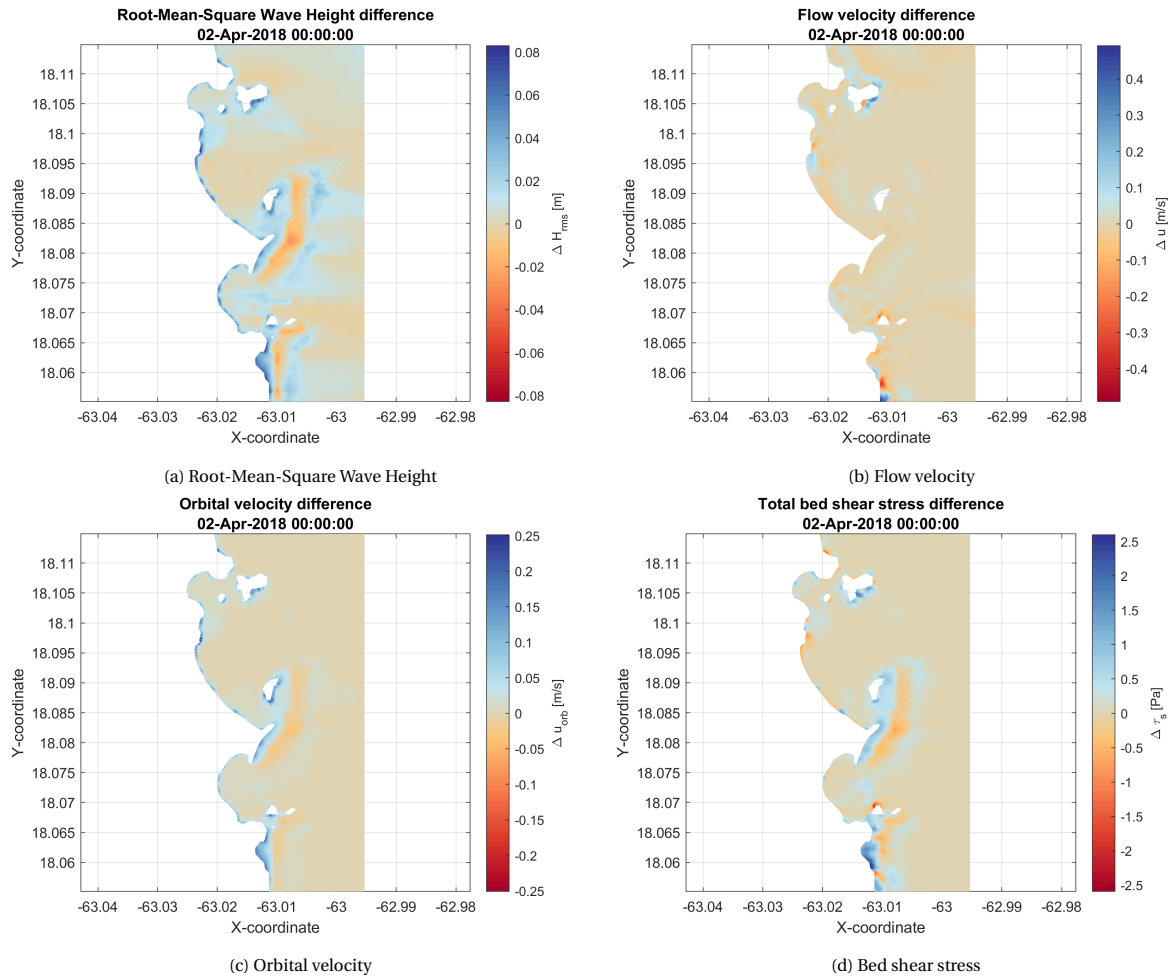


Figure D.4: Impact of wave set-up activation on hydrodynamics. The difference of the hydrodynamic forces are shown when the wave set-up is activated and deactivated in D-Waves. The wave height and orbital velocities slightly decrease on top of the reefs.

The wave-induced bed shear stress is also found to be smaller than the total bed shear stress (Figure D.5) as expected from the literature and implementation of the bed shear stress. This model setup makes thus physically more sense and has been used for further analysis.

This implies that the wave set-up in the coupled Flow-Wave model is not computed appropriately when it is not activated explicitly in D-Waves. The wave-induced bed shear stresses are unreliably large, whilst the increase of the orbital velocities is not that substantial. There might also be a possibility that the adopted model setup results in a model artifact. However, the coupled Flow-Wave model has not been officially released yet and it is known that other Flow-Wave couple issues exist. This might, therefore, be another software technical issue. This analysis also shows that a careful interpretation of the model output is a necessity. Note that the total bed shear stress is almost equal to the case when the wave set-up is deactivated in D-Waves. Therefore, it is not expected that the deactivation of the wave set-up in D-Waves would lead to significant differences with regard to the morphological changes.

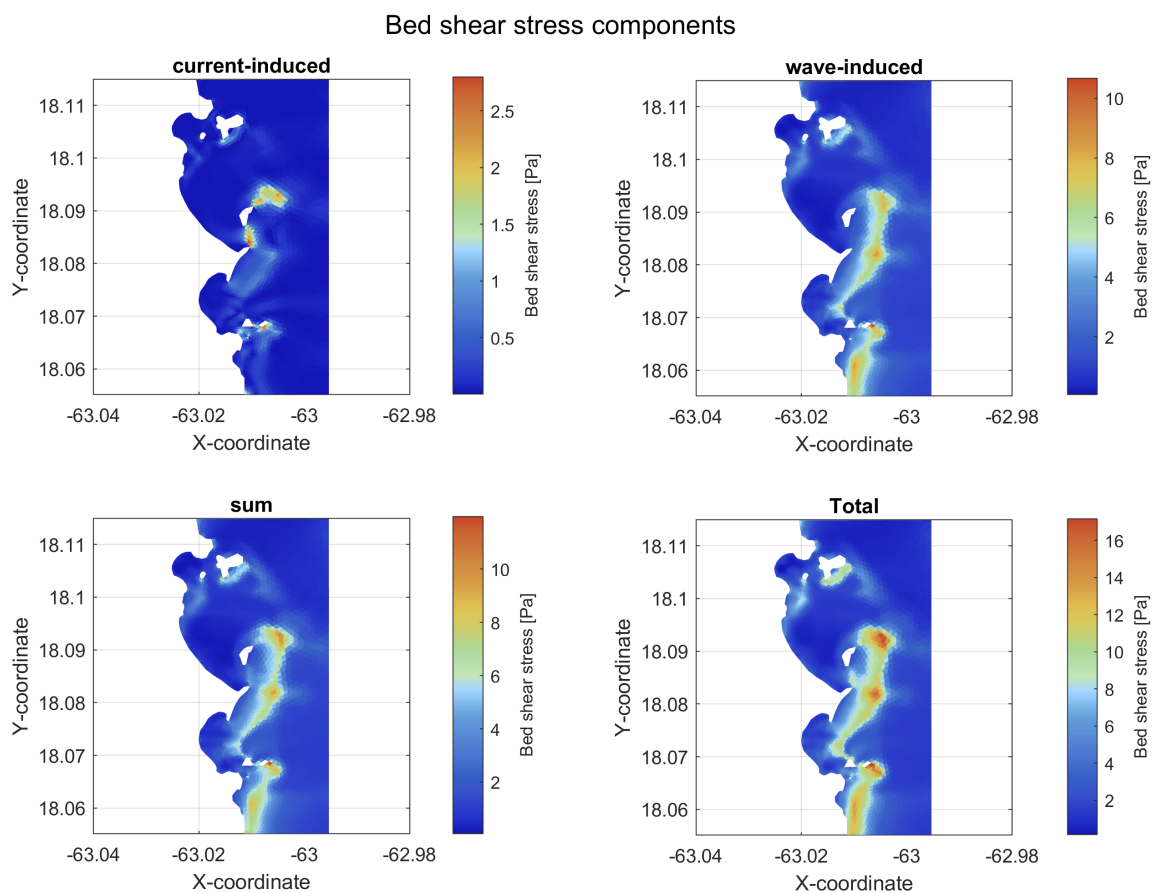


Figure D.5: Bed shear stress components with wave set-up activated in D-Waves. The wave-induced bed shear stress component did reduce with one order of magnitude and the total bed shear stress is now larger the sum of the individual components. Note that the total bed shear stress is almost equal to the case when the wave set-up is not activated.

E

Morphological sensitivity analysis

Wave conditions of a certain magnitude and waveform need to be present to propagate sufficient wave energy into the sheltered bays and transport the sediment. The wave height and wave period have therefore been varied to assess under which wave conditions the sediment transport becomes apparent. Moreover, the morphological changes for different wave directions and sediment characteristics are investigated.

E.1. Wave height

Small wave conditions ($H_s = 0.5\text{m}$) do not cause significant coastal erosion (Figure E.1). Only around Caye Verte, a larger sediment flux can be observed due to the high concentrated flows and large wave energy. The morphological changes of the coastal bays start to become apparent from an offshore significant wave height of 1m (Figure E.2). The (RMS) wave height increased slightly up to 10cm (Figure E.3). However, this small increase of wave energy inside the bays is enough to significantly increase the bed shear stresses and coastal erosion in the shallow regions.

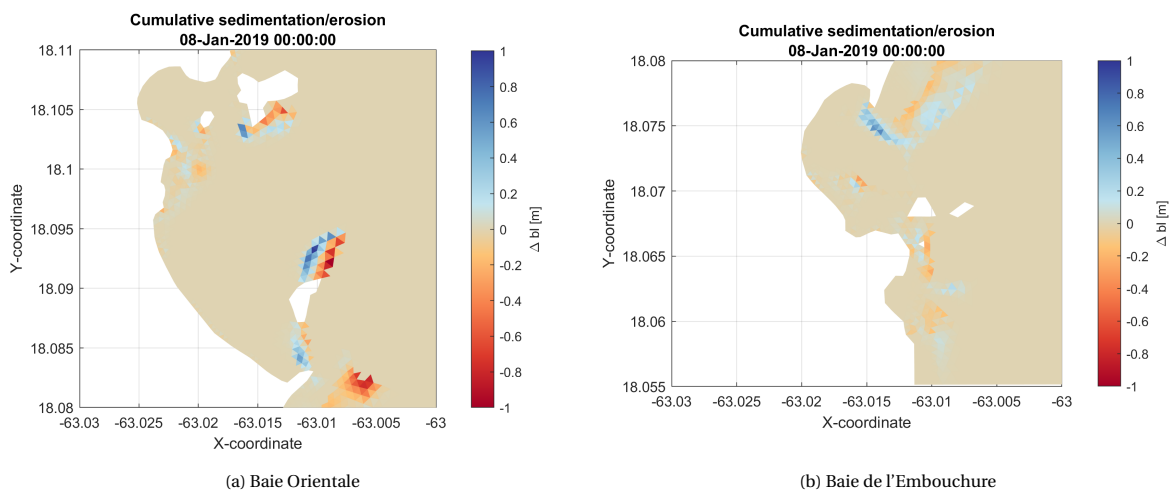


Figure E.1: Morphological changes in coastal bays for regular wave climate ($H_s = 0.5\text{m}$). The small wave conditions ($H_s = 0 - 0.5\text{m}$) do not propagate sufficient wave energy inside the bays to cause significant coastal erosion.

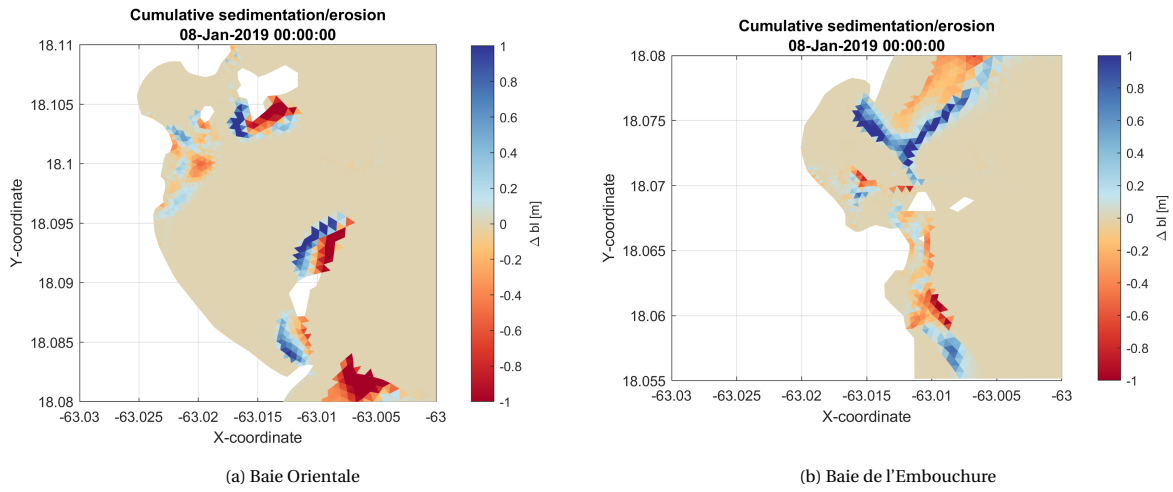


Figure E.2: Morphological changes in coastal bays for regular wave climate ($H_s = 1\text{m}$). The coastal erosion in the bays starts to become prominent.

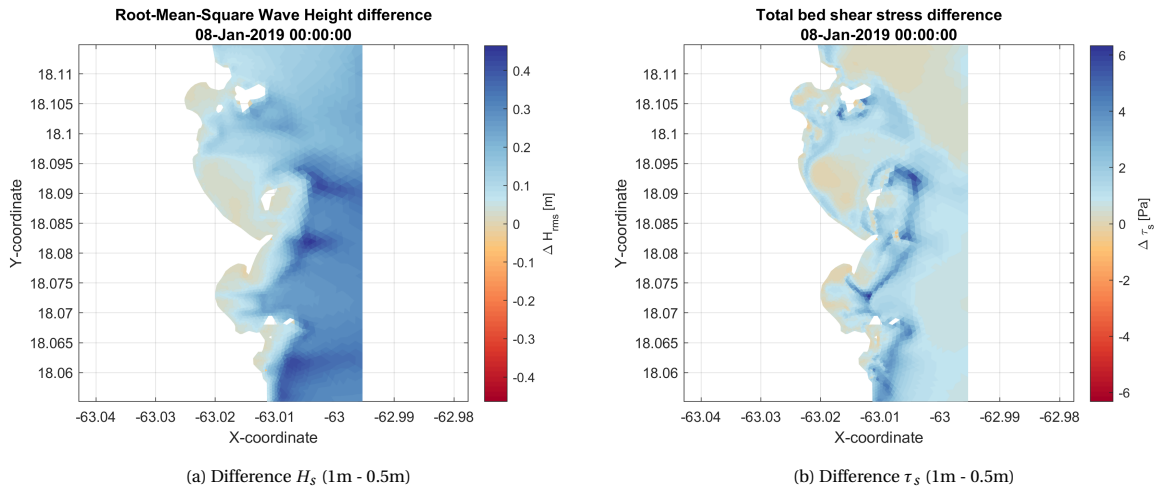


Figure E.3: Difference of wave height and bed shear stresses between normal ($H_s=1.0\text{m}$) & small ($H_s=0.5\text{m}$) wave conditions. The wave height increases slightly inside the bays, however this small increase is enough to significantly increase the bed shear stress in the shores.

E.2. Wave period

A characteristic of the swell wave climate is the large wavelength over the wave height ratio. Therefore, different simulations have been run in which the (mean) wave period has been varied. Whilst, the significant wave height has been kept fixed ($H_s=1.5\text{m}$).

The longer waves shift more towards the reefs, which increases the (RMS) wave height up to 60cm in front of the reefs (Figure E.4). The longer waves also propagate more wave energy into the sheltered bays. However, this is rather limited (up to 10cm) due to the prevailing depth-induced wave breaking on top of the reefs.

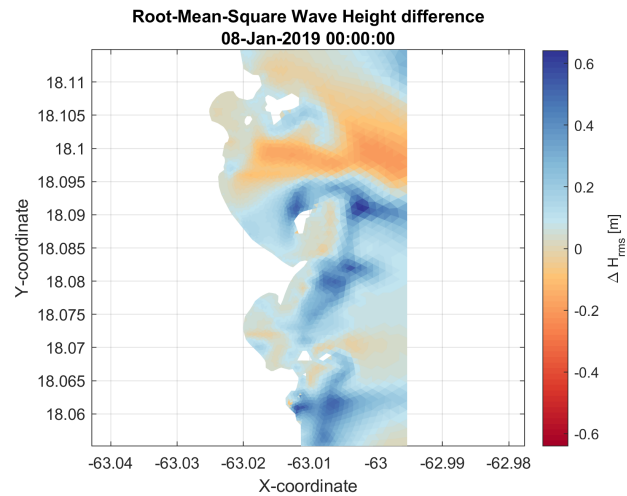


Figure E.4: Wave height difference between long ($T_m=13s$) and short ($T_m=5s$) waves. The longer waves propagate more wave energy into the sheltered bays. But remarkably, the longer waves are smaller than the shorter waves, in the exposed region in Baie Orientale.

Remarkable is that the longer waves are smaller than the shorter waves, in the exposed region in Baie Orientale. This is caused by the influences of the neighboring island (Île Tintamarre) on the diffraction patterns of the wave field. The wave diffraction around the island can also be observed in reality (Figure E.6). Longer waves from the north diffract further around the island towards the entrance of Baie Orientale and interact with the straight incoming waves (Figure E.5). The non-linear wave-wave interactions do not result in a direct energy dissipation but in a re-distribution of the wave energy. Especially, the Triad-interactions are important in shallow waters and transfer wave energy from the lower frequencies to the larger frequencies. This increases the wave steepness and dissipation of wave energy.

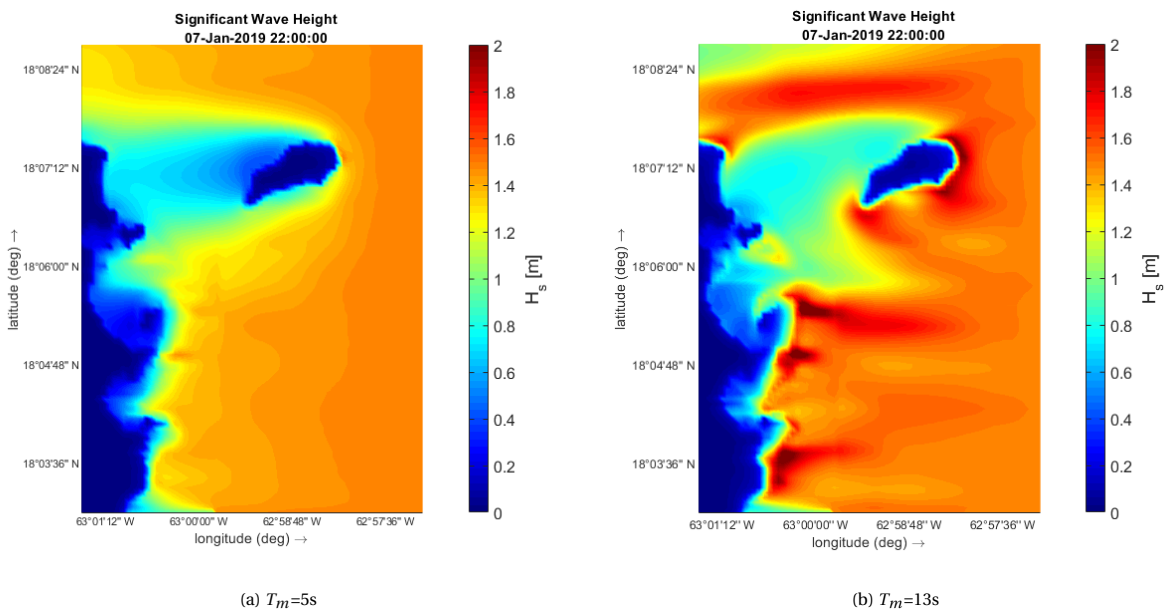


Figure E.5: Simulated diffraction around Île Tintamarre. Longer waves diffract relatively further around the island.

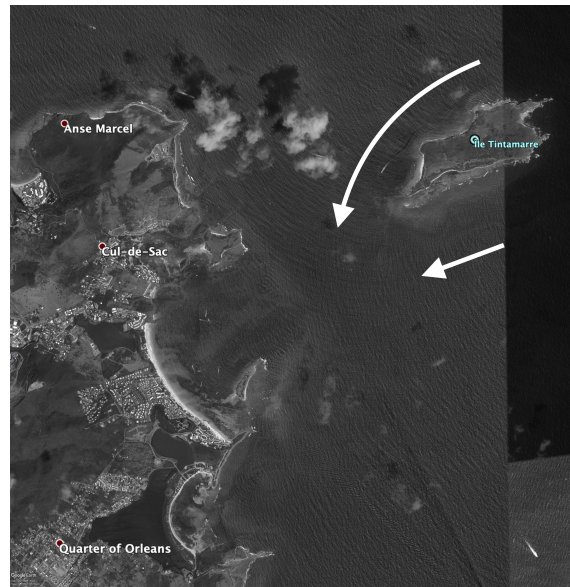


Figure E.6: Observed diffraction around Île Tintamarre. The white arrows indicate the wave rays and reveal the diffraction pattern around island. Adopted from (Google Earth, 2014).

The shift of the longer waves and increased wave energy inside the bays also affects the morphological development of the coastal bays (Figure E.7). The sediment transport increases within the bays and is further directed towards the shore. The southward sediment fluxes in front of the headland and beneath Baie de l'Embouchure are also larger.

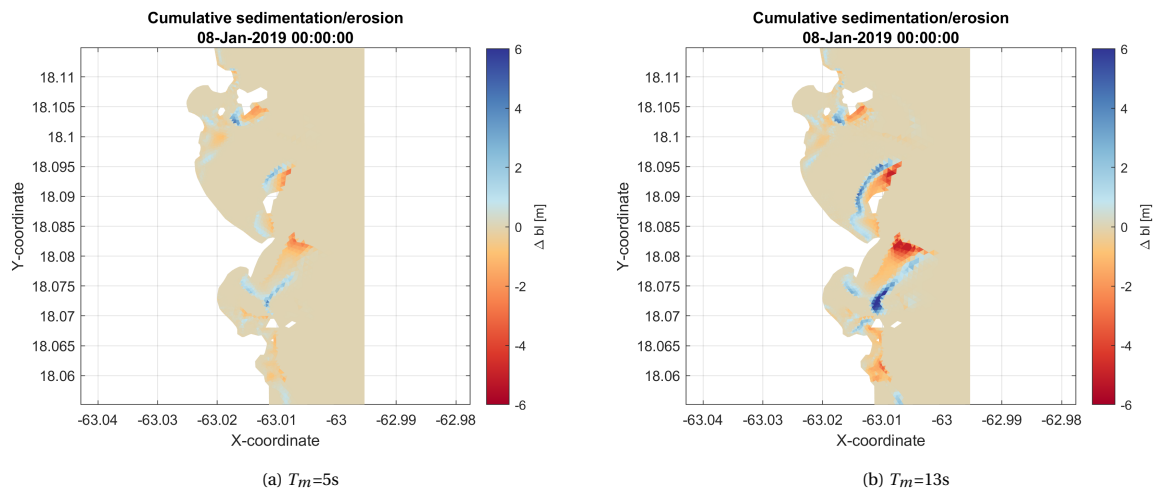


Figure E.7: Sensitivity of morphological changes for different wave periods. The shift of the longer waves and increased wave energy inside the bays leads to larger sediment fluxes.

E.3. Wave direction

Two simulations have been assessed, one with a wave direction from the East-North-East and another from East-South-East. The wave direction has a significant influence on the direction of the transported sediment

(Figure E.8). The uniformity of the wave directions is reflected in the sediment fluxes. Therefore, the dynamic wave climate, in reality, would smoothen the uniform pattern of the sediment fluxes.

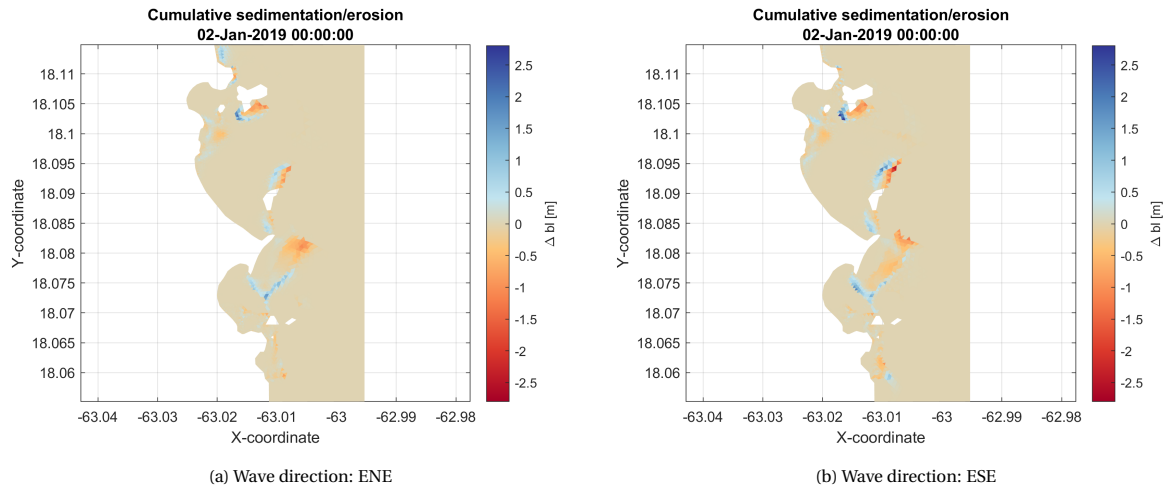


Figure E.8: Sensitivity of morphological changes for different wave directions. The uniformity of the wave directions is reflected in the morphological changes.

E.4. Sediment grain size

The sediment characteristics vary non-uniformly in the bays. The median sediment grain size has, therefore, been varied and shows that finer sediment particles are transported much more easily compared to coarser particles (Figure E.9). Differences in the sediment characteristics are, therefore, expected to influence the rates of sediment transport, type of transport and how far the sediment is transported.

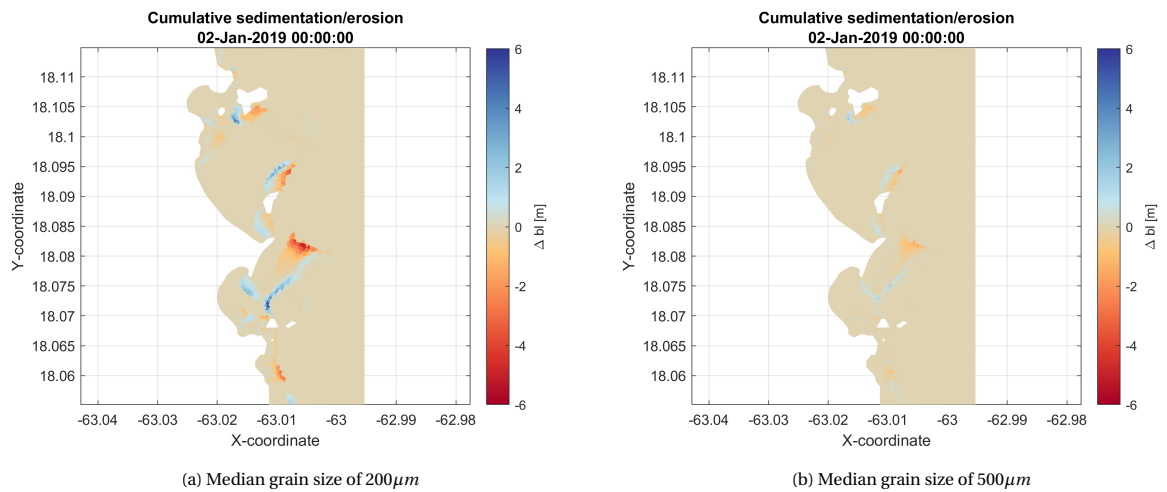


Figure E.9: Sensitivity of morphological changes for different sediment properties. The finer sediment particles are transported much more easily compared to coarser particles.

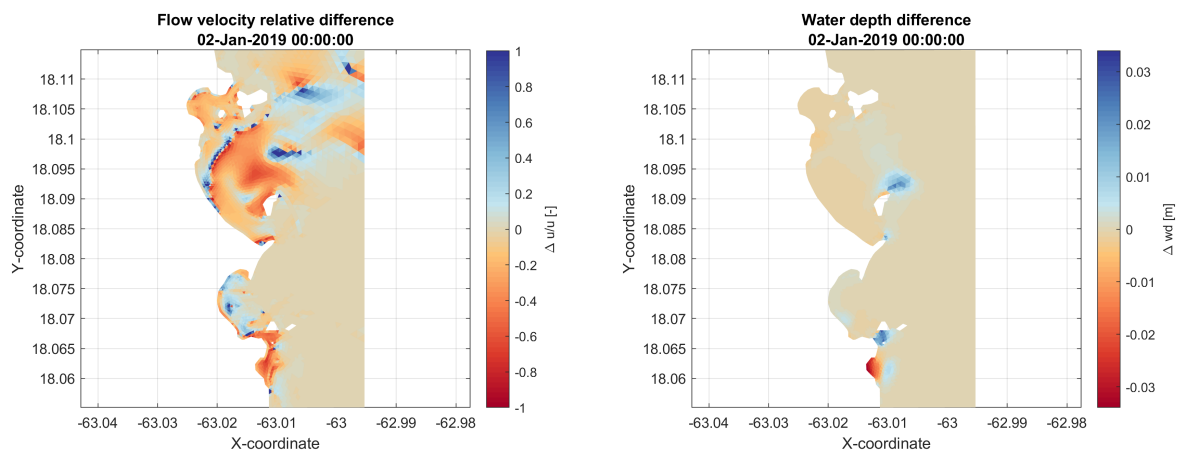
F

Hydrodynamic attenuation by seagrass

F.1. Attenuation under regular wave climate

Flow attenuation

The impact of seagrass on the flow velocities can be observed in Figure F.1a. The circulation flow in Baie Orientale is significantly weakened. Moreover, the circulation flow slightly shifts towards the ocean and is a direct consequence of the shear exerted by the seagrass. Another cause is the subtle vegetation-induced setup (Figure F.1b) which decreases the pressure gradient that drives the circulation flow. The smaller circulation flows in Baie de l'Embouchure increase in magnitude, whilst the flow velocities at the shore reduce over almost the entire shoreline.



(a) Impact of seagrass on flow velocities. The values have been normalized and the attenuation is indicated in red.

(b) The seagrass meadows induce a subtle water level increase in the bays indicated in blue.

Figure F.1: Impact of seagrass on flow and water level. The flow velocity in Baie Orientale is substantially attenuated and shifts slightly towards the ocean. This might also partially be caused by subtle seagrass-induced water level increase.

Wave attenuation

The waves are predominantly dissipated by the reefs and to a lesser extent attenuated by the seagrass meadows. The impact of the seagrass is prominent in the shallow areas around Caye Verte and in Baie de l'Embouchure (Figure F.2).

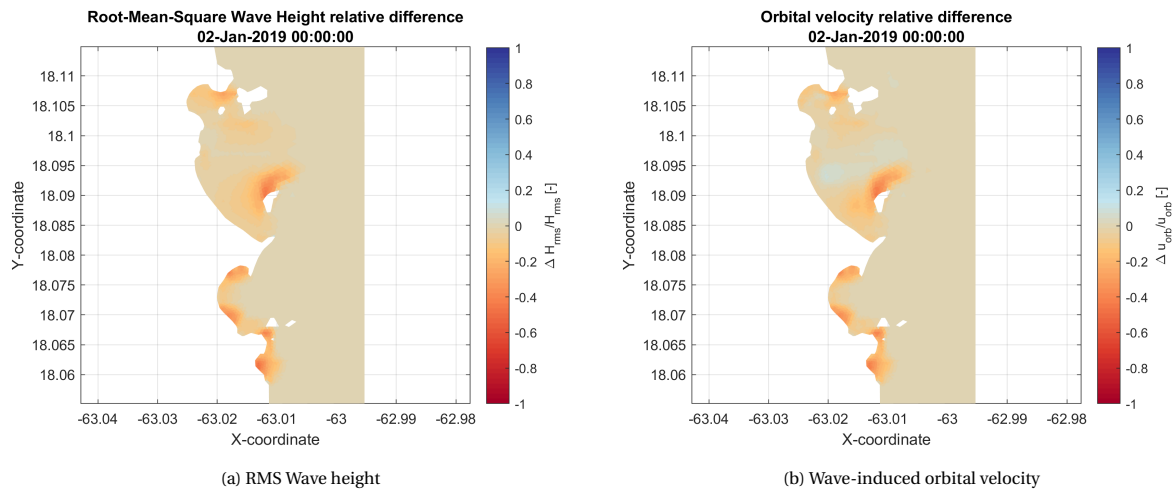


Figure E2: Impact of seagrass on wave forces. The values have been normalized and the attenuation is indicated in red. The attenuation of the wave forces is restricted to the shallow regions and where the seagrass meadows are present.

The transformation of the waves across the exposed part of Baie Orientale is shown in Figure E3. The seagrass meadows reduce the wave height over almost the entire stretch of the bay. The highest impact can be found where the seagrass meadows are located. Especially, nearby the shore the seagrass attenuates a large portion of the wave energy (up to 15%).

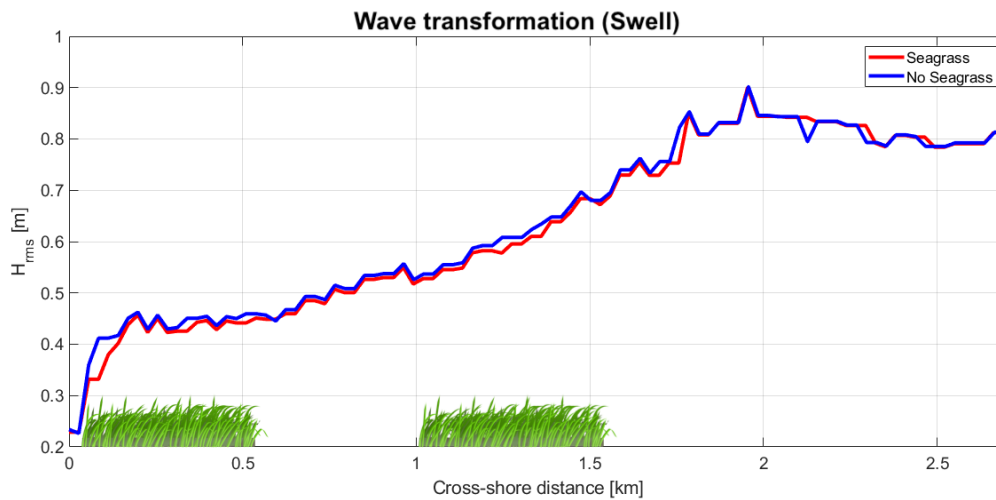


Figure E3: Wave propagation and transformation in the exposed area of Baie Orientale (A-A' as indicated in Figure 4.5). The waves shoal and reach a (RMS) wave height up to 90cm. Thereafter, the wave energy dissipates at the entrance of the bay. The seagrass meadows result in a slightly larger rate of dissipation over the entire stretch, but the impact is more noticeable in the areas where the seagrass is present.

Note that the indicated seagrass between 1 and 1.5 km is actually not present at the cross-section itself but a little bit southward.

Reduction of bed shear stresses

The bed shear stress has been lowered significantly in the shallow areas, likewise the wave attenuation (Figure E4). The reduction reaches locally values up to 60%, whilst the reduction in the northern part of Baie Orientale is less significant (approximately 10%).

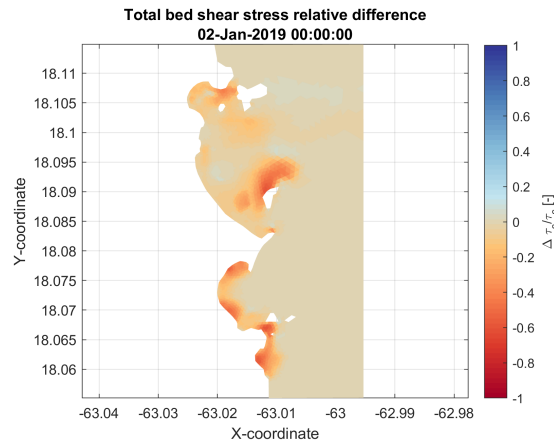


Figure E4: Impact of seagrass on bed shear stresses. The values have been normalized and the attenuation is indicated in red. The reduction of the bed shear stresses is especially noticeable in the shallow regions and where the seagrass is present.

E2. Attenuation under extreme storm event

The spatial attenuation patterns of the hydrodynamic forces during the extreme storm event can be observed in Figure E5 and are similar to the regular wave climate.

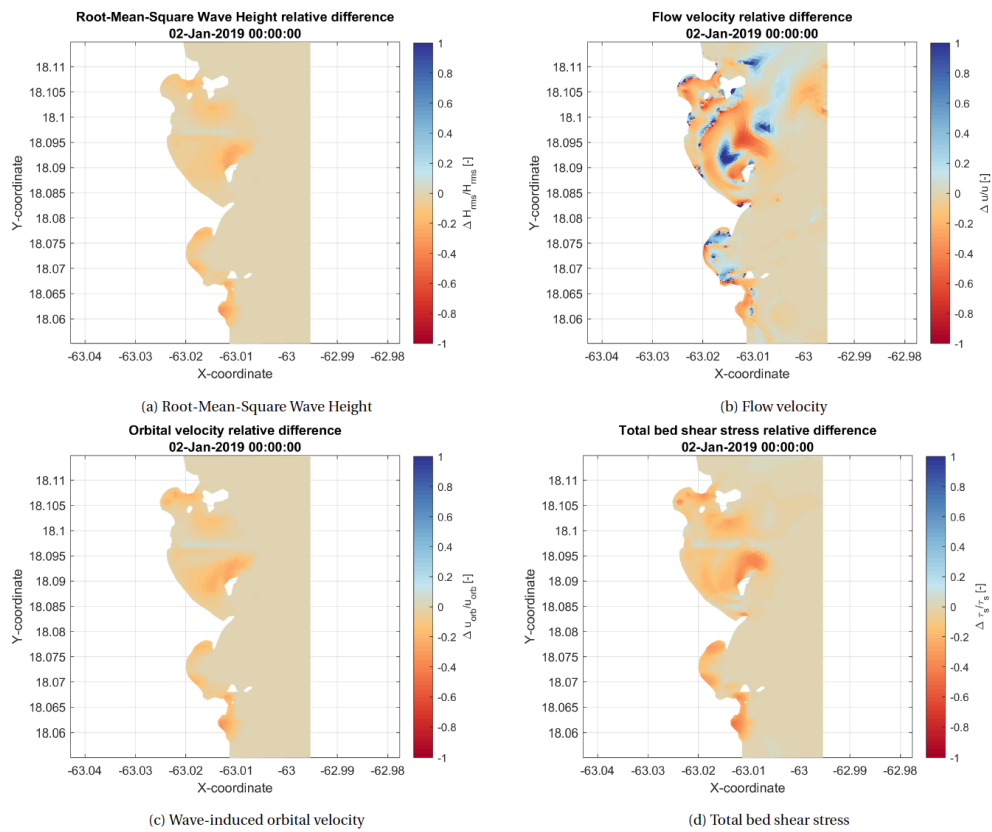


Figure E5: Hydrodynamic attenuation under the extreme storm event.

E.3. Hydrodynamic sensitivity to vegetation characteristics

The impact of different vegetation characteristics on the hydrodynamic attenuation has been assessed, in which the characteristics have been increased and decreased by 50%. The relative differences of the spatially-averaged hydrodynamic attenuation for the different vegetation characteristics can be seen in Figure E.6.

The vegetation height has a substantial impact on the attenuation of the flow velocities. The impact of the vegetation height on the waves (forces) and bed shear stresses is found to be also significant but is almost equally important as the impacts of the vegetation density, diameter, and bulk drag.

The vegetation exerts a certain drag on the flow and hence does have an effect on the attenuation of the flow velocities. However, the impact of the reduced flows on the waves is insignificant in these wave-dominated bays. The bed shear stress is dominated by both the waves and the flows and, therefore, the impact of the drag coefficient is slightly larger compared to the waves but could be still regarded as insignificant. Vice versa, the waves are dominant in the initiation of the circulation flows inside the bays and, therefore, the bulk drag coefficient does have a significant effect on the attenuation of the flow velocities.

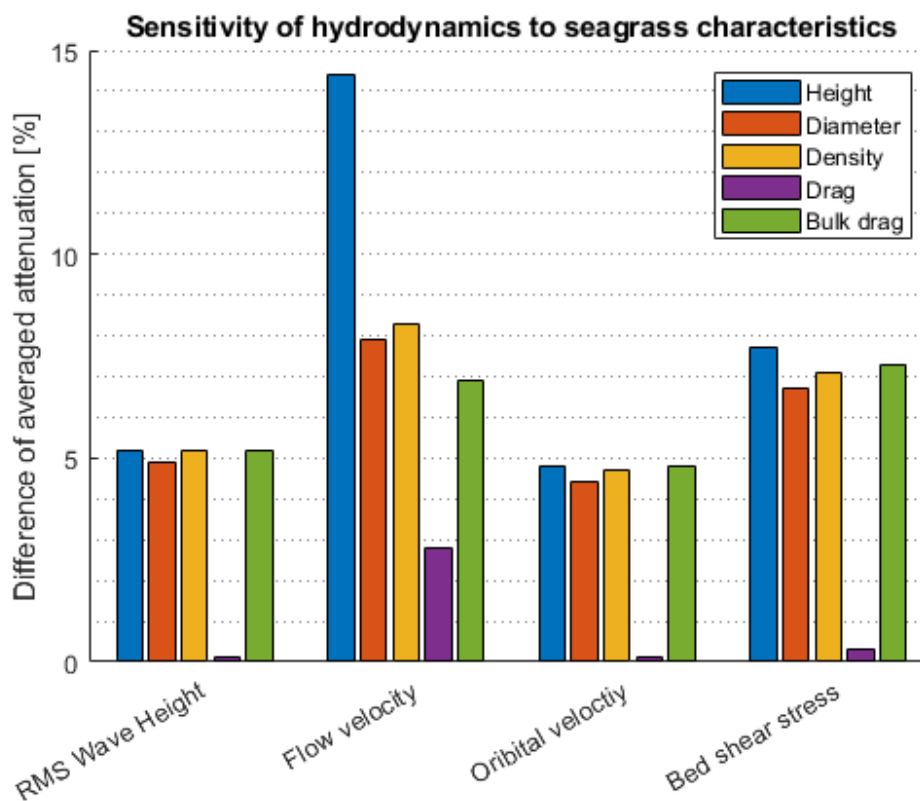


Figure E.6: Hydrodynamic sensitivity for the vegetation characteristics (+/-50%). The vegetation height has a significant impact on the attenuation flows and waves. However, the impact of the vegetation height on the waves is almost equally important as the impacts of the vegetation density, diameter, and bulk drag. The drag coefficient only has a significant effect on the attenuation of the flow velocities.